ADAPTIVE CRUISE CONTROL ON AN ELECTRIC ROBOTIC VEHICLE

ADAPTIVE CRUISE CONTROL ON AN ELECTRIC ROBOTIC VEHICLE

By

Liang Wang, B.Eng.

A Thesis
Submitted to the School of Graduate Studies
In Partial Fulfillment of the Requirements
For the Degree of
Master of Applied Science

McMaster University

Master of Applied Science (2015)	McMaster University
(Mechanical Engineering)	Hamilton, Ontario, Canada

TITLE:	Adaptive Cruise Control on an Electric Robotic Vehicle
AUTHOR:	Liang Wang
SUPERVISOR:	Dr. Fengjun Yan
NUMBER OF PAGES:	xii, 141

ABSTRACT

Adaptive Cruise Control (ACC), mostly equipped on high end vehicles, is an optional cruise control system which automatically adjusts the vehicle speed and maintains a safe distance ahead.

The control strategy for ACC, which has been developed for decades, is still well worth being researched. In this thesis, a hierarchical architecture was proposed, which consists of a supervisory controller and vehicle level controller.

Three control methods, named linear quadratic regulator (LQR), robust LQR, and composite nonlinear feedback (RCNF) control respectively were applied to upper level system as supervisory controllers. The active disturbance rejection control (ADRC) was chosen as vehicle level controller.

An electric robotic vehicle was built for demonstration and validation. Simulations and experiments were carried out with detailed discussions. Characteristics of these controllers were discussed and further studied.

ACKNOWLEDGEMENTS

This research was undertaken thanks to the help of my supervisor Dr. Fengjun Yan for his guidance in control strategy selection and financial support for building experimental platform. Special appreciation goes to Mr. Cam Fisher for his help and support in MARC.

Many thanks to the Department of Mechanical Engineering and its fellows, as well as McMaster University, where two years of my memory goes. Also gratitude to the country of Canada for its beauty and friendly people, and its open mind towards international students.

I would like to thank all my friends for their love and support, which equip me with courage and determination even in the darkest days.

At last, I am grateful to my parents for their over 20 years' love and continuous support.

TABLE OF CONTENTS

LIST OF FIGURES

LIST OF TABLES

CHAPTER 1

INTRODUCTION

1.1 Vehicle Automation and Adaptive Cruise Control (ACC)

There were nearly 6,420,000 vehicle accidents happened in the United States in 2005, suffering from which the financial cost exceeded 230 billion dollars and approximately 2.9 million people reported injured and 42,636 people confirmed killed [1].

90% accidents occur due to human errors, where distraction, poor judgment and lack of awareness are potentially responsible to share the blame [2]. The increasing numbers of traffic accidents and congestion have already become a severe social problem, urging governmental, academic and industrial entities to come up with effective measures cooperatively.

To reduce the risk of car accidents, increase road capacity, optimize fuel consumption and improve comfort and vehicle performance, research on vehicle automation never stops.

1.1.1 History of ACC

While the history of automation could probably go back to as early as 1930s [3], the focus on vehicular side began relatively late due to rudimentary electronics and sensory technology. The first try was the conventional cruise control (CCC) system, which can be traced back to the 1950s. At that time the earliest CCC system did not offer much functionality for it only used mechanical parts to hold the throttle in a fixed position. Later during 1950s to 1960s, these controllers were equipped with proportional feedback to provide full throttle when vehicle dropped 6-10 mph below the desired cruising velocity. In 1980s, with development in technology of assembly, microchips, sensors and component integration, CCC systems were gradually made more effective, reliable and robust. At the same period of time, the term adaptive cruise control (ACC) was adopted and massive researches were launched to contribute to the art of vehicle automation.

But the development history of ACC system began well before the term emerged, which traced back as early as 1960s [4,5]. Diamond and Lawrence [6] proposed an automatically controlled highway system (ACHS) to deal with increasing traffic congestion in April 1966. Levine and Athans [7] applied the theory of optimal control to a densely packed string of high-speed moving vehicles to regulate their position and speed using the simplest three-vehicle string model. Shladover [8] classified these systems into 13 controller structures by the difference in sources of feedback information, which was further discussed by Fenton's group at Ohio State University in 1968 for analyzing highway automation [9]. They proposed several requirements the controller structure must meet [9-12], which became a basis for later ACC controller's design.

By 1980s, driving situation developed more and more severe due to the relatively lagging construction of infrastructure of transportation system compared to the rapid expansion in the number of vehicles around world, hence, forcing the pursuit of the implementation of ACC systems [13,14]. Through the late of 1980s towards the beginning of 1990s, research plans were launched by United States, Europe and Japan almost the same time [15].

In Europe, the eight-year PROMETHEUS programme was initiated on 1 October 1986. 16 automotive companies, 56 electronics and supplier companies and 115 basic research institutes [14] participated. One of its main objectives was to provide European automotive and supplier industries a framework for cooperative development to gain competitive advantages over other continents [8,14].

In this programme, the term ‘ACC’ was defined and an ACC system was described in detail by Broqua et al. [16]. Distance-warning systems, ACC and ‘light convoy’, were defined by Zhang [17] as several longitudinal control levels. A modelling framework was also defined by Zhang and Benz [18] to evaluate the performance and safety of ACC.

At the end of the PROMETHEUS programme in 1994, the opportunity was greatly reduced for continued research with ACC systems [19]. Most subsequent projects began to focus on the evaluation and evolution of different ACC systems [20].

In United States, 1986, a study of automation in vehicle-highway systems by the California Department of Transportation’s (Caltrans) and the Institute of Transportation Studies at the University of California Berkeley led to the development of a state-wide programme called PATH [8,13]. Caltrans-PATH was involved in serial of other projects covering the areas such as collision warning, vehicle control and automation concepts [21].

In 1988, Caltrans and PATH created the Mobility 2000 with their counterparts in other states to expand the project to nationwide [22], which contributed to group intelligent vehicle highway system (IVHS) technologies into four functional areas: ATMS, ADIS, CVO and AVCS [22,23]. The first generation of ACC systems falls within the scope of AVCS.

In latter part of Caltrans and PATH project, a serial of field operation tests were conducted by Fancher's group [24–26] from July 1996 to October 1999 and General Motors Corporation [27] from 1999 to determine the safety effects, vehicle performance, user-acceptance and deployment issues of ACC systems.

In the late 1980s and the early 1990s, five ministries of the Japanese government initiated several projects concerning vehicle automation to improve the traffic condition, which later on stimulated the organization of Vehicle, Road and Traffic Intelligence Society (VERTIS) in 1994 and the Advanced Cruise-Assist Highway System Research Association (AHSRA) in September 1996 [28].

During this period, most of the research was conducted by private automotive companies and their suppliers, thus making it difficult to come up with a clear picture of the development of ACC systems. But some useful information can still be accessed such as: fully automated vehicles developed by Mazda, Mitsubishi and Toyota were tested on tracks [13]. Afterwards, the mainly focus was switched to the development of autonomous active safety systems, crash avoidance system and full-speed ACC system in the 1990s.

Currently, ACC is not only a technical term, but also becomes a popular marketing means. Nowadays, most automakers have equipped ACC systems on their high-end vehicles, with a trend extending this feature towards mid-range ones [21,29]. Vehicles with Full speed range ACC (with the ability to bring the vehicle to a fully stop) are listed in the table below.

Region	Full speed range ACC vehicles
Europe	**Audi** A8, A7 (2010+), A6 (2011+), Q7 (2007+), A3 (2013+), Q5 (2013+) / **Bentley** Continental GT (2009+) / **BMW** 2007 5-series, 2011+ X5 excl Diesel, 2013 3-series, i3 / **Land Rover** Range Rover (2013+) / **Mercedes-Benz** 2006 S, B, E, CLS, CL (2009+); A, CLA, M, G, GL (2013+) / **Porsche** Panamera (2010+); Cayenne (2011+), Cayman (2013+), Boxster (2012+) / **Seat** León (2012+) / **Skoda** Octavia (2013+), Fabia (2014+) / **Volkswagen** Phaeton (2010+), Passat B8 (2014+), Touareg (2011+) Golf Mk7 (2013+), Polo (2014+) / **Volvo** All Volvo models 2015+
United States	**Cadillac** XTS, ATS, SRX (2013+), ELR, Escalade (2015+ Premium trim) / **Chevrolet** Impala (2014+) / **Chrysler** 200c (2015+) / **Jeep** Cherokee (Limited and TrailHawk Models) / Grand Cherokee Stop & Go / **Tesla** Model S (2015+)
Asia	**Acura** 2014 RLX, 2014 MDX, 2015 TLX, RDX / **Infiniti** EX (2010+) / **Lexus** 2006 LS 460, 2013 GS hybrid / **Mitsubishi** Outlander (2014+) / **Nissan** Murano (2015+), Maxima (2016+) / **Subaru** Legacy, Outback (2013+) Forester (2014) / **Hyundai** Equus (2012+), Genesis (2015+), Sonata (2015+) / **Kia** Cadenza (2014+), Sedona (2015+), K900 (2015+)

Table 1.1 Vehicles with full speed range ACC

1.1.2 Issues of ACC

From 2001 to present, technical problems of ACC have been gradually fixed and more attention has been paid to other issues brought by ACC.

Firstly, human issues (such as driver behavior, user acceptance and human–machine issues), are concerned during the design and test processes of automatic systems that assist or replace human operator in safety critical tasks [30]. But unlike technical research, self-report questionnaires are usually applied to determine the different needs and different driving styles of various drivers falling into diverse age groups and with massive kinds of driving behaviors [31,32].

As for traffic perspective, notwithstanding ACC systems are stated as comfort systems by automakers, the systems are still considered to have traffic safety, capacity and stability benefits by researchers [13]. For this reason, standards or framework to assess the safety benefits of ACC systems or similar systems are proposed [33,34]. A number of investigations and evaluations have also been conducted by researchers funded by governments and/or automakers [18,35-38]. Some researchers conducted preliminary microscopic or macroscopic traffic flow simulations and limited traffic flow field operational tests in [39–41] trying to judge whether ACC systems have benefits towards traffic capacity. But due to differences in their simulation models, their results are sometimes controversial.

Environmental issues have been demonstrated as well. Bose and Ioannou [42–44] demonstrated that, during rapid acceleration transients, fuel consumption and air pollution levels can be reduced by 28.5% and 60.6%, respectively, if ACC penetration is 10%.

Marketing issues are highly concerned by automakers to reduce potential investing risk before broad deployment of ACC system. Though publications in this aspects are rare and considered as commercial secret, automakers have declared ACC systems are welcomed by customers as a valuable stress-reliever for highway driving [32,37,45-50].

Because of marketing issues mentioned above, legal issues of ACC systems are not discussed in publications. However, some discussions were proposed for similar systems [51-56], which are also applicable for ACC systems.

Several other issues besides the ones mentioned above were also presented by researchers. While in this thesis, designing control strategies are the main focus with performance and safety considered as first priority.

1.2 Novelty and Contribution

This thesis presents a complete design process for ACC systems, including control methodology demonstration, system modeling, design of supervisory and vehicle level controllers, simulations, experimental platform configuration and results with analysis.

A hierarchical control structure was proposed, which separates the controllers into supervisory and vehicle level ones.

Three different controlling strategies, i.e. traditional linear quadratic regulator (LQR), robust linear quadratic regulator (RLQR) and composite nonlinear feedback (CNF), were successively adopted as the supervisory controllers, and disturbance rejection control (ADRC) was selected as the vehicle level one, where, to the best of my knowledge, RLQR, CNF, and ADRC are seldom applied to ACC research area.

An electric robotic vehicle was constructed as experimental platform, which is highly configurable to be fully autonomous in the future. Simulation and experimental data was collected with detailed analysis, providing a guidance with characteristics and performance of these controllers towards the future design of ACC systems.

1.3 Thesis Outline

This thesis consists of 6 chapters.

Chapter 1 presents a brief introduction of ACC in both historical and potential issue aspects, demonstrating the fundamental knowledge of ACC system and problems it encounters. Novelty and contribution was clarified here, then thesis outline stated, as a sketch to grasp the whole structure and key points.

In Chapter 2, further details and explanations focusing on the technical side of ACC system were given with schematics. Discussion was made for current research advances of ACC control strategies, which offers a better understanding towards the overall mainstream ideas on ACC controller design process.

Chapter 3 presents a hierarchical control structure with several carefully selected control methods, which were divided into supervisory and vehicle level ones and illustrated with mathematical algorithms and diagrams.

Chapter 4 of this thesis mainly focuses on system modeling and simulations. Detailed processes were given and results were compared among different methods for their performance and characteristics.

An electric robotic vehicle was constructed as the platform in Chapter 5 to provide a way to validate control strategies. Experiments were carried out with detailed discussion and analysis to demonstrate their performance, effectiveness and properties.

The last Chapter 6 consists of the conclusion and future work recommendation, which illustrates a potential possibility for later research.

CHAPTER 2
ARCHITECTUAL AND RESEARCH ADVANCES OF ACC

2.1 Architecture of ACC System

ACC is an optional cruise control system for road vehicles which automatically adjusts speed and maintains a safe distance between following and preceding vehicles ahead.

ACC is normally considered an extension version of conventional cruise control (CCC) with the existence of range sensors (such as radar, lidar or a video camera). In the control process, if the preceding vehicle is absent, an ACC-equipped vehicle travels at a user defined speed, much like the CCC system. When the preceding vehicle is detected by sensors, the ACC system applies a control methodology which calculates and then estimates whether the situation is safe or not. If the system determines that the situation is unsafe, control activities are made to automatically adjust the position of throttles and/or brakes. Generally, the ACC system applies a maximum braking deceleration of around $0.5g$ [57]. An example of ACC system activated on highway can be described as below:

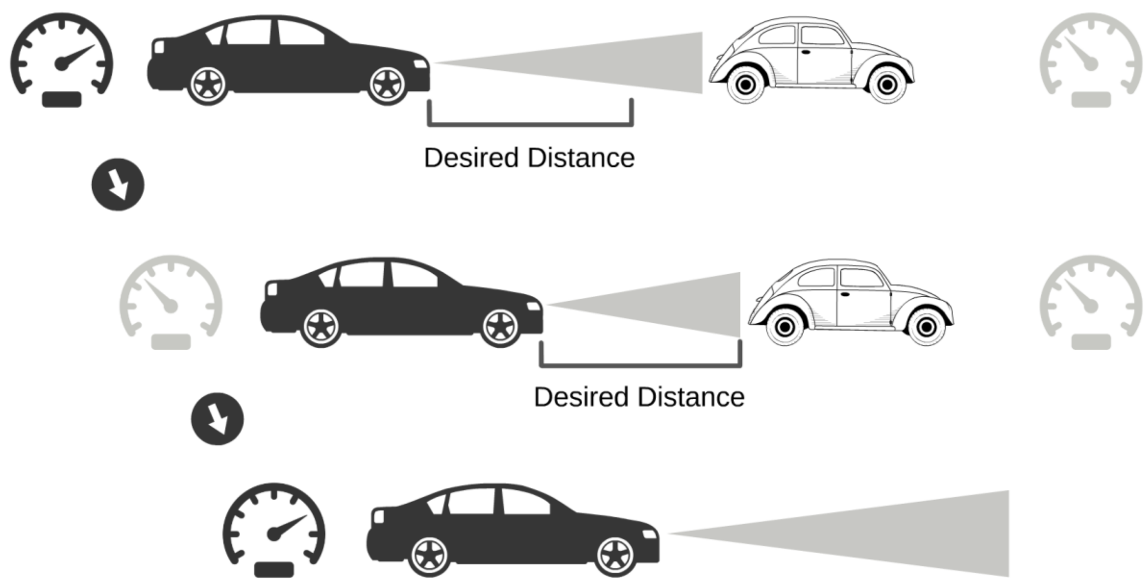

Figure 2.1 ACC system activated on highway

The term ACC was first described as adaptive intelligent cruise control (AICC), which was proposed in the PROMETHEUS programme in Europe. But later, the term AICC was considered to be inappropriate for the use of the word ‘intelligent’, which gives an illusion of the unrealistic performance. Therefore the ‘ACC’ is finally adopted to refer to autonomous longitudinal control strategy which not only offer comfort to driving operator but potential increased safety conditions.

ACC systems are configured by a common electronic control units (ECUs) and an additional one. The common ECUs are some standard ECUs with slight modification to make them suitable for the control task. The additional one, called ACC control module and specially designed, contains a range sensor and the ACC controller [29]. In the early generation, sensors like long range radar (LRR) and light detection and ranging (Lidar) are commonly used [58]. In later generation, mid-range and short-range radar, video camera and thermal radiation sensors are supposed to be used to improve the performance [58,59]. Discussions and comparisons between various sensors are made by some researchers [58-62].

Human machine interface (HMI) is also a concern by researchers, especially by automakers to improve the user acceptance of ACC system. The design objective of HMI is to make the driver always feels that the he or she is provided with vehicle's best support and meanwhile still possesses the full control privilege of the vehicle [58,63].

Several other sensors are needed to enhance the ACC system performance, including curve sensors (usually contains the steering angle sensor, yaw rate sensor, lateral acceleration sensor, navigation system and video camera) and velocity sensors. These sensors provide the driver with the prediction of future road situations, especially beneficial while driving along curves or performing a lane change [29].

Lingyun proposed a four-part system architecture for ACC system in [64] according to the research of [29,58,65-67], which are signal collecting (SC), signal processing (SP), signal actuating (SA) and signal displaying (SD) parts, as demonstrated in the figure below.

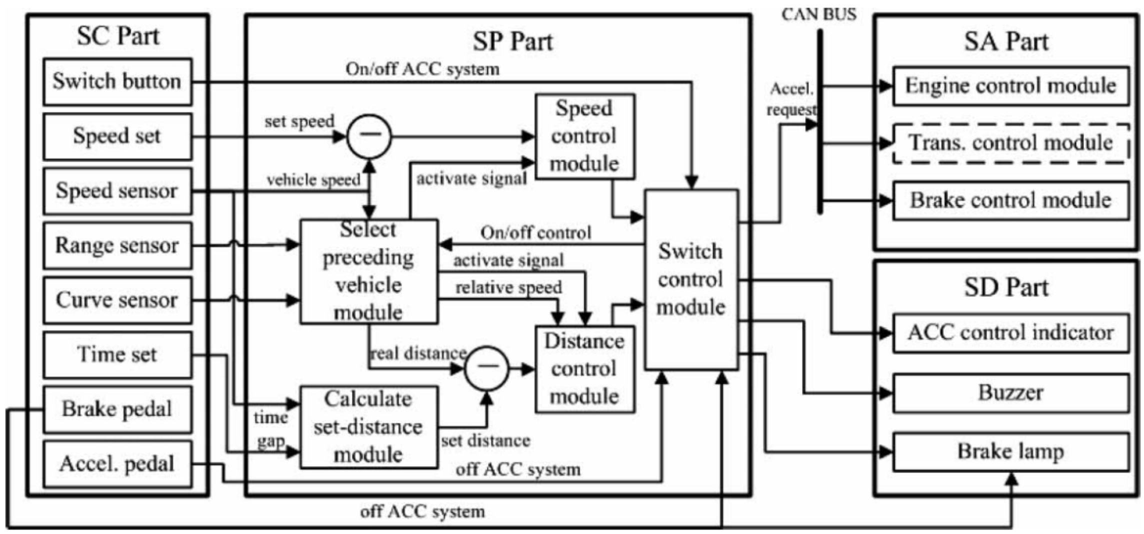

Figure 2.2 ACC system architecture

The operating process is as follows:

1) The switch control module detects the ON/OFF signal during driving and, if the switch button is pressed to ON with speed set by the driver, activate the ACC system then the range sensor starts to detect.
2) If the driving situation is safe, which means the preceding vehicle is absent or far away traveling at a high speed, the system will maintain a steady speed like CCC system.
3) If the driving situation is not safe, which implies the preceding vehicle is too close or running slowly, the system will automatically adjust the throttle and brake to keep a proper distance ahead. Under severe condition that the deceleration capability of the ACC system is insufficient, buzz is activated and vehicle control privilege will request to turn back over to driver.

4) If the switch button is set to Off during driving or brake or acceleration pedal is applied by driver, the ACC control system will be turn off.

2.2 Research Advances

2.2.1 Spacing Policy

The control methodology is perhaps the most researched area in ACC. ACC system control design begins with the selection of spacing policy, which refers to the desired steady state distance between two successive vehicles. Early design can trace back to 1950s [68]. During the early research process of this topic, five different kinds of spacing policies have been proposed: constant distance, constant time headway (CTH), constant safety factor, constant stability and constant acceptance, where the CTH spacing policy is chosen by automakers with the consideration of feasibility, stability, safety, capability and reliability factors [69–74]. Various design of spacing policy also can be found in [75-83].

2.2.2 Hierarchical Architecture

Typically, hierarchical architecture is adopted for ACC controllers [58], including the supervisory controller (also named upper level controller or ACC controller) and the vehicle level controller (also named lower level controller or longitudinal controller).

The supervisory controller firstly determines the kinematics of the vehicle to fulfil the control objectives. Then the vehicle level controller receives signal from supervisory controller to adjust throttle (or motor input if applied to an electric vehicle) and/or brake command to track the desired the kinematics [4,58] and demanded by the supervisory controller. Therefore, supervisory controller is more environmental focused and vehicle level controller is more model focused of the controlled vehicle itself (if error based control methodology like PID or ADRC is not adopted).

2.2.2.1 Supervisory Controller

The design methodology of supervisory controller can roughly divided into two aspects: the human behavior based and mathematical calculated.

The human behavior based method typically adopts neural network and fuzzy logic in controller design. Trained by real human beings, these controllers can imitate the safe car following behavior of humans [84] and offer a natural and comfortable feeling to drivers when the system is activated, which is an advantage over the mathematical calculated one in this aspect.

Pomerleau’s autonomous land vehicle (ALVINN) [85] was one of the earliest research to use machine learning for autonomous vehicle control. The vehicle consisted of a computer vision system, based on neural network, which was able to learn to correlate observations of the road to the correct action to take. Thiriez [86] also proposed a neural network based learning scheme to determine the path of the vehicle in a collision avoidance maneuver.

Naranjo et al. [87] demonstrated a fuzzy adaptive cruise controller focusing on providing driving strategies and regulating actuation of the engine throttle in 2003. They also proposed a fuzzy control approach in 2007 providing an alternative solution for nonlinear automotive control problems compared to conventional analytical control method [88]. In 2008, Abdullah et al. [89] integrated the fuzzy control method and tuning supervisor with a generalized learning model to form a multiple-controller framework for ACC.

Mathematical based supervisory controller is an alternative to human behavior based method and has been well studied and applied by a decent number of researchers.

Gain scheduling were adopted to provide an adaptive scheme for controllers. Ng et al. [90] proposed a reinforcement learning based gain scheduling method for the adaptive control system. Shakouri et al. [91] applied gain scheduling to (proportional-integral) PI and linear quadratic (LQ).

Optimal control method is favored by some researchers to balance various design objectives in practical implementation. Fuel consumption typically possesses the first priority in such design process, especially when the controller is equipped in heavy duty trucks [75]. Linear quadratic regulator (LQR) [91] and model predictive control (MPC) method are usually adopted, where the MPC is sometimes made explicit [92,93] or multi-objective [83].

Multi-target tracking was also considered to imitate the practical road condition, studied by many researchers [94-101].

While traditional ACC only deals with the relation between one single vehicle and its environment outside, cooperative adaptive cruise control (CACC) requires communication between different vehicles to obtain a better control results, which was studied by some researchers. De Bruin et al. [102] gave an overview on how such a system can be designed. Naus et al. [103] focused on the feasibility of the implementation setup in real practice for CACC. And the communication aspect of such system was researched by van Eenennaam et al. [104].

2.2.2.2 Vehicle Level Controller

In vehicle level controller design, engine and brake models are usually studied.

Swaroop et al. [105] proposed an input/output linearization method to handle the nonlinearities of the engine. Gerdes and Hedrick [106] designed sliding controllers showing successful tracking of kinematics in simulation and experiment. Schiehlen and Fritz [107] compared several different linear and nonlinear controller for engine design. Similar work were carried out in [108]. Some researchers like Mayr [109] skipped the modeling of engine and driveline, and instead introduced a simplified longitudinal model.

For brake models, an example can be found in [110]. Application of sliding mode controller for nonlinear brake models was studied by Yi and Chung [111]. Druzhinina et al conducted a series of researches to verify the compression brake control designs for heavy truck [112-114] and experimental results was analyzed in [115].

CHAPTER 3
CONTROL STRATEGIES

Although control systems of various type can trace back to antiquity, the dynamics analysis of the centrifugal governor, conducted by the physicist James Clerk Maxwell in 1868, entitled On Governors [116], marked the beginning of more formal research into the field of control methodology.

Nowadays, most people are familiar with the methods and techniques of what is known as “classical control”. The systems or plants considered to apply classical control methods are linear and time invariant and have a single input and a single output.

The primary objective to use classical control design is to stabilize a plan, whereas the secondary aims may include a certain transient response, bandwidth, disturbance rejection, steady state error, and robustness to system variations or uncertainties.

Designing methods cover analytical ones, graphical ones, and empirically based knowledge. But performance are limited for higher-order systems, multi-input systems or system do not have the properties assumed in classical control methods.

In contrast to the frequency domain analysis of the classical control theory, modern control theory utilizes the time-domain state space representation. It de-empiricize control system design and can present solutions to a wider range class of control problems than classical control systems.

3.1 Supervisory Controller Selection

3.1.1 Linear Quadratic Regulator (LQR)

3.1.1.1 Introduction

Optimal control is one particular type of modern control methodology, which not only possesses the ability to stabilize the system, but is supposed to be the best possible solution towards a system of a particular type.

Linear optimal control is a special category of optimal control, where the controller, and the hardware controlling device are constrained to be linear. Methods that achieve linear optimal control are termed linear quadratic (LQ) methods, and the controllers are called linear quadratic regulators (LQR).

LQR design for time invariant system largely reflects a matter of control law synthesis, summarized in [117], as follows:

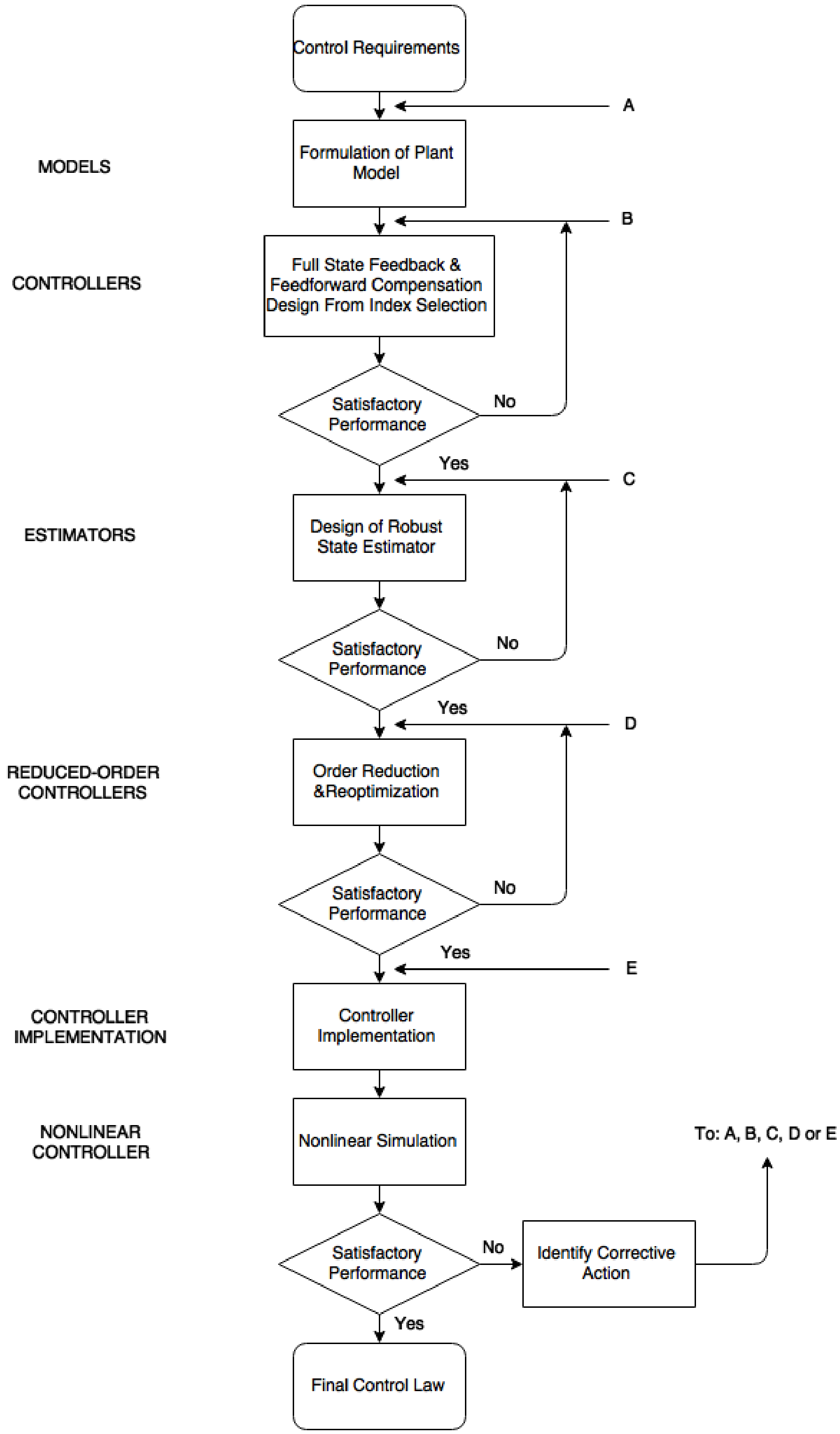

Figure 3.1 Control law synthesis process

The first step in control design is to formulate a mathematical problem, embodied in the top two blocks. The controller design process follows in next two blocks, where whether all the states can be measures becomes an index for if there is a need to proceed the estimator design described in next two blocks. Generally, for the natural properties of the plant or with the help of an estimator, the states of controller can be reduced to simplify the whole process. The final step is to implement the controller to judge if it meets the design requirements.

3.1.1.2 Finite-horizon linear time-invariant (LTI) continuous time LQR

The linear finite dimensional continuous-time systems can be represented by equations as follows:

$$\dot{x}(t) = Ax(t) + Bu(t)$$

$$y(t) = Cx(t)$$

A, B, and C are constant matrices. If their dimensions are respectively $n \times n$, $n \times m$, $n \times p$, the n vector $x(t)$ denotes the system state at time t, and the p vector $y(t)$ denotes the system output at time t.

Consider the system above with $x(t_0)$ given. Q and R are defined as constant matrix. Let $F(t)$ be a positive semidefinite matrix. Define the quadratic performance index (QPI, i.e. cost function).

$$J = \frac{1}{2} x^T(t_1)F(t_1)x(t_1) + \int_{t_0}^{t_1} (x^T(t)Qx(t) + u^T(t)Ru(t) + 2x^T(t)Nu(t))dt$$

And minimization problem as the task of finding an optimal control $u(t)$, $t \in [t_0, t_1]$, minimizing the QPI J.

Assume t_1 is finite. To solve the problem, Hamilton-Jacobi equation can be used. An outline of the problem solution is as follows:

1) The QPI J, if it exists, must be of the form $x^T(t)Px(t)$, where P is a symmetric matrix.
2) If J exists, check if P satisfies a nonlinear differential equation, i.e. a matrix Riccati equation.
3) Establish existence of J.
4) Find the optimal control.

Detailed demonstration process with linear time variant (LTV) situation can be found in [117].

The optimal control solution is given as follows:

$$u(t) = -Kx(t)$$

Where

$$K = R^{-1}(B^T P(t) + N^T)$$

And P is found by solving the continuous time Riccati differential equation:

$$A^T P(t) + P(t)A - (P(t)B + N)R^{-1}(B^T P(t) + N^T) + Q = -\dot{P}(t)$$

With the boundary condition:

$$P(t_1) = F(t_1)$$

3.1.1.2 Finite-horizon LTI discrete time LQR

For a discrete time linear system described as:

$$\mathrm{x}_{k+1} = Ax_k + Bu_k$$

With a QPI defined as:

$$J = \sum_{k=0}^{N} (x_k^T Q x_k + u_k^T R u_k + 2x_k^T N u_k)$$

The optimal control sequence minimizing the QPI is given by:

$$u_k = -F_k x_k$$

Where

$$F_k = (R + B^T P_k B)^{-1}(B^T P_k A + N^T)$$

And P_k is found iteratively backwards in time by the dynamic Riccati equation:

$$P_{k-1} = A^T P_k A - (A^T P_k B + N)(R + B^T P_k B)^{-1}(B^T P_k A + N^T) + Q$$

From terminal condition $P_N = Q$.

u_N is not define, since x is driven to its final state x_N by $Ax_{N-1} + Bu_{N-1}$.

3.1.2 Robust Linear Quadratic Regulator (RLQR)

Traditional LQR has the ability to minimize the QPI, which can be easily acquired using modern computer programs, therefore it has been widely applied in controlling linear plants [118-121]. But one disadvantage with LQR is that it lacks the robust property when parameter perturbations and external disturbances exists. To obtain a better performance, Liu et al. [122] proposed a robust LQR method for linear systems under the guideline of planes cluster approaching mode (PCAM). A nonlinear item $f_n(\cdot)$ is introduced into the control law, which, combined with the linear item, guarantees the global asymptotic stability and optimal control results when disturbance exists, which can be described as below:

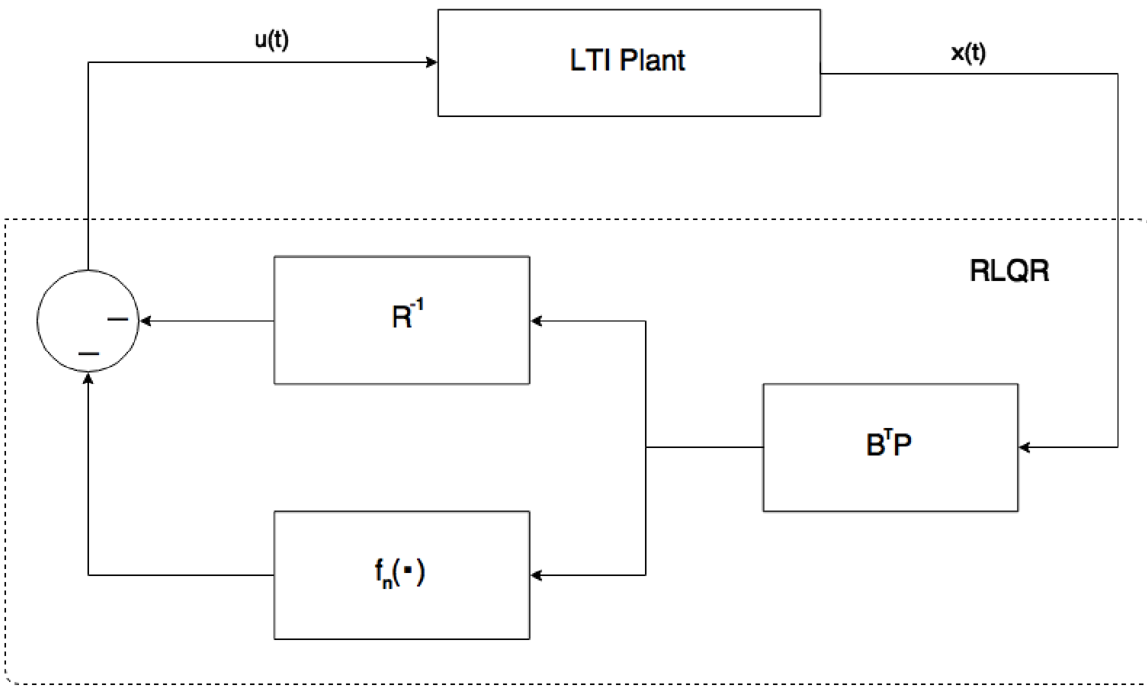

Figure 3.2 Demonstration of RLQR control law

Define a LTI system with multiple control inputs:

$$\dot{x}(t) = Ax(t) + B[u(t) + d(t)]$$

Where $x(t) \in \mathbb{R}^n$ is the state vector ($n \geq 2$), $u(t) \in \mathbb{R}^m$ is the control input vector ($m \geq 2$), $d(t) \in \mathbb{R}^m$ is the equivalent disturbances vector, $A \in \mathbb{R}^{n\times m}$ and $B \in \mathbb{R}^{n\times m}$ are constant matrices.

Assume system above is controllable, and choose the QPI with infinite time interval as:

$$J = \frac{1}{2}\int_0^\infty [x^T(t)Qx(t) + u^T(t)Ru(t)]dt$$

Where the terminal state vector $x(\infty)$ is free, $Q \in \mathbb{R}^{n\times n}$ and $R \in \mathbb{R}^{n\times n}$ are usually chosen as symmetric positive definite matrices. Without considering the equivalent disturbances in system described above, the goal of LQR is to find the optimal control to minimize QPI.

Assume $d(t)$ is norm-bounded. The control input vector $u(t)$ is designed as:

$$u(t) = u_1(t) + u_2(t)$$

The linear item in $u(t)$ is:

$$u_1 = -R^{-1}B^T Px(t)$$

And the nonlinear item is:

$$u_2(t) = \begin{cases} -\dfrac{B^T Px(t)}{\|B^T Px(t)\|}\delta(t) & B^T Px(t) \neq 0 \\ 0 & B^T Px(t) = 0 \end{cases}$$

Where $P \in \mathbb{R}^{n\times n}$ is symmetric positive definite, and $\delta(t)$ is positive.

If the following two conditions are both satisfied,

1) P is the solution of MARE:

$$A^T P + PA - PBR^{-1}B^T P + Q = 0$$

2) The gain of nonlinear item:

$$\delta(t) > \|d(t)\|_2$$

System will possess global asymptotic stability.

The LTV system control input algorithm and proof for its system stability can be found in [122].

Note that in this method, the disturbance is made equivalent to share the same matrix B with input, which may not be practical with some situations. Therefore, some modifications are made below to extend this method to more general cases.

Consider the system as follows:

$$\dot{x}(t) = Ax(t) + Bu(t) + Dd(t) \tag{3.1.1}$$

Where $x(t) \in \mathbb{R}^n$ is the state vector ($n \geq 2$), $u(t) \in \mathbb{R}^m$ is the control input vector ($m \geq 2$), $d(t) \in \mathbb{R}^m$ is the equivalent disturbances vector, $\in \mathbb{R}^{n\times m}$, $B \in \mathbb{R}^{n\times m}$ and , $D \in \mathbb{R}^{n\times m}$ are constant matrices where $B \neq D$.

Assume system above is controllable, and choose the QPI with infinite time interval as:

$$J = \frac{1}{2}\int_0^\infty [x^T(t)Qx(t) + u^T(t)Ru(t)]dt$$

Where the terminal state vector $x(\infty)$ is free, $Q \in \mathbb{R}^{n\times n}$ and $R \in \mathbb{R}^{n\times n}$ are usually chosen as symmetric positive definite matrices. Without considering the equivalent disturbances in system described above, the goal of LQR is to find the optimal control to minimize QPI.

Assume $d(t)$ is norm-bounded. The control input vector $u(t)$ is designed as:

$$u(t) = u_1(t) + u_2(t) \tag{3.1.2}$$

The linear item in $u(t)$ is:

$$u_1 = -R^{-1}B^T P x(t) \tag{3.1.3}$$

And the nonlinear item is:

$$u_2(t) = \begin{cases} -\frac{B^T P x(t)}{\|B^T P x(t)\|}\delta(t) & B^T P x = D^T P x \\ 0 & B^T P x \neq D^T P x \end{cases} \tag{3.1.4}$$

Where $P \in \mathbb{R}^{n\times n}$ is symmetric positive definite, and $\delta(t)$ is positive.

If the following two conditions are both satisfied,

3) P is the solution of MARE:

$$A^T P + PA - PBR^{-1}B^T P + Q = 0 \tag{3.1.5}$$

4) The gain of nonlinear item:

$$\delta(t) > \frac{\|B^T Px(t)\|_2}{\|D^T Px(t)\|_2}\|d(t)\|_2 \tag{3.1.6}$$

System will possess global asymptotic stability.

Note the only difference made in control law is the update of condition (3.1.6) and proof for this modification is given as follows:

Choose a Lyapunov function:

$$V = x^T Px$$

Differentiating the function above about time gets:

$$\dot{V} = \dot{x}^T Px + x^T \dot{P}x + x^T P\dot{x}$$

Substituting (3.1.1) in the function above gets:

$$\dot{V} = (Ax + Bu + Dd)^T Px + x^T \dot{P}x + x^T P(Ax + Bu + Dd)$$

Then substituting (3.1.2) in gets:

$$\dot{V} = (Ax + Bu_1)^T Px + x^T P(Ax + Bu_1) + x^T \dot{P}x + (Bu_2 + Dd)^T Px + x^T P(Bu_2 + Dd)$$

For $(Bu_2 + Dd)^T Px$ is a scalar quantity, there is:

$$(Bu_2 + Dd)^T Px = x^T P(Bu_2 + Dd)$$

Then the derivative of Lyapunov function can be simplified into:

$$\dot{V} = (Ax + Bu_1)^T Px + x^T P(Ax + Bu_1) + x^T \dot{P} x + 2x^T P(Bu_2 + Dd)$$

Which divides $\dot{V}$ into two parts:

$$f_1 = (Ax + Bu_1)^T Px + x^T P(Ax + Bu_1) + x^T \dot{P} x$$

$$f_2 = 2x^T P(Bu_2 + Dd)$$

Substituting (3.1.3) in f_1 gets:

$$f_1 = x^T \left(A^T P + PA - PBR^{-1}B^T P + \dot{P}\right)x - (B^T Px)^T R^{-1}(B^T Px)$$

R is symmetric positive definite, therefore R^{-1} exists and is also symmetric positive definite, which can be demonstrated as follows:

If R is symmetric positive definite, then all of its eigenvalues are positive, so 0 is not an eigenvalue of R. Therefore, the equation $Rx = 0$ has only the trivial solution $x = 0$ and so R is invertible. Also we have:

$$x^T Rx > 0 \qquad \text{for all nonzero } x \in C^n$$

Let $y = Rx$, and y is nonzero for x is nonzero and R is positive definite, which gives

$$y^T R^{-1} y = (Rx)^T R^{-1} Rx = x^T R^T x = x^T Rx > 0$$

For all nonzero $y \in C^n$.

Therefore R^{-1} exists and is symmetric positive definite if R is symmetric positive definite.

If condition (3.1.5) is satisfied, f_1 can be transformed into:

$$f_1 = -x^T Qx - (B^T Px)^T R^{-1} (B^T Px)$$

Obviously, $f_1 \leq 0$ always exists, and $f_1 = 0$ only when $x = 0$.

Then, substituting (3.1.4) into f_2 gives:

1) When $B^T Px = D^T Px$ (i.e. $x = 0$ for $B \neq D$), $f_2 = 0$.
2) When $B^T Px \neq D^T Px$ (i.e. $x \neq 0$), f_2 can be transformed into:

$$f_2 = (B^T Px)^T u_2 + (D^T Px)^T d \leq [(B^T Px)^T u_2 + |(D^T Px)^T d|]$$
$$= \left[-(B^T Px)^T \frac{B^T Px}{\|B^T Px\|_2} \delta + |(D^T Px)^T d| \right]$$

For $(B^T Px)^T B^T Px = \|B^T Px\|_2^2$, f_2 can be simplified as follows:

$$f_2 \leq [-\|B^T Px\|_2 \delta + |(D^T Px)^T d|]$$

Based on Cauchy-Schwarz inequality in [129]:

$$|(D^T P x)^T d| \leq \|D^T P x\|_2 \|d\|_2$$

Then f_2 can be further simplified as:

$$f_2 \leq [-\|B^T P x\|_2 \delta + \|D^T P x\|_2 \|d\|_2]$$

Therefore, if condition (3.1.6) is satisfied, we have $f_2 < 0$ and system is stable against disturbance.

In a word, $\dot{V} = f_1 + f_2 \leq 0$ always exists, and $\dot{V} = 0$ only when $x = 0$. Thus using the input (3.1.2)-(3.1.4), the system will possess global asymptotic stability.

3.1.3 Composite Nonlinear Feedback (CNF) Control

3.1.3.1 Theory Development

Every physical system in our world has nonlinearities, and many control system are sufficiently nonlinear that linear techniques can malfunction sometimes. Traditionally, when dealing with control objectives like tracking and targeting, time optimal control (TOC) is often adopted. But traditional TOC is not robust when system uncertainties and disturbance exists. To overcome the disadvantages of TOC, Chen [123] improved the theory of composite nonlinear feedback control, in which the control input consists of a linear feedback item and a nonlinear feedback one without switching elements. The linear feedback part is designed for a quick response with a closed-loop system with a small damping ratio, at the same time not to exceed the actuator limits. The nonlinear feedback part is applied to increase the damping ratio when system output approach the target reference to reduce overshoot.

Different situations are presented by Chen in [123]: 1) the state feedback case, 2) the full order measurement feedback case, 3) the reduced order measurement feedback case.

Consider the system with input saturation as follows:

$$\begin{cases} \dot{x} = Ax + Bsat(u), \qquad x(0) = x_0 \\ y = C_1 x \\ h = C_2 x \end{cases} \tag{3.1.7}$$

Where $x \in \mathbb{R}^n$, $u \in \mathbb{R}$, $y \in \mathbb{R}^p$, and $h \in \mathbb{R}$ are respectively the state, control input, measurement output and controlled output. A, B, C_1 and C_2 are appropriate dimensional constant matrices, and sat: $\mathbb{R} \to \mathbb{R}$ represents the actuator saturation defined as:

$$sat(u) = sign(u) \min\{u_{max}, |u|\}$$

With u_{max} defining the saturation level of the input. The following assumptions are required:

1) (A, B) is stabilizable;
2) (A, C_1) is detectable;

3) (A, B, C_2) is invertible and has no zeros at $s = 0$.

A. State Feedback Case

Step 1. Design a linear feedback law

$$u_L = Fx + Gr$$

Where r is the target reference and F is chosen such that 1) $A + BF$ is an asymptotically stable matrix, and 2) the closed-loop system $C_2(sI - A - BF)^{-1}B$ has certain desired properties such as a small damping ratio. F can be designed using H_∞ approaches, as well as robust and tracking technologies given in [124].

G is a scalar and given by:

$$G = -[C_2(A + BF)^{-1}B]^{-1}$$

And r is a step command input.

Step 2. Compute:

$$H := [1 - F(A + BF)^{-1}B]G$$

And let:

$$x_e := -(A + BF)^{-1}BGr$$

Given a positive definite matrix $W \in \mathbb{R}^{n\times n}$, solve the following Lyapunov equation:

$$(A+BF)'P + P(A+BF) = -W$$

For $P > 0$. Such P always exists since $A + BF$ is asymptotically stable. Then the nonlinear feedback control item $u_N(t)$ is given by:

$$u_N = \rho(r,y)B'P(x - x_e)$$

Where $\rho(r,y)$ is any non-positive function locally Lipschitz in y. The method for selecting W and $\rho(r,y)$ can be found in [124].

Step 3. The control input can be derived combining the linear and nonlinear item to form a CNF controller:

$$u = u_L + u_N = Fx + Gr + \rho(r,y)B'P(x - x_e)$$

B. Full-Order Measurement Feedback Case

Generally, full state feedback case is not practical, therefore CNF control system using measurement feedback is needed.

Step 1. A linear full order measurement feedback control law is given as follows:

$$\Sigma_F := \begin{cases} \dot{x}_v = (A + KC_1)x_v - Ky + Bsat(u_L) \\ u_L = F(x_v - x_e) + Hr \end{cases}$$

Where r is the reference input and x_v is the state of the controller. F and K are gain matrices and are designed such that $A + BF$ and $A + KC_1$ are asymptotically stable and the closed-loop system has the desired properties. G and H are given in case A.

Step 2. Given a positive definite matrix $W \in \mathbb{R}^{n \times n}$, solve the following Lyapunov equation with $P > 0$:

$$(A + BF)'P + P(A + BF) = -W$$

Step 3. The linear control item is combine to form the following CNF control law.

$$\begin{cases} \dot{x}_v = (A + KC_1)x_v - Ky + Bsat(u) \\ u = F(x_v - x_e) + Hr + \rho(r, y)B'P(x - x_e) \end{cases}$$

Where $\rho(r, y)$ is any non-positive function locally Lipschitz in y. x_e is defined in case A.

C. Reduced-Order Measurement Feedback Case

In general, it's not necessary to estimate all the measurable states in case B. Therefore a dynamic controller with dynamical order is designed.

Step 1. Assume C_1 is in the form of:

$$C_1 = [I_p \quad 0]$$

The system (3.1.7) in can be rewritten as:

$$\begin{cases} \begin{pmatrix} \dot{x}_1 \\ \dot{x}_2 \end{pmatrix} = \begin{bmatrix} A_{11} & A_{12} \\ A_{21} & A_{22} \end{bmatrix} \begin{pmatrix} x_1 \\ x_2 \end{pmatrix} + \begin{bmatrix} B_1 \\ B_2 \end{bmatrix} sat(u) \\ y = [I_p \quad 0] \begin{pmatrix} x_1 \\ x_2 \end{pmatrix} \\ h = C_2 \begin{pmatrix} x_1 \\ x_2 \end{pmatrix}, \qquad x_0 = \begin{pmatrix} x_1 \\ x_2 \end{pmatrix} \end{cases}$$

Let F be chosen such that 1) $A + BF$ is asymptotically stable and 2) $C_2(sI - A - BF)^{-1}B$ has desired properties. And let K_R be chosen such that $A_{22} + K_R A_{12}$ is asymptotically stable. F and K_R can be designed using appropriate control technique described in case A.

Step 2. Given a positive definite matrix $W \in \mathbb{R}^{n\times n}$, solve the following Lyapunov equation with $P > 0$:

$$(A + BF)'P + P(A + BF) = -W$$

Given another positive definite matrix $W_R \in \mathbb{R}^{(n-p)\times(n-p)}$, with:

$$W_R > F_2' B' P W^{-1} P B F_2$$

Solve the following Lyapunov equation with $Q_R > 0$:

$$(A_{22} + K_R A_{12})' Q_R + Q_R (A_{22} + K_R A_{12}) = -W_R$$

Step 3. Divide F referring to x_1 and x_2:

$$F = [F_1 \quad F_2]$$

The reduced-order CNF controller law can be derived as:

$$\begin{cases} \dot{x}_v = (A_{22} + K_R A_{12})x_v + (B_2 + K_R B_1 sat(u) + [(A_{21} + K_R A_{11}) - (A_{22} + K_R A_{12})K_R]y \\ u = F\left[\begin{pmatrix} y \\ x_v - K_R y \end{pmatrix} - x_e\right] + Hr + \rho(r,y)B'P\left[\begin{pmatrix} y \\ x_v - K_R y \end{pmatrix} - x_e\right] \end{cases}$$

Where $\rho(r, y)$ is any non-positive function locally Lipschitz in y. And H and x_e are defined in case A.

Theorems and proves can be accessed in [124].

For a summary, an illustration of CNF control strategy in different cases can be described as follows, which also works for RCNF to be introduced in the next section:

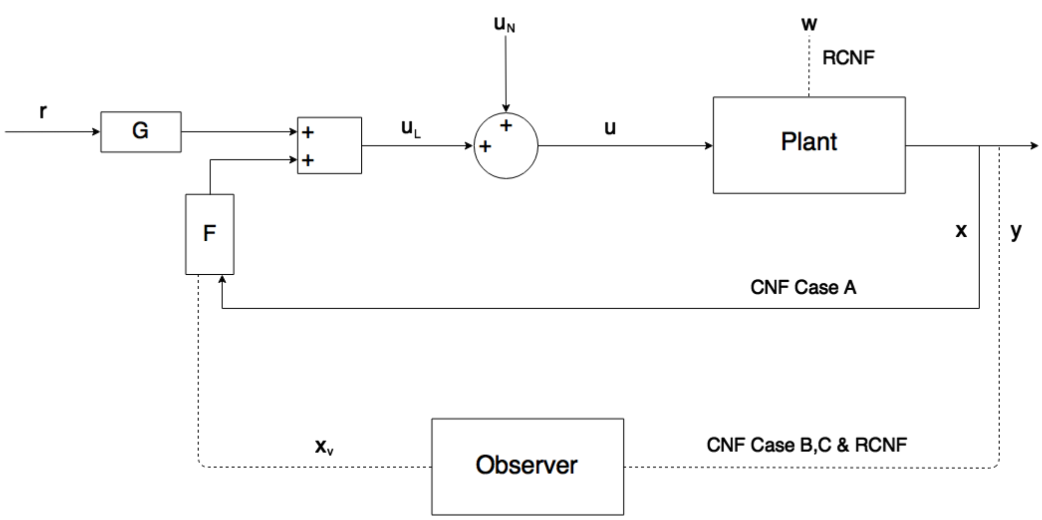

Figure 3.3 Illustration of CNF control strategy in different cases

3.1.3.2 Robust Composite Nonlinear Feedback (RCNF) Control

Though the fact that the CNF can track the reference fairly quick and yield a better performance than the time optimal control, it lack a mechanism to compensate disturbance. Thus a robust version of CNF is proposed by Cheng and Hu in [125], which treats the unknown disturbance as an extended state variable to be augmented with the plant. The new approach is claimed to not only retain the quick response property of the original CNF but have the ability to reject disturbance and uncertainties. Their work is based on [7], where the disturbance is limited to a constant.

Consider a linear system with an input saturation and an unknown bounded disturbance with a limit rate of change as follows:

$$\begin{cases} \dot{x} = Ax + Bsat(u) + Ew \qquad x(0) = x_0 \\ y = C_1 x \\ h = C_2 x \end{cases}$$

Where $x \in \mathbb{R}^n$, $u \in \mathbb{R}$, $y \in \mathbb{R}^p$, $h \in \mathbb{R}$ and $w \in \mathbb{R}$ are respectively the state, control input, measurement output and controlled output and disturbance of the system. A, B, C_1, C_2 and E are appropriate dimensional constant matrices, and sat: $\mathbb{R} \to \mathbb{R}$ represents the actuator saturation defined as:

$$sat(u) = sign(u)\min\{u_{max}, |u|\}$$

With u_{max} defining the saturation level of the input. The following assumptions are required:

1) (A, B) is stabilizable;
2) (A, C_1) is detectable;
3) (A, B, C_2) is invertible and has no zeros at $s = 0$;
4) w is bounded unknown disturbance with limited variation rate;
5) h is a subset of y, i.e. h is also measurable.

Take disturbance w as an additional state and augment it into the system above as follows:

$$\begin{cases} \dot{\bar{x}} = \bar{A}x + \bar{B}sat(u) + E\dot{w} \\ y = \bar{C}_1\bar{x} \\ h = \bar{C}_2\bar{x} \end{cases} \tag{3.1.8}$$

Where

$$\dot{\bar{x}} = \begin{pmatrix} x \\ w \end{pmatrix}, \bar{A} = \begin{bmatrix} A & E \\ 0 & 0 \end{bmatrix}, \bar{B} = \begin{bmatrix} B \\ 0 \end{bmatrix}, N = \begin{bmatrix} 0 \\ 1 \end{bmatrix}$$

$$\bar{C}_1 = [C_1 \quad 0], \bar{C}_2 = [C_2 \quad 0]$$

Where $(\bar{A}, \bar{C}_1)$ should be detectable.

Next, the design of RCNF control law will be divided into four steps.

Step 1. Design a linear state feedback control law with disturbance compensation term as below:

$$u_L = [F \quad F_w] \binom{x}{w} + Gr$$

Where F is chosen such that 1) $A + BF$ is an asymptotically stable matrix, and 2) the closed-loop system $C_2(sI - A - BF)^{-1}B$ has should have a dominant pair with a small damping ratio. G is a scalar and given by:

$$G = -[C_2(A + BF)^{-1}B]^{-1}$$

And F_w is chosen as:

$$F_w = G[C_2(A + BF)^{-1}E]$$

Where (A, B, C_2) is assumed to have no invariant zeros at $s = 0$.

Step 2. Given a positive definite matrix $W \in \mathbb{R}^{n \times n}$, solve the following Lyapunov equation with $P > 0$:

$$(A + BF)'P + P(A + BF) = -W$$

Solution is always existent as $A + BF$ is asymptotically stable. Define:

$$\begin{cases} G_e := -(A + BF)^{-1}BG \\ G_w := (A + BF)^{-1}(BF_w + E) \\ x_e := G_e r + G_w w \end{cases}$$

The nonlinear feedback portion u_N is given by:

$$u_N = \rho(e)F_n(x - x_e)$$

Where $F_n = B'P$ and $\rho(e)$ is a smooth, non-positive function of $|e|$ with $e = h - r$. The method for selecting W and $\rho(e)$ is given in [125].

Step 3. Assume C_1 is already in the following form,

$$C_1 = [I_p \quad 0]$$

The first p element of state vector, denoted by x_1 is already available and need not to be estimated. Only the remaining $n - p$ elements of state vector, denoted by x_2, and the unknown disturbance w. Define:

$$\bar{x}_2 = \begin{pmatrix} x_2 \\ w \end{pmatrix}$$

Then the matrices in (3.1.8) can be rewritten as:

$$\bar{A} = \begin{bmatrix} A_{11} & A_{12} \\ A_{21} & A_{22} \end{bmatrix}, \bar{B} = \begin{bmatrix} B_1 \\ B_2 \end{bmatrix}, N = \begin{bmatrix} 0 \\ N_1 \end{bmatrix}$$

Choose the proper matrix $K \in \mathbb{R}^{(n-p+1)\times p}$ such that the poles of $A_{22} + KA_{12}$ are placed in proper location in the open left half plane. Then the reduce observer is given as follows:

$$\begin{cases} x_v = A_v x_v + Bsat(u) + B_y \cdot y \\ \begin{pmatrix} \hat{x}_2 \\ \widehat{w} \end{pmatrix} = x_v - Ky \end{cases} \tag{3.1.9}$$

Where

$$\begin{cases} A_v = A_{22} + KA_{12} \\ B_u = B_2 + KB_1 \\ B_y = A_{21} + KA_{11} - (A_{22} + KA_{12})K \end{cases}$$

Step 4. Combine the linear feedback part with nonlinear feedback part, the RCNF control law is given as:

$$\begin{cases} u = [F \quad F_w] \begin{pmatrix} y \\ \hat{x}_2 \\ \widehat{w} \end{pmatrix} + Gr + \rho(e) F_n \left[\begin{pmatrix} y \\ \hat{x}_2 \end{pmatrix} - \hat{x}_e \right] \\ \hat{x}_e \coloneqq G_e r + G_w \widehat{w} \end{cases}$$

Where $\hat{x}_2$ and $\widehat{w}$ are given in (3.1.9).

3.2 Vehicle Level Controller Selection

3.2.1 Proportional-Integral-Derivative (PID) Control

PID is particularly rather a primitive and simplified implementation of basic principle in error-based feedback control, where the error e between reference v and plant output y as well as its derivative and integration are used in a linear combination to produce the control law:

$$u = K_P e + K_I \int_0^t e d\tau + K_D \frac{de}{dt}$$

PID is widely applied in industry for its properties of model independence and easy tuning and configuration. PID is effective in such a way, proposed in [126]:

Let the system possesses the form as follows:

$$\begin{cases} \dot{x}_1 = x_2 \\ \dot{x}_2 = a_1 x_1 + a_2 x_2 + bu \\ y = x_1 \end{cases} \tag{3.2.1}$$

And let:

$$\begin{cases} e = v - y = v - x_1 = e_1 \\ \dot{e}_1 = -\dot{x}_1 = e_2 \\ \ddot{e} = -\ddot{x}_1 \end{cases}$$

And the error dynamic can be seen as:

$$\begin{cases}\dot{e}_1 = e_2\\ \dot{e}_2 = a_1e_1 + a_2e_2 - a_1v - bu\end{cases}$$

Denoting $e_0 = \int_0^t ed\tau$, then $\dot{e}_0 = e = e_1$, and u becomes

$$u = k_0e_0 + k_1e_1 + k_2e_2$$

Then the error equation can be rewritten as:

$$\begin{cases}\dot{e}_0 = e_1e_2\\ \dot{e}_1 = e_2\\ \dot{e}_2 = -bk_0\left(e_0 + \dfrac{a_1}{bk_0}v\right) + (a_1 - bk_1)e_1 + (a_2 - bk_2)e_2\end{cases}$$

Which is asymptotically stable if:

$$\begin{cases}bk_0 > 0, (bk_1 - a_1) > 0, (bk_2 - a_2) > 0\\ (bk_1 - a_1)(bk_2 - a_2) > bk_0\end{cases}$$

That is, $e_1 = e = v - x_1 \to 0$, or $x_1 \to v$, is met if the gains k_0, k_1, and k_2 are selected to satisfy the equation above for the given range of $a_1, a_2, b \neq 0$.

It is obvious that for most plans of form (3.2.1), a set of PID gains can be easily found.

3.2.2 Active Disturbance Rejection Control (ADRC)

3.2.2.1 Theory Development

Although PID possesses a lot of advantages, there still exist some issues, as stated in [126].

1) Set point is often given as a step function, not appropriate for most dynamics systems because it requires the control signal to make a sudden jump.
2) PID is often implemented without the D part because of the noise sensitivity.
3) The weight sum K_P, K_I and K_D are simple but may not be the optimal solution.
4) The integral term, while critical to rid of steady state error, introduces other problems such as saturation and reduced stability margin due to phase lag.

These limitations prompt Han to develop a novel control method named ADRC proposed in [126].

To avoid these four issues stated above, four solutions are given correlatively by Chen.

A. Set point Jump

A time optimal solution is given and transferred into discrete form for avoidance of numerical error while implemented in discrete time situation.

For the discrete time system:

$$\begin{cases} v_1 = v_1 + hv_2 \\ v_2 = v_2 + hu \end{cases} \qquad |u| \le r$$

The time optimal solution is obtained as:

$$u = fhan(v_1 - v, v_2, r_0, h_0)$$

Where h is the sampling period, r_0 and h_0 are controller parameters, and $fhan(v_1, v_2, r_0, h_0)$ is given by:

$$\begin{cases} d = h_0 r_0^2, \;\; a_0 = h_0 v_2, \;\; y = v_1 + a_0 \\ a_1 = \sqrt{d(d + 8|y|)} \\ a_2 = a_0 + sign(y)(a_1 - d)/2 \\ s_y = (sign(y + d) - sign(y - d))/2 \\ a = (a_0 + y - a_2)s_y + a_2 \\ s_a = (sign(a + d) - sign(a - d))/2 \\ fhan = -r_0\left(\dfrac{a}{d} - sign(a)\right)s_a - r_0 sign(a) \end{cases}$$

B. Tracking Differentiator

PID is commonly implemented that a differentiation of the input v is obtained by approximation which is sensitive to noise. Thus following approximation is proposed:

$$\dot{v}(t) \approx \frac{v(t - \tau_1) - v(t - \tau_2)}{\tau_2 - \tau_1}$$

Which can be implemented using the first order transfer function.

$$w_1(s) = \frac{1}{\tau_2 - \tau_1}\left(\frac{1}{\tau_1 s + 1} - \frac{1}{\tau_2 s + 1}\right), \quad \tau_2 > \tau_1 > 0$$

C. Nonlinear Feedback Combination

An alternative nonlinear function is proposed as:

$$\begin{cases} fal(e,a,\delta) = \begin{cases} \dfrac{e}{\delta^{1-\alpha}}, & |x| \le \delta \\ |e|^{\alpha} sign(e), & |x| \ge \delta \end{cases} \\ fhan(x_1, x_2, r, h_0) \end{cases}$$

That sometimes provides better results in practice as claimed in [126].

D. Total Disturbance Estimation and Rejection via ESO

Consider the system:

$$\begin{cases} \dot{x}_1 = x_2 \\ \dot{x}_2 = f(x_1, x_2, w(t), t) + bu \\ y = x_1 \end{cases} \tag{3.2.2}$$

If $F(t) = f(x_1, x_2, w(t), t)$ is treated as an additional state variable $x_3 = F(t)$, and let $\dot{F}(t) = G(t)$ while $G(t)$ is unknown, the system can be rewritten as:

$$\begin{cases} \dot{x}_1 = x_2 \\ \dot{x}_2 = x_3 + bu \\ \dot{x}_3 = G(t) \\ y = x_1 \end{cases}$$

Which is always observable. After constructing an extended state observer and implementing it in discrete form with a sampling period of h, we obtain:

$$\begin{cases} e = z_1 - y \\ fe = fal(e, 0.5, \delta), \;\; fe_1 = fal(e, 0.25, \delta) \\ z_1 = z_1 + hz_2 - \beta_{01} e \\ z_2 = z_2 + h(z_3 + bu) - \beta_{02} fe \\ z_3 = z_3 - \beta_{03} fe_1 \end{cases}$$

The observer gains can be selected as:

$$\beta_{01} = 1, \;\; \beta_{02} = \frac{1}{2h^{0.5}}, \;\; \beta_{03} = \frac{2}{5^2 h^{1.2}}$$

The control input u and system output y are the inputs to ESO, allowing the control law $(u_0 - F(t))/b$ to reduce (3.2.2) to a cascade integral form of:

$$\begin{cases} \dot{x}_1 = x_2 \\ \dot{x}_2 = u_0 \\ y = x_1 \end{cases}$$

Which can be easily controlled by a PD controller.

By combining the four solutions together, ADRC can be derived, and the topology is shown in figure below.

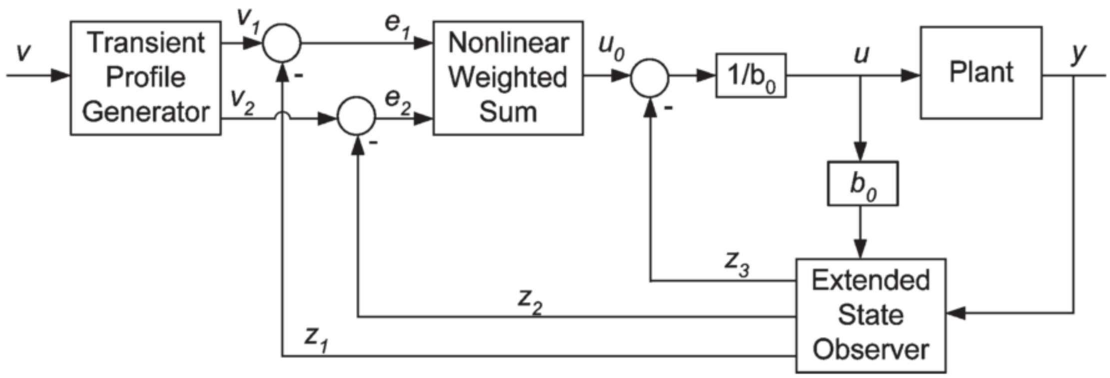

Figure 3.4 ADRC topology

There are four tuning parameters r, c, h_1 and b_0, respectively denote amplification coefficient, damping coefficient, precision coefficient and rough approximation of the coefficient b.

The ADRC control law can be formed as:

$$
\begin{cases}
fv = fhan(v_1 - v, v_2, r_0, h) \\
v_1 = v_1 + hv_2 \\
v_2 = v_2 + hfv \\
e = z_1 - y \\
fe = fal(e, 0.5, h), \quad fe_1 = fal(e, 0.25, h) \\
z_1 = z_1 + hz_2 - \beta_{01} e \\
z_2 = z_2 + h(z_3 + b_0 u) - \beta_{02} fe \\
z_3 = z_3 - \beta_{03} fe_1 \\
e_1 = v_1 - z_1, \quad e_2 = v_2 - z_2 \\
u = -\dfrac{fhan(e_1, ce_2, r, h_1)}{b_0}
\end{cases}
$$

Two alternative control law can be selected as:

$$\begin{cases} u = -\dfrac{\beta_1 e_1 + \beta_2 e_2 - z_3}{b_0} \\ u = \dfrac{\beta_1 fal(e_1, \alpha_1, \delta) + \beta_2 fal(e_1, \alpha_1, \delta) - z_3}{b_0}, \quad 0 < \alpha_1 < 1 < \alpha_2 \end{cases}$$

Proof and detailed information can be found in [126].

3.2.2.2 A Simplified Form of ADRC

Though ADRC seems to be a good alternative to PID control, its complicated form causes some problems in practical implementation. Hence, a simplified version of ADRC is proposed by Gao in [127], which greatly reduces the difficulty to for designers.

Consider the system with a form of:

$$\begin{cases} \dot{x} = Ax + Bu + Eh \\ y = Cx \end{cases}$$

With

$$A = \begin{bmatrix} 0 & 1 & 0 \\ 0 & 0 & 1 \\ 0 & 0 & 0 \end{bmatrix}, B = \begin{bmatrix} 0 \\ b \\ 0 \end{bmatrix}, C = \begin{bmatrix} 1 & 0 & 0 \end{bmatrix}, E = \begin{bmatrix} 0 \\ 0 \\ 1 \end{bmatrix}$$

Design a state observer as follows:

$$\begin{cases} \dot{z} = Az + Bu + L(y - \hat{y}) \\ \hat{y} = Cz \end{cases}$$

With the observer gain $L = [\beta_1, \beta_2, \beta_3]^T$ selected appropriately, the observer can estimate the state of the system above.

To simplify the tuning process, the observer gains could be parameterized as:

$$L = [3\omega_0, 3\omega_0^2, w_0^3]^T$$

While the bandwidth ω_0 is the only tuning parameter.

The control law can be rewritten as:

$$\begin{cases} u = \dfrac{-z_3 + u_0}{b} \\ u_0 = k_p(r - z_1) - k_d z_2 \end{cases}$$

Where r is the set point. The controller tuning can further be simplified with $k_d = 2\omega_c$, and $k_p = \omega_c^2$. ω_c is the closed-loop bandwidth proposed by Gao in [128]. The control law can be illustrated more explicitly by the diagram as follows:

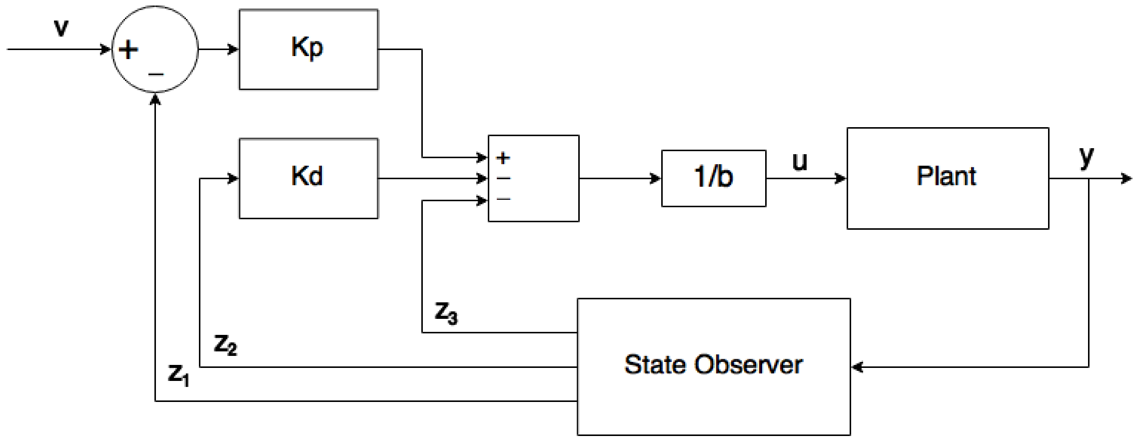

Figure 3.5 Simplified ADRC topology

Therefore, a simplified ADRC is proposed, named parameterized linear ADRC or LADRC. For stability analysis or other detailed proof, please refer to [127].

CHAPTER 4
SYSTEM MODELING AND SIMULATION

4.1 Spacing Policy

As mentioned in Chapter 2, the design process of ACC system usually begins with the selection of spacing policy, which refers to the desired steady state distance between two successive vehicles. Policies such as constant distance, constant time headway (CTH), constant safety factor, constant stability and constant acceptance were proposed as different methodology, where the CTH is chosen by automakers as well as a lot of researchers to implement in academic or practical activities.

In CTH theory, with respect to inter vehicular longitudinal dynamics, two state variables are normally defined:

$$\begin{cases} \Delta d = d - d_{des} \\ \Delta v = v_p - v_f \end{cases} \quad (4.1.1)$$

Where Δd, d, d_{des}, Δv, v_p and v_f respectively denote the clearance error, actual distance between two vehicles, desired inter vehicular distance, speed error, the proceeding vehicle speed and the following vehicle speed.

d_{des} is defined as:

$$d_{des} = \tau_h v_f + d_0$$

Where τ_h is the constant time headway, d_0 denotes the pre-set stopping distance. Note τ_h is normally set around $2.5s$ for heavy duty vehicles like trucks, but should be chosen smaller for passenger vehicles.

The clearance error Δd is typically considered with the first priority and should always converge to 0 if possible in control design to maintain a safe distance between proceeding vehicle and following vehicle.

Generally, CTH is an effective and simple method, where the speed of the flowing vehicle itself is considered, therefore providing a more reliable policy over a constant distance.

In this thesis, the constant time headway τ_h is chosen as $0.5s$, and the preset stopping distance d_0 is selected as $5m$, such that the desired inter vehicular distance follows:

$$d_{des} = \begin{cases} 20\ m & v_f = 30m/s\ (108km/h) \\ 10\ m & v_f = 10m/s\ (36km/h) \end{cases}$$

Which corresponding to the situations of low traffic density and traffic congestion respectively.

4.2 System Modeling

As mentioned in Chapter 2, hierarchical architecture is adopted for ACC controllers [58], including the supervisory controller (also named upper level controller or ACC controller) and the vehicle level controller (also named lower level controller or longitudinal controller.

The supervisory controller firstly determines the kinematics of the vehicle to fulfil the control objectives. Then the vehicle level controller receives signal from supervisory controller to adjust throttle (or motor input if applied to an electric vehicle) and/or brake command to track the desired the kinematics [4,58] outputted by the supervisory controller.

These two controllers are combined to stabilize the system and optimize the control results. A topology, is give below, which describes the relationship between different levels of control system.

This topology is specially drafted for this thesis, for normal ACC systems are implemented in gasoline vehicles.

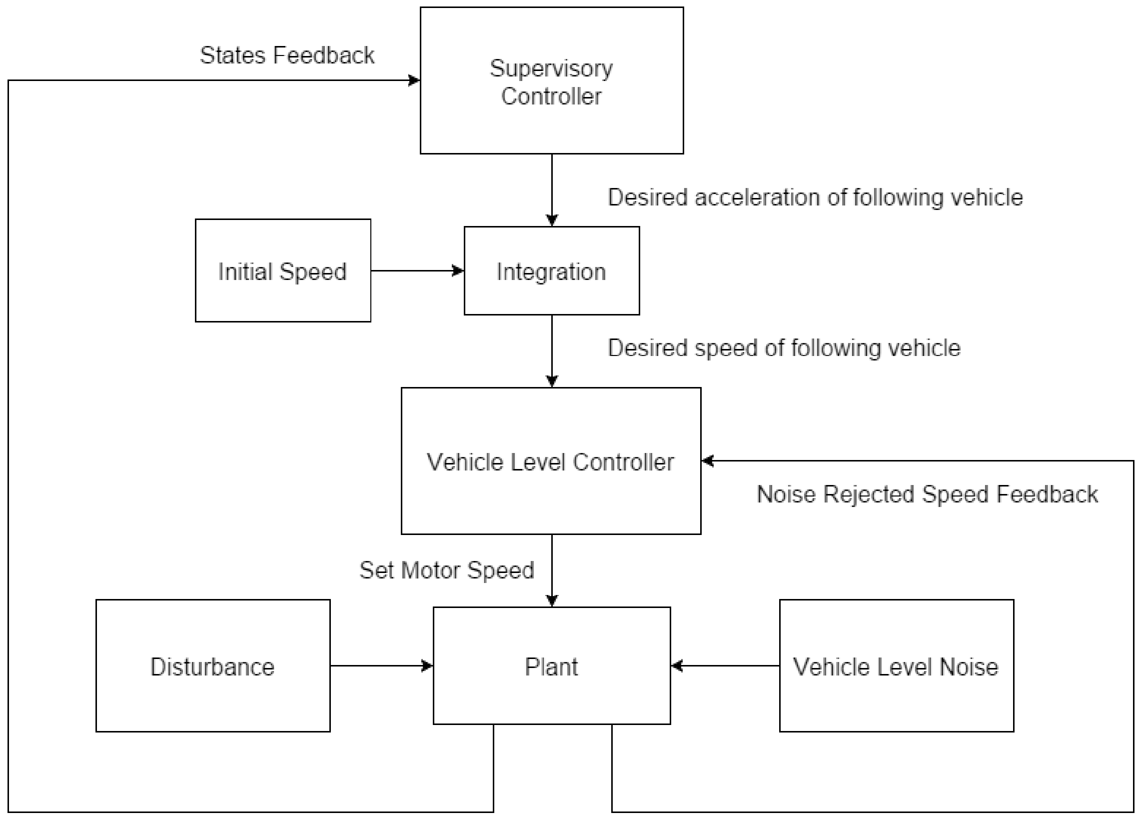

Figure 4.1 Hierarchical architecture of control system in this thesis

In a complete control process, the supervisory controller collects data of system states from the sensors in vehicle plant and calculates the desired acceleration. This signal is integrated as desired speed of following vehicle and is sent to vehicle level controller as reference. The vehicle level controller calculates the desired speed command according to reference and the speed feedback to reject noise in vehicle plant, then regulates motor speeds in plant using PWM method.

In the system modeling process, which will be discussed later in this section, the proceeding vehicle speed is selected as the disturbance, which is commonly used in ACC system design. And the vehicle level controller is selected to solve the problem of noise.

In this chapter, the supervisory controllers and vehicle level controller are modelled and simulated separately, which will be combined together to perform the experiment in Chapter 5.

For accuracy, the low level controller and plant are not neglected but simplified as a time delay transfer function to denote their properties in the supervisory controller design process. Which can be described as:

$$a_f = \frac{K_L}{T_L s + 1} a_{fdes}$$

Where K_L denotes the system gain, which should be set to 1 to comply the relationship between a_f and a_{fdes} , T_L denotes the time constant, a_f and a_{fdes} denotes the actual acceleration and the desired acceleration of following vehicle respectively. For a summary, these algorithms can be augmented into a diagram to illustrate the relationship mutually as follows:

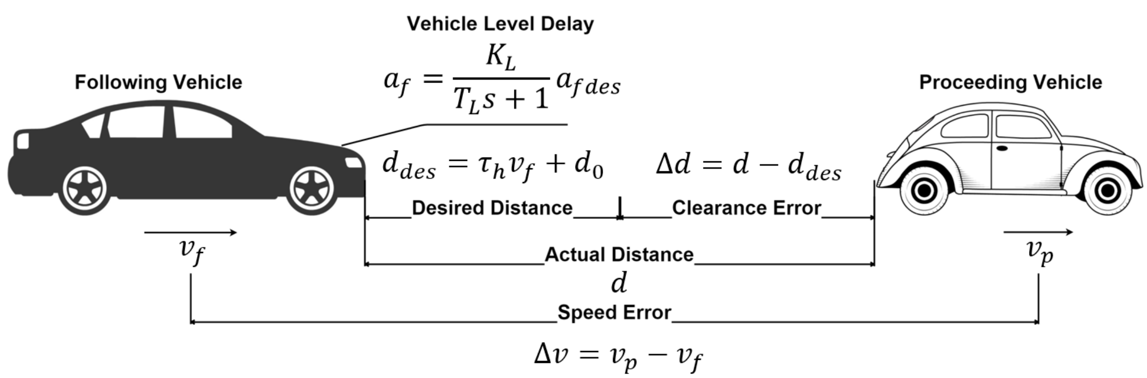

Figure 4.2 Illustration of spacing policy and vehicle level delay

Consider the system with the form:

$$\dot{x} = Ax + Bsat(u) + Ew$$

$$y = C_1 x, \;\; h = C_2 x$$

$$x = [\Delta d \quad \Delta v \quad a_f]^T$$

$$sat(u) = sign(u) \min\{u_{max}, |u|\}$$

Where $x \in \mathbb{R}^n$ denotes the state vector, $y \in \mathbb{R}^p$ and $h \in \mathbb{R}$ are measurable and controlled output, $sat(u)$ denotes the control input with saturation referring to control input $u \in \mathbb{R}$, u_{max} defining the saturation level of the input and $w \in \mathbb{R}$ denotes the disturbance. Δd and Δv are defined in (4.1.1).

Let:

$$u = a_{fdes}, \;\; w = a_p$$

Where a_p is the acceleration of the preceding vehicle.

The matrices can be derived as:

$$A = \begin{bmatrix} 0 & 1 & -\tau_h \\ 0 & 0 & -1 \\ 0 & 0 & -\frac{1}{T_L} \end{bmatrix}, \;\; B = \begin{bmatrix} 0 \\ 0 \\ \frac{1}{T_L} \end{bmatrix}, \;\; E = \begin{bmatrix} 0 \\ 1 \\ 0 \end{bmatrix}$$

$$C_1 = \begin{bmatrix} 1 & 0 & 0 \\ 0 & 1 & 0 \end{bmatrix}, \;\; C_2 = \begin{bmatrix} 1 & 0 & 0 \end{bmatrix}$$

Where A, B, E, C_1, C_2 are all constant matrices, therefore it is a LTI system.

4.2.1 LQR Control Strategy Configuration

For the system given in Chapter 4.2, a conventional LQR controller can be design as:

$$u = -Kx$$

$$K = R^{-1}B^T P$$

With the QPI is given by:

$$J = \frac{1}{2}\int_{t_0}^{t_f} [x^T(t)Qx(t) + u^T(t)Ru(t)]dt$$

Where Q and R denote the weight factor for QPI and will be configured in simulation and experiment.

P is found by solving the continuous time Riccati differential equation

$$A^T P + PA - PBR^{-1}B^T P + Q = 0$$

With Condition I, which is proposed and will be further explained in simulation section later, where parameters are selected as:

$$\tau_h = 0.5,\ \ d_0 = 5,\ \ T_L = 0.1,\ \ K_L = 1,\ \ Q = \begin{bmatrix} 10 & 0 \\ 0 & 1 \end{bmatrix},\ \ R = 1 \qquad (4.1.2)$$

P can be calculated:

$$P = \begin{bmatrix} 5.8204 & 1.1939 & -0.3162 \\ 1.1939 & 1.4756 & -0.1841 \\ -0.3162 & -0.1841 & 0.0298 \end{bmatrix}$$

Note, this condition, with parameters selected as in (4.1.2), will be reused to calculate relative values and matrices in RLQR and RCNF later for demonstration. But more conditions with different values for u_{max}, T_L, Q and R will be applied in simulations, and new values will be updated automatically but not stated again in thesis.

4.2.2 RLQR Control Strategy Configuration

Also consider the system given in 4.2, the RLQR control input is designed as:

$$u(t) = u_1(t) + u_2(t)$$

The linear item in $u(t)$ is:

$$u_1 = -R^{-1}B^T P x(t)$$

And the nonlinear item is:

$$u_2(t) = \begin{cases} -\dfrac{B^T P x(t)}{\|B^T P x(t)\|}\delta(t) & B^T P x = D^T P x \\ 0 & B^T P x \neq D^T P x \end{cases}$$

Where $P \in \mathbb{R}^{n\times n}$ is symmetric positive definite, and $\delta(t)$ is positive, which is selected to satisfy:

$$\delta(t) > \frac{\|B^T P x(t)\|_2}{\|D^T P x(t)\|_2}\|d(t)\|_2$$

Since the RLQR can be regarded as a traditional LQR control input with an additional nonlinear item, P carries the same values as the one in LQR mentioned previous section.

4.2.3 RCNF Control Strategy Configuration

Consider the system proposed in 4.2, follow the steps described in section 3.1.3.2 to design a RCNF controller.

Step 1. Design a linear state feedback control law with disturbance compensation term as below:

$$u_L = [F \quad F_w]\begin{pmatrix} x \\ w \end{pmatrix} + Gr$$

Where F is chosen such that 1) $A + BF$ is an asymptotically stable matrix, and 2) the closed-loop system $C_2(sI - A - BF)^{-1}B$ has should have a dominant pair with a small damping ratio.

The poles to be placed are selected as:

$$Poles_1 = [-5 + 0.1i \quad -5 - 0.1i \quad -2];$$

Such that:

$$F = [5.0020 \quad 2.0000 \quad -0.2000]$$

G is a scalar and given by:

$$G = -[C_2(A + BF)^{-1}B]^{-1} = -5.0020$$

And F_w is calculated as:

$$F_w = G[C_2(A + BF)^{-1}E] = 0.2000$$

Step 2. Given a positive definite matrix $W \in \mathbb{R}^{n \times n}$, solve the following Lyapunov equation with $P > 0$:

$$(A + BF)'P + P(A + BF) = -W$$

Where W is chosen as:

$$\begin{bmatrix} 0.01 & 0 & 0 \\ 0 & 0.01 & 0 \\ 0 & 0 & 0.01 \end{bmatrix}$$

And P is derived:

$$P = \begin{bmatrix} 0.0341 & 0.0079 & -0.0001 \\ 0.0079 & 0.0132 & -0.0006 \\ -0.0001 & -0.0006 & -0.0005 \end{bmatrix}$$

Define:

$$\begin{cases} G_e \coloneqq -(A+BF)^{-1}BG \\ G_w \coloneqq (A+BF)^{-1}(BF_w+E) \\ x_e \coloneqq G_e r + G_w w \end{cases}$$

Then G_e and G_w are given by:

$$G_e = \begin{bmatrix} 1 \\ 0 \\ 0 \end{bmatrix}, \quad G_w = \begin{bmatrix} 0 \\ 0.5000 \\ 1.0000 \end{bmatrix}$$

r is the reference and should be chosen as 0 to make Δd converged to 0 all the time.

The nonlinear feedback portion u_N is given by:

$$u_N = \rho(e) F_n (x - x_e)$$

Where $F_n = B'P = [-0.0010 \quad -0.0064 \quad 0.0047]$

$\rho(e)$ is a smooth, non-positive function of $|e|$ with $e = h - r$ as follows:

$$\rho(e) = -\beta e^{-\alpha\alpha_0|e|} = -\beta e^{-\alpha\alpha_0|h|}$$

With $r = 0$ and:

$$\alpha_0 = \begin{cases} \dfrac{1}{|e_0|} & if\ e(0) \neq 0 \\ 1 & if\ e(0) = 0 \end{cases}$$

Where:

$$e_0 = C_2 x(0)$$

α and β are chosen as:

$$\alpha = 10, \;\; \beta = 20$$

Step 3. Assume C_1 is already in the following form,

$$C_1 = [I_p \quad 0]$$

The first p element of state vector, denoted by x_1 is already available and need not to be estimated. Only the remaining $n - p$ elements of state vector, denoted by x_2, and the unknown disturbance w. Define:

$$\bar{x}_2 = \begin{pmatrix} x_2 \\ w \end{pmatrix}$$

Then the matrices in (3.1.8) can be rewritten as:

$$\bar{A} = \begin{bmatrix} A_{11} & A_{12} \\ A_{21} & A_{22} \end{bmatrix}, \bar{B} = \begin{bmatrix} B_1 \\ B_2 \end{bmatrix}, N = \begin{bmatrix} 0 \\ N_1 \end{bmatrix}$$

Where matrices are derived as:

$$A_{11} = \begin{bmatrix} 0 & 1 \\ 0 & 0 \end{bmatrix}, A_{12} = \begin{bmatrix} -0.5000 & 0 \\ -1.0000 & 1.0000 \end{bmatrix}, A_{21} = \begin{bmatrix} 0 & 0 \\ 0 & 0 \end{bmatrix}, A_{22} = \begin{bmatrix} -10 & 0 \\ 0 & 0 \end{bmatrix}$$

$$B_1 = \begin{bmatrix} 0 \\ 0 \end{bmatrix}, \quad B_2 = \begin{bmatrix} 10 \\ 0 \end{bmatrix}, \quad N_1 = \begin{bmatrix} 0 \\ 1 \end{bmatrix}$$

Choose the proper matrix $K \in \mathbb{R}^{(n-p+1)\times p}$ such that the poles of $A_{22} + KA_{12}$ are placed in proper location in the open left half plane.

Poles are chosen as:

$$Poles_2 = [-5 + 0.1i \quad -5 - 0.1i]$$

Then the reduced order observer is given as follows:

$$\begin{aligned} x_v &= A_v x_v + Bsat(u) + B_y \cdot y \\ \begin{pmatrix} \hat{x}_2 \\ \hat{w} \end{pmatrix} &= x_v - Ky \end{aligned}$$

Where:

$$A_v = A_{22} + KA_{12} = \begin{bmatrix} -5.2000 & 0.2000 \\ 9.7500 & -4.800 \end{bmatrix}$$

$$B_u = B_2 + KB_1 = \begin{bmatrix} 10 \\ 0 \end{bmatrix}$$

$$B_y = A_{21} + KA_{11} - (A_{22} + KA_{12})K = \begin{bmatrix} -50.0200 & -8.0000 \\ 49.9800 & -34.8900 \end{bmatrix}$$

Step 4. Combine the linear feedback part with nonlinear feedback part, the RCNF control law is given as:

$$\begin{cases} u = [F \quad F_w] \begin{pmatrix} y \\ \hat{x}_2 \\ \hat{w} \end{pmatrix} + Gr + \rho(e) F_n \left[\begin{pmatrix} y \\ \hat{x}_2 \end{pmatrix} - \hat{x}_e \right] \\ \hat{x}_e \coloneqq G_e r + G_w \hat{w} \end{cases}$$

4.2.4 ADRC Control Strategy Configuration

Consider the system formed in 4.2 and apply the simplified parameterized linear ADRC proposed by Gao in [127]. With:

$$A = \begin{bmatrix} 0 & 1 & 0 \\ 0 & 0 & 1 \\ 0 & 0 & 0 \end{bmatrix}, B = \begin{bmatrix} 0 \\ b \\ 0 \end{bmatrix}, C = [1 \quad 0 \quad 0], E = \begin{bmatrix} 0 \\ 0 \\ 1 \end{bmatrix}, L = \begin{bmatrix} 3\omega_0 \\ 3\omega_0^2 \\ \omega_0^3 \end{bmatrix}$$

The control law can be rewritten as:

$$\begin{cases} u = \dfrac{-z_3 + u_0}{b} \\ u_0 = k_p(r - z_1) - k_d z_2 \end{cases}$$

Where r is the set point. The controller tuning can further be simplified with $k_d = 2\omega_c$, and $k_p = \omega_c^2$. ω_c is the closed-loop bandwidth.

There are only three parameters needed to be selected, i.e. ω_0, ω_c, and b, which is further discussed in the simulations and experiments.

4.3 Simulation

4.3.1 Supervisory Controller Simulation

In this section, simulations for LQR, RLQR and CNF are carried and results are compared mutually with illustrations, which mainly focus on controllers' performance to converge Δd to 0.

A discussion about parameter selection is proposed, where the selection of u_{max}, T_L, Q and R are further studied.

To offer a better understanding of the workflow of ACC system, a diagram is given below to illustrate the workflow of a typically ACC equipped vehicle on highway.

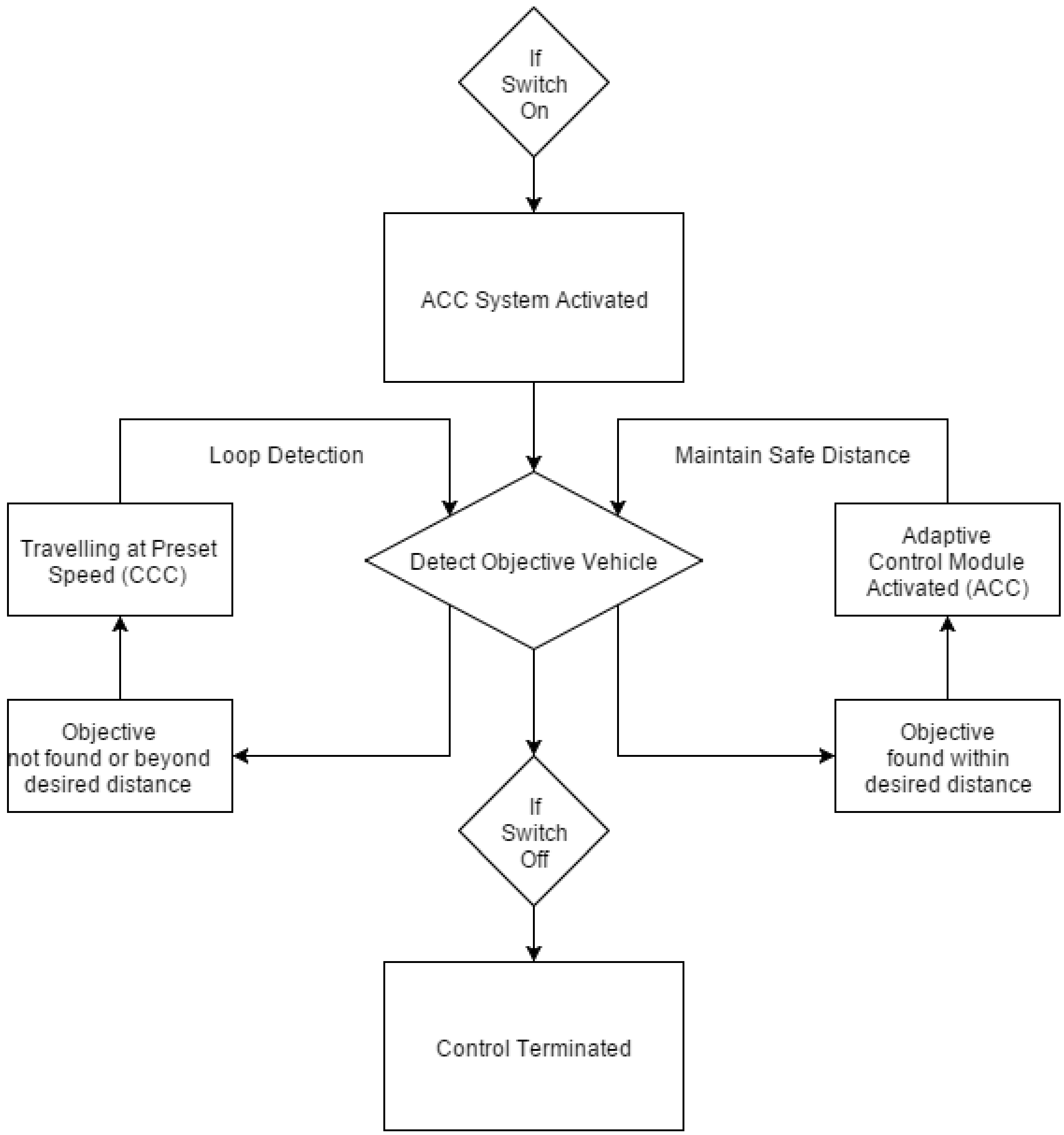

Figure 4.3 Workflow of ACC system

According to the diagram above, the decision made by the system to switch from CCC to ACC depends on whether the objective vehicle is detected and within the desired distance. Therefore, the actual ACC control algorithm is only a part of the whole system. For simplicity, simulations with only CCC activated will not be given.

There are two situations when the actual ACC control module is activated, which is classified as follows:

1) The detected vehicle gradually emerges within the desired distance. i.e. d_{des}, which means the following vehicle proceeds a constant speed while the proceeding vehicle is about to decelerate.
2) The detected vehicle suddenly appears within the desired distance, which means it was already there when the ACC module was activated. The proceeding vehicle may possess a positive or negative acceleration, where the negative one denotes a worse situation.

Situation 2) is generally worse than 1), whereas, the controller performance can be more clearly illustrated with 1), which provides designers more freedom to choose the emerging time of proceeding vehicle, and is selected in this thesis to perform the simulation and experiments.

Consider the proceeding vehicle with an acceleration described below:

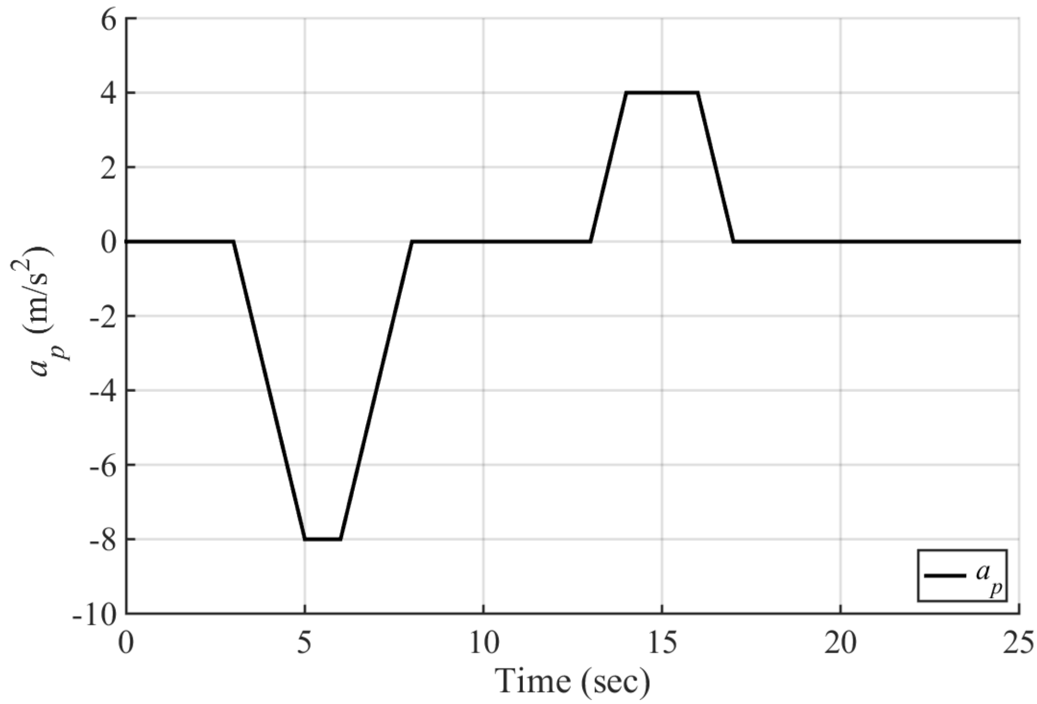

Figure 4.4 Acceleration variation of proceeding vehicle

Which denotes the proceeding vehicle gradually applies a deceleration at $t = 3$ which reaches its maximum value $a_{pdmax} = -8$ at $t = 5$ then gradually cancels, and accelerates at $t = 13$ to a max acceleration $a_{pamax} = 4$ at $t = 14$ then gradually cancels.

Note, the max braking deceleration of most vehicles on market are around $10m/s^2$, and the max acceleration for most commercial vehicles is around $5m/s^2$, therefore the situation is enough severe to test the control strategies.

The initial condition is designed as follows:

$$V_{f0} = 30\,m/s\ (108km/h), \quad x = \begin{bmatrix} 0 \\ 0 \\ 0 \end{bmatrix}$$

Where V_{f0} denotes the travelling speed of following vehicle at $t = 0$, and for $x =$ [0 ; 0 ; 0], according to (4.1.1), we have:

$$d_{desi} = d_i$$

Where d_i is the actual initial distance between two vehicles, which means at $t = 0$, the following vehicle maintains the very desired distance behind the proceeding vehicle. According to Figure 4.4 where the acceleration of proceeding vehicle remains 0 until $t =$ 3, the two vehicles will maintain a same constant speed, i.e. V_{f0}, in the first 3 seconds.

Then with $\tau_h = 0.5$ and $d_0 = 5$, which are mentioned in the section of system modeling, d_i is derived as:

$$d_i = 20m$$

A summary of parameter selection in simulation can be given as follows:

	$\tau_h = 0.5$	$d_0 = 5$	$V_{f0} = 30$	$d_i = 20$
	$x_0 = [0 ; 0 ; 0]$		$K_L = 1$	$T_s = 0.001$
RCNF	$\alpha = 10$		$\beta = 20$	$r = 0$
	$Pole_1 = [-5 + 0.1i \;\; -5 - 0.1i \;\; -2]$			
	$Pole_1 = [-5 + 0.1i \;\; -5 - 0.1i]$			$W = 0.01I_3$
ADRC	$\omega_0 = 10000$		$\omega_c = 5000$	$b = 20000$

Table 4.1 Parameter selection in simulations

Next, simulations are conducted in five cases with parameters selected as follows:

Case	u_{max}	T_L	Q	R	Remark
I	6	0.1	$\begin{bmatrix} 10 & 0 \\ 0 & 1 \end{bmatrix}$	1	General Case
II	10	0.1	$\begin{bmatrix} 10 & 0 \\ 0 & 1 \end{bmatrix}$	1	Effective Braking
III	6	0.5	$\begin{bmatrix} 10 & 0 \\ 0 & 1 \end{bmatrix}$	1	Large Delay
IV	6	0.1	$\begin{bmatrix} 10 & 0 \\ 0 & 0.01 \end{bmatrix}$	0.01	Safety with (R)LQR
V	6	0.1	$\begin{bmatrix} 20 & 0 \\ 0 & 5 \end{bmatrix},$	10	Comfort with (R)LQR

Table 4.2 Parameter selection for different simulation cases

Except Case II, the input saturation is set as $u_{max} = 6$, which denotes the braking system of following vehicles is not that good as proceeding vehicles. The max deceleration of it is only $6m/s^2$, which could cause tens of meters more in braking distance than proceeding vehicle. These severe cases are designed to fully test the performance of different control strategies. In Case II, input saturation is set to 10 to check the controller performance with effective braking systems.

T_L is generally set to 0.1 to denote a minor delay of vehicle level controller and plant, but is set to 0.5 in Case III to indicate an aged car system or mechanical problems which may cause delay.

In the first three cases, Q and R are set to denote a relatively high demand on safety, where the weight factor of Δd denotes the controlling strength put in safety. The weight factor for Δv represents an objective to maintain the same speed with proceeding vehicle, and weight factor for a_{fdes} is selected to minimize jerk cause by large acceleration.

In Case IV, Q and R are set to offer the highest priority in safety aspect. While in Case V, comfort reason acquires more consideration in the control process.

For a summary, Case I can be regarded as a general case for reference. Case II is the one with effective braking system. Case III has the largest time delay. Case IV puts more weight on safety aspects with LQR and RLQR. And Case V puts more weight on comfort aspects with LQR and RLQR.

In the simulations, $\Delta d, \Delta v, u$ and d are selected to demonstrate the performance of each controller, where Δd and Δv denote the measurable states of the system, which are clearance error and the speed error respectively, and Δd is also the controlled output. u is the control input, i.e. the desired acceleration a_{fdes} for following vehicle. d is the actual distance between two vehicles.

Simulation time is set to $25s$ to track the whole process of acceleration and deceleration of the proceeding vehicle. The results are plotted with dotted line for LQR, dashed line for RLQR and solid line for RCNF respectively.

Note that safety aspect possesses the first priority during control process, which means the performance of these controllers can be greatly reflected by the graph of Δd.

Simulations in Case I are carried out with results shown below:

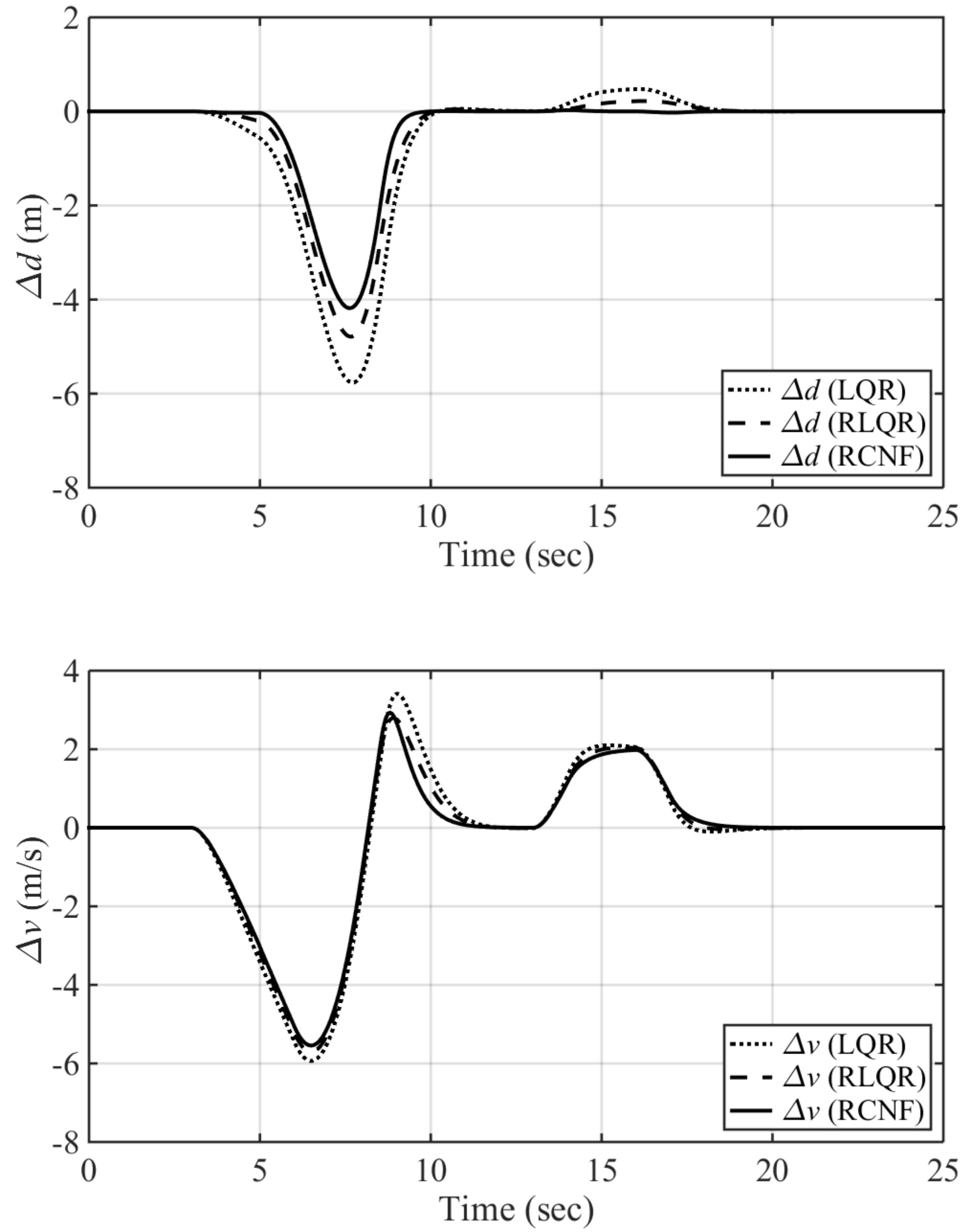

Figure 4.5 Simulation results for Δd and Δv in Case I (General Case)

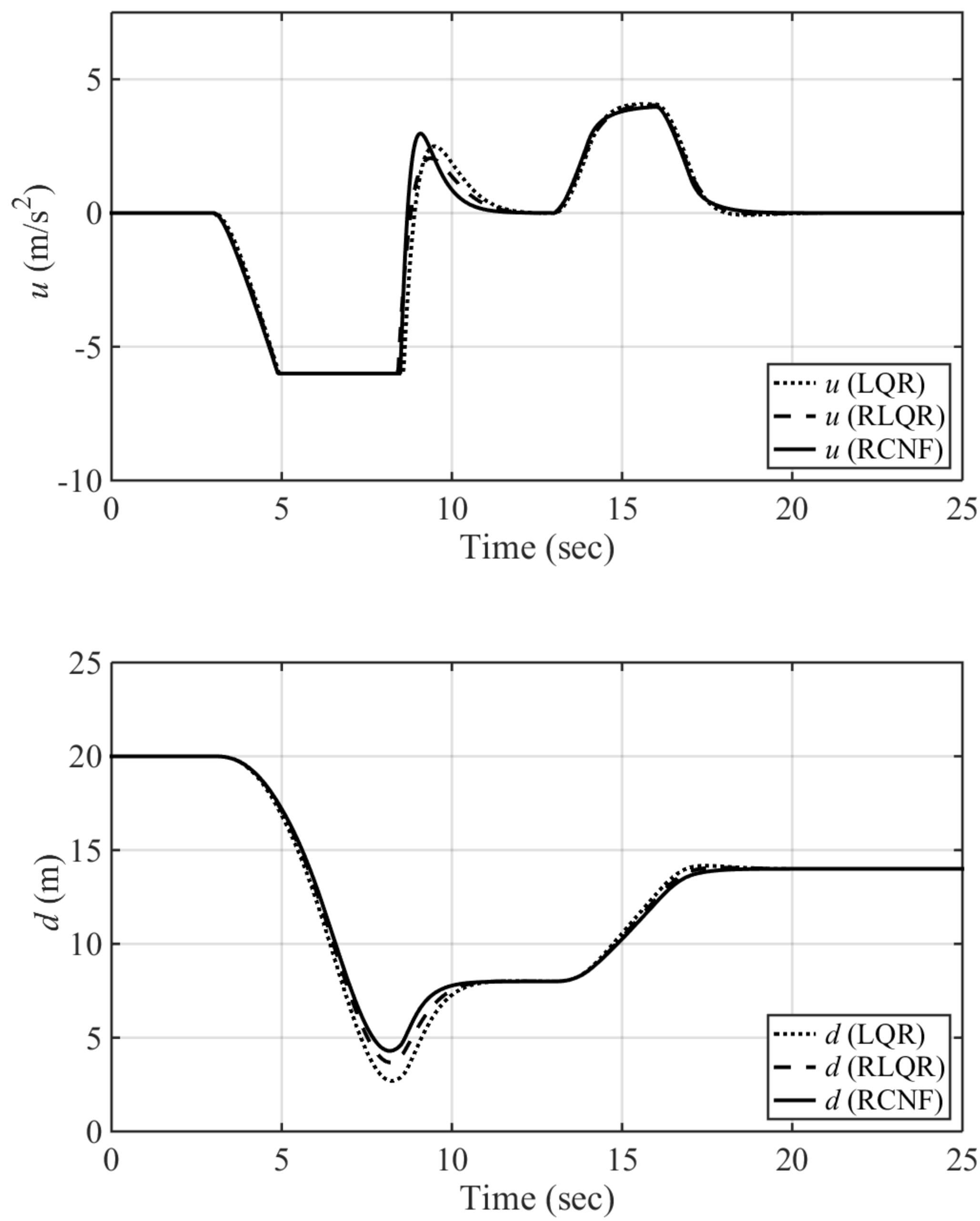

Figure 4.6 Simulation results for u and d in Case I (General Case)

With the parameters selected in Table 4.1 for Case I, RCNF demonstrates a better performance to converge Δd to 0 with the least overshoot in both deceleration and acceleration process.

Note that with $u_{max} = 6 < a_{pdmax}$, overshoot cannot be eliminated by all means.

The controlling process of Δv possesses a similar objective with Δd, which can be summarized as: the less overshoot, the better, where RCNF also denotes the best performance.

The direct reason for the difference in performance lies in the response time of input, which is graphed in Figure 4.6. It can be clearly seen that, at the ascending edge around $t = 8$, the input of RCNF offers a quicker response, which is also indicated at other ascending and descending edge.

In the graph of d, i.e. actual distance between two vehicles, for RCNF demonstrates the safest properties with an overall largest braking deceleration, i.e. input u, its decelerating distance is approximately $1m$ less than LQR and $0.5m$ than RLQR. And with the slowest increasing of acceleration, RCNF is able to keep Δd at 0 with almost no overshoot, shown in Figure 4.5.

RLQR generally stands in the second place between RCNF and LQR. It provides a performance superior than LQR for the existence of the nonlinear feedback part in the control input, which offers the ability to reject overshoot to some degree.

Meanwhile, for the reason that weigh factors of Q and R are also distributed to minimize jerks, LQR and RLQR show a more comfortable ride compared to RCNF, which can be demonstrated in Figure 4.6, where quick response of RCNF input also brings more jerks. Though there is always a tradeoff between safety and comfort in ACC design, safety always goes first.

Next, simulations for Case II are carried out, where following vehicle is equipped with a not worse or even better braking system than the proceeding vehicle and results are as follows:

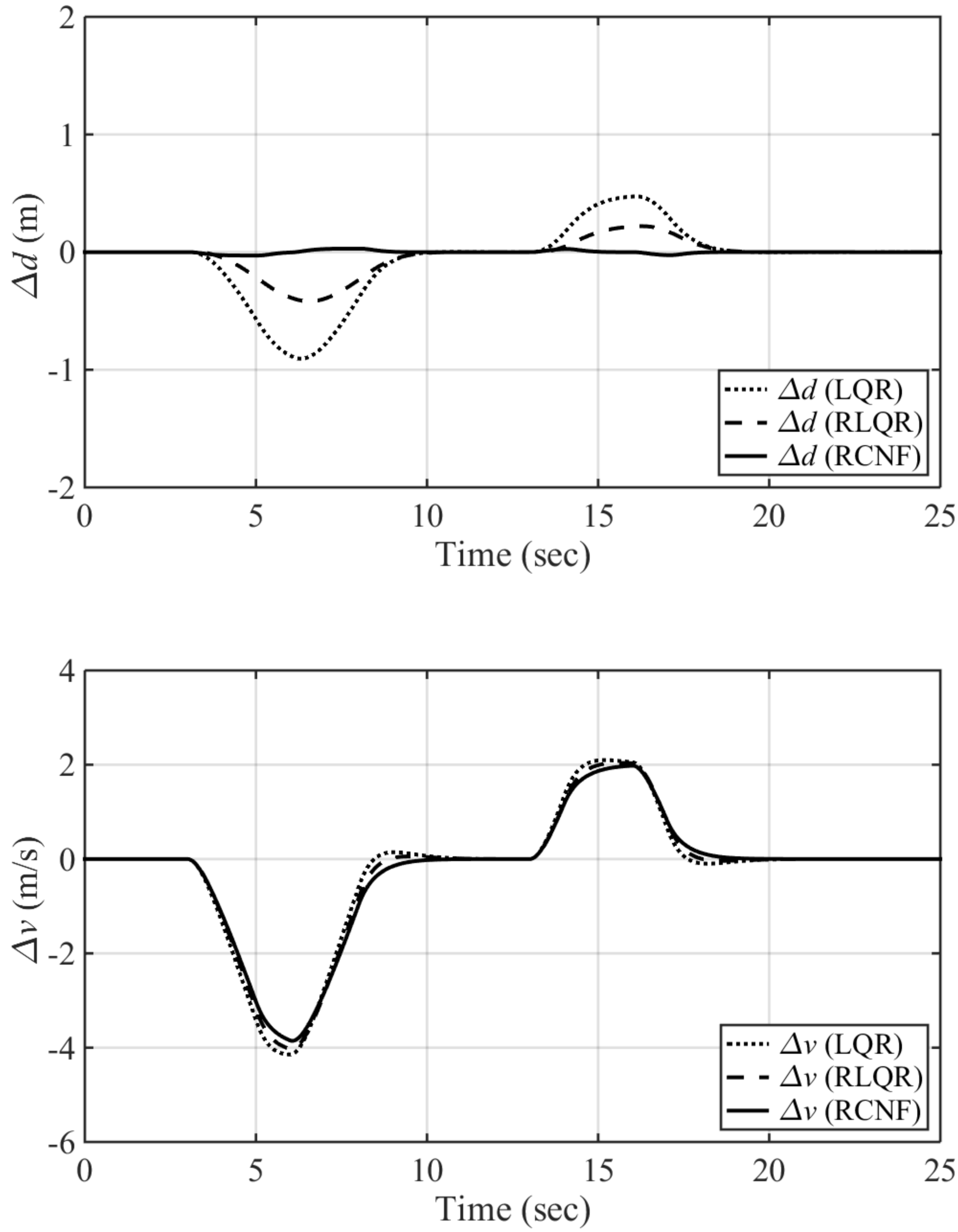

Figure 4.7 Simulation results for Δd and Δv in Case II (Effective Braking)

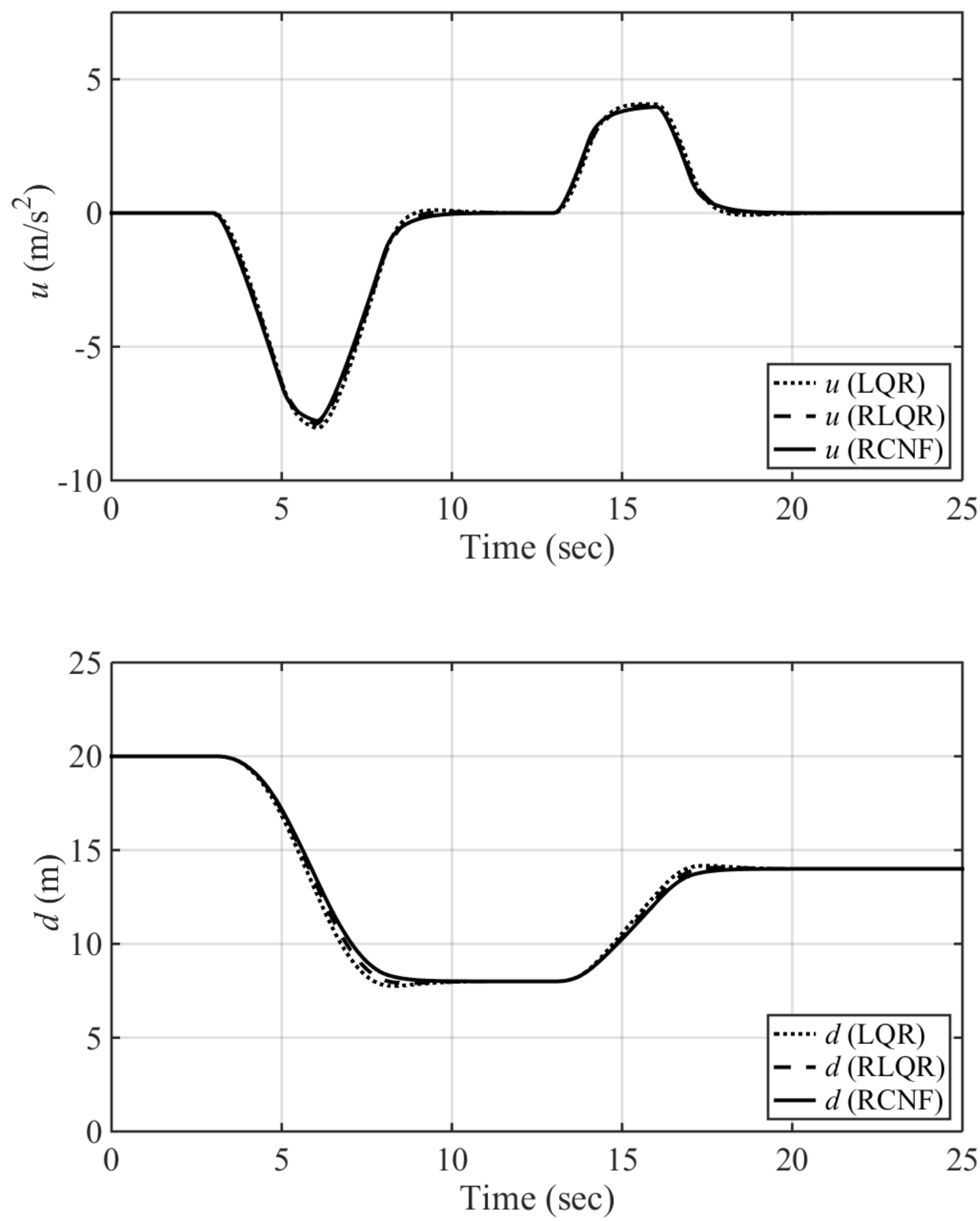

Figure 4.8 Simulation results for u and d in Case II (Effective Braking)

In this set of simulation, RCNF denotes a much better performance on reducing the overshoot of Δd and Δv, which represents its outstanding ability with a control objective of tracking targets.

The input of RCNF still provides a quicker response, which on contrary also offers a less comfortable ride.

All three controllers have the ability to deal with the most severe cases if the following vehicle possesses a superior braking system than the proceeding one, which is reflected in the graph of d in Figure 4.8. RLQR and LQR have a little more overshoot than RCNF in the deceleration process, but not as much as the case with a smaller input saturation of 6.

Then, in Case III, we reset u_{max} to 6 and change T_L to 0.5, which means there are more delays on the vehicle level, which in real world is generally caused by aging of the vehicle and/or mechanical problems.

Simulations results are as follows:

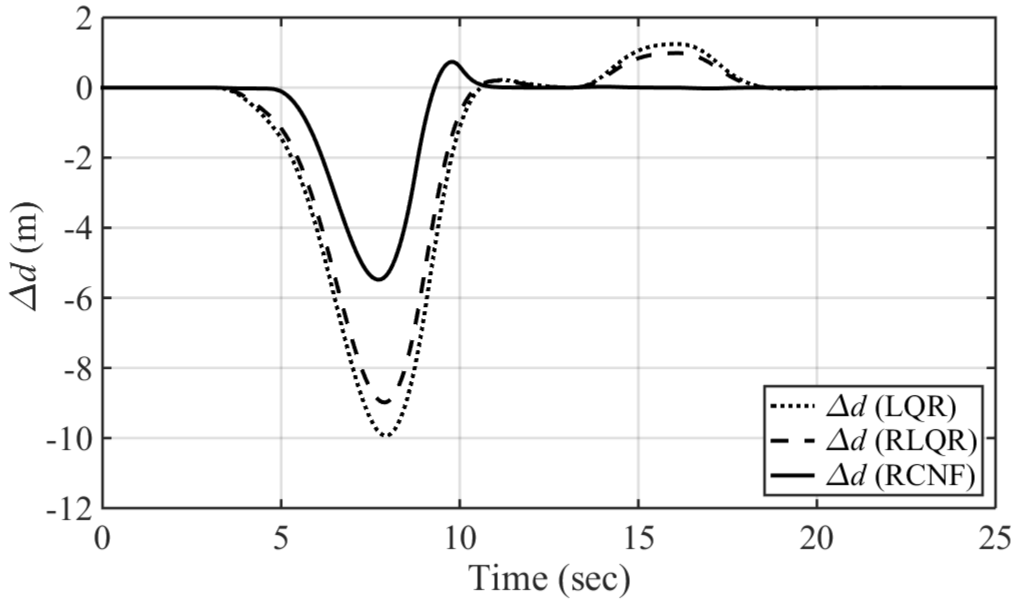

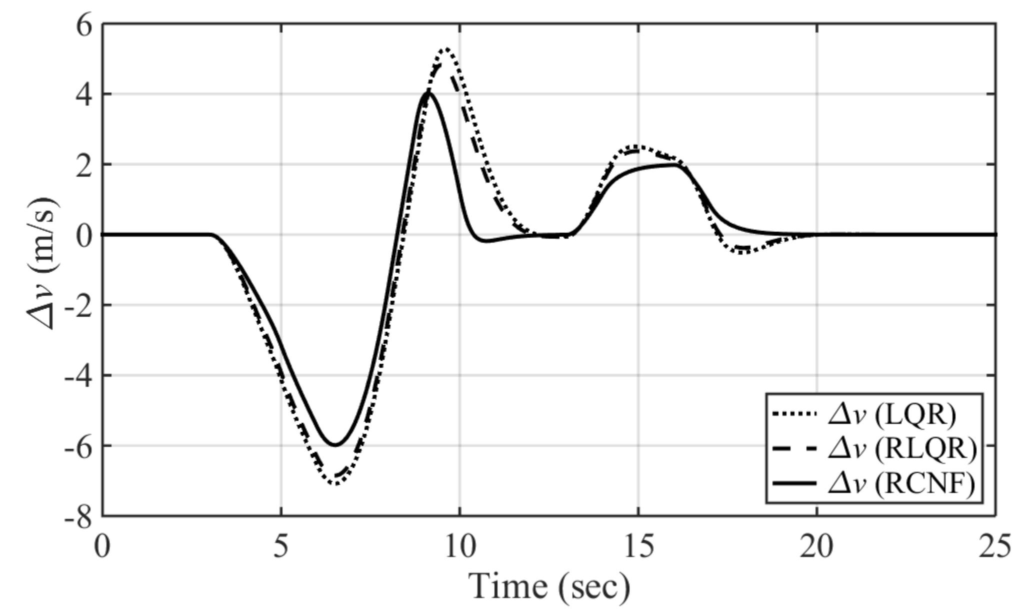

Figure 4.9 Simulation results for Δd and Δv in Case III (Large Delay)

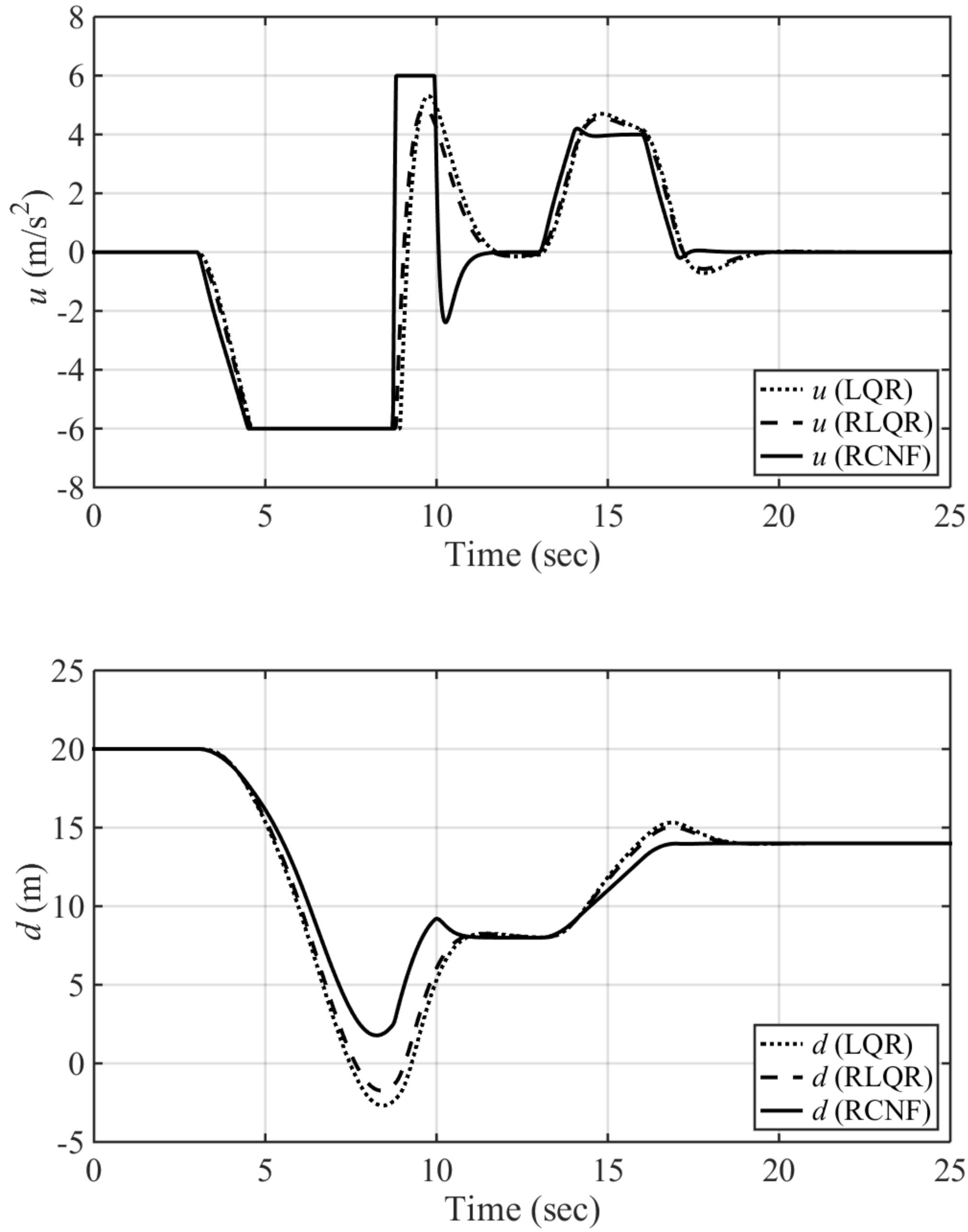

Figure 4.10 Simulation results for u and d in Case III (Large Delay)

This set of simulations are the severest ones considered in this thesis.

The RCNF is still the best one to maintain a safe driving situation. Thought the overshoot is slightly larger than that in Figure 4.5, it is superior compared to LQR and RLQR, which indicates that RCNF possesses more resistance to aging and mechanical lagging in vehicle level. Δv shows the similar trend with Δd, which was already fully discussed in previous two cases, which needs not to be illustrated here.

Figure 4.10 denotes a quick and heavy variation of the RCNF input, which may cause large discomfort. But compared to the graph of d below, the sacrifice of comfort is deserved in this case for the vehicles equipped with RLQR and LQR both made a crash.

Actually, the weight factor in RLQR and LQR can greatly affect the performance of these two controller. In the upcoming simulations, the QPI is resized referring to different design needs.

Firstly, Case IV is tested, where the QPI almost only consists of the weight factor of Δd, which denotes safety holds the highest priorities.

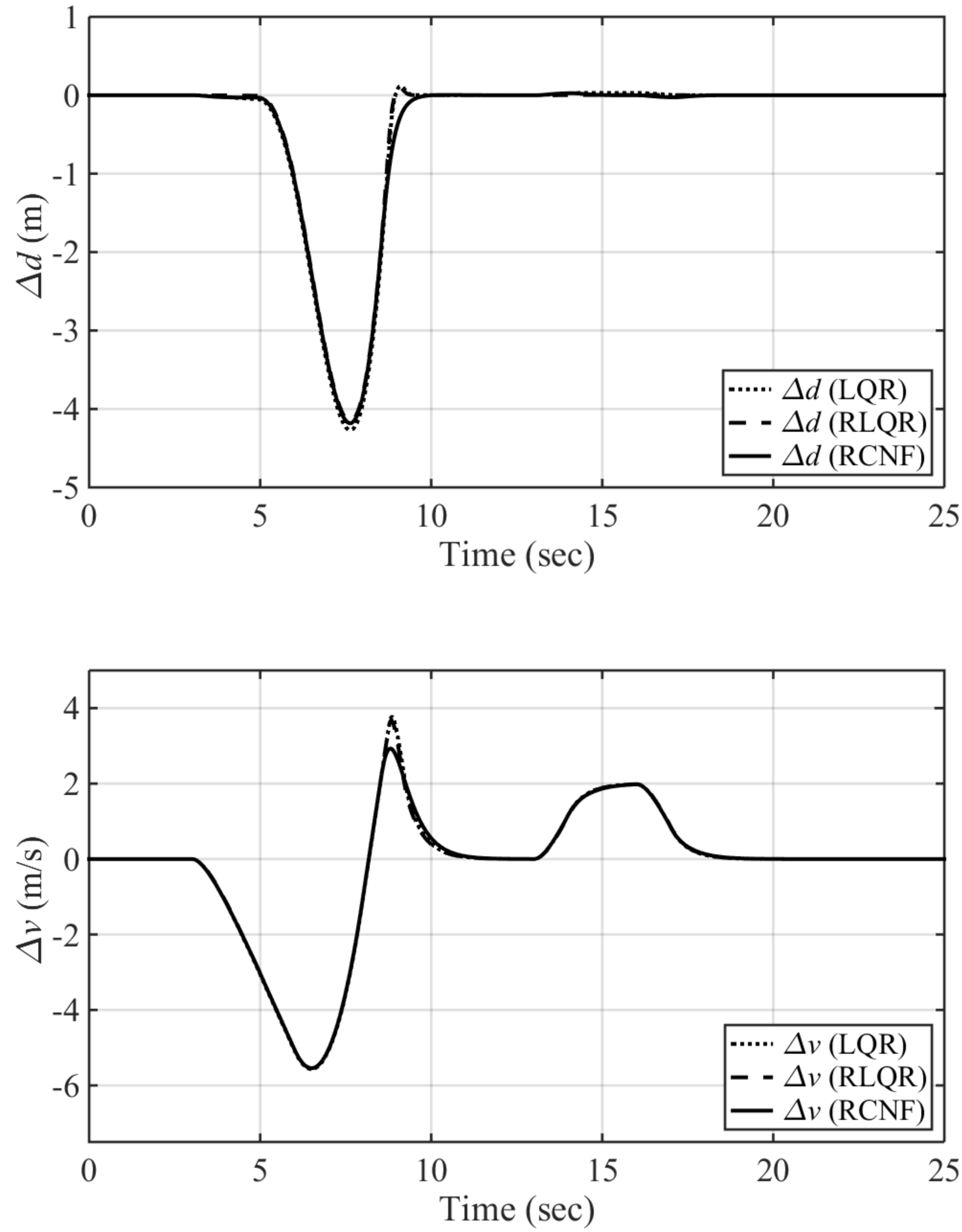

Figure 4.11 Simulation results for Δd and Δv in Case IV (Safety with (R)LQR)

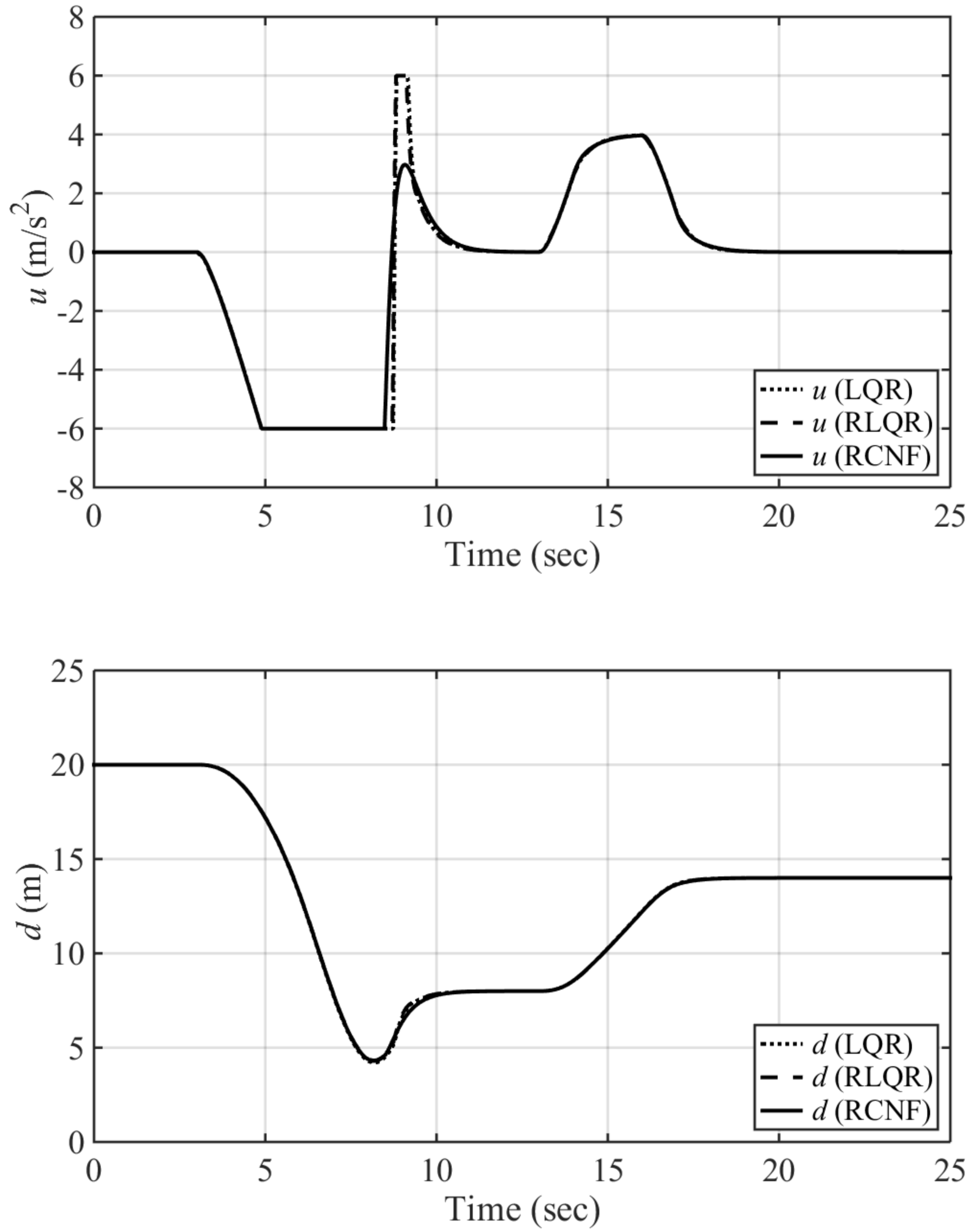

Figure 4.12 Simulation results for u and d in Case IV (Safety with (R)LQR)

In this case, the RLQR and LQR possess almost the same overall ability to converge Δd to 0 as RCNF with the new set of weight matrices, but comfort is sacrificed, as shown in the graph of input, u transits abruptly with large variations .

If the weight matrices Q and R are chosen such that safety and comfort are balanced, which is preferred by some automakers and drivers, simulations can be carried out with parameters stated in Case V. Results are as follows:

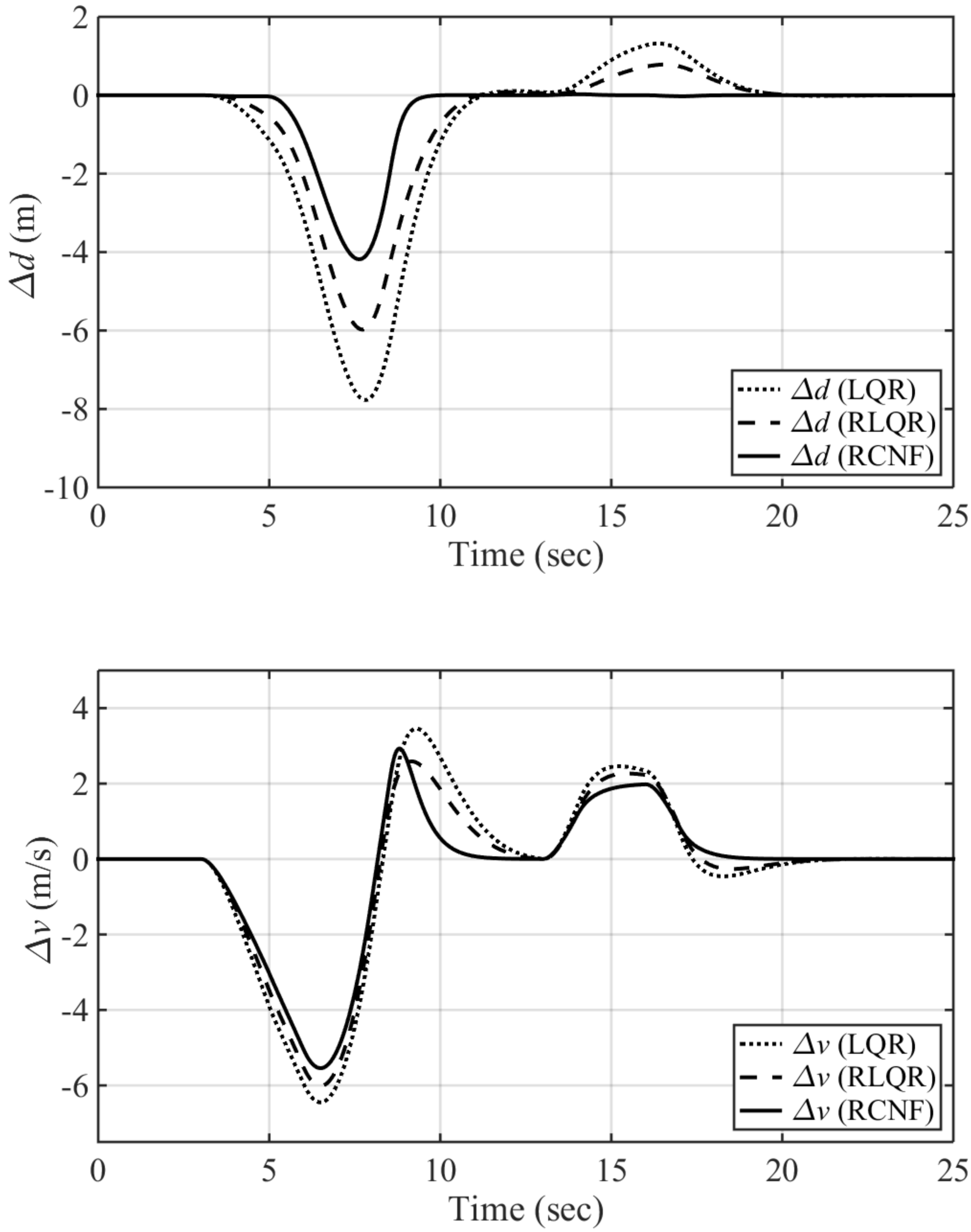

Figure 4.13 Simulation results for Δd and Δv in Case V (Comfort with (R)LQR)

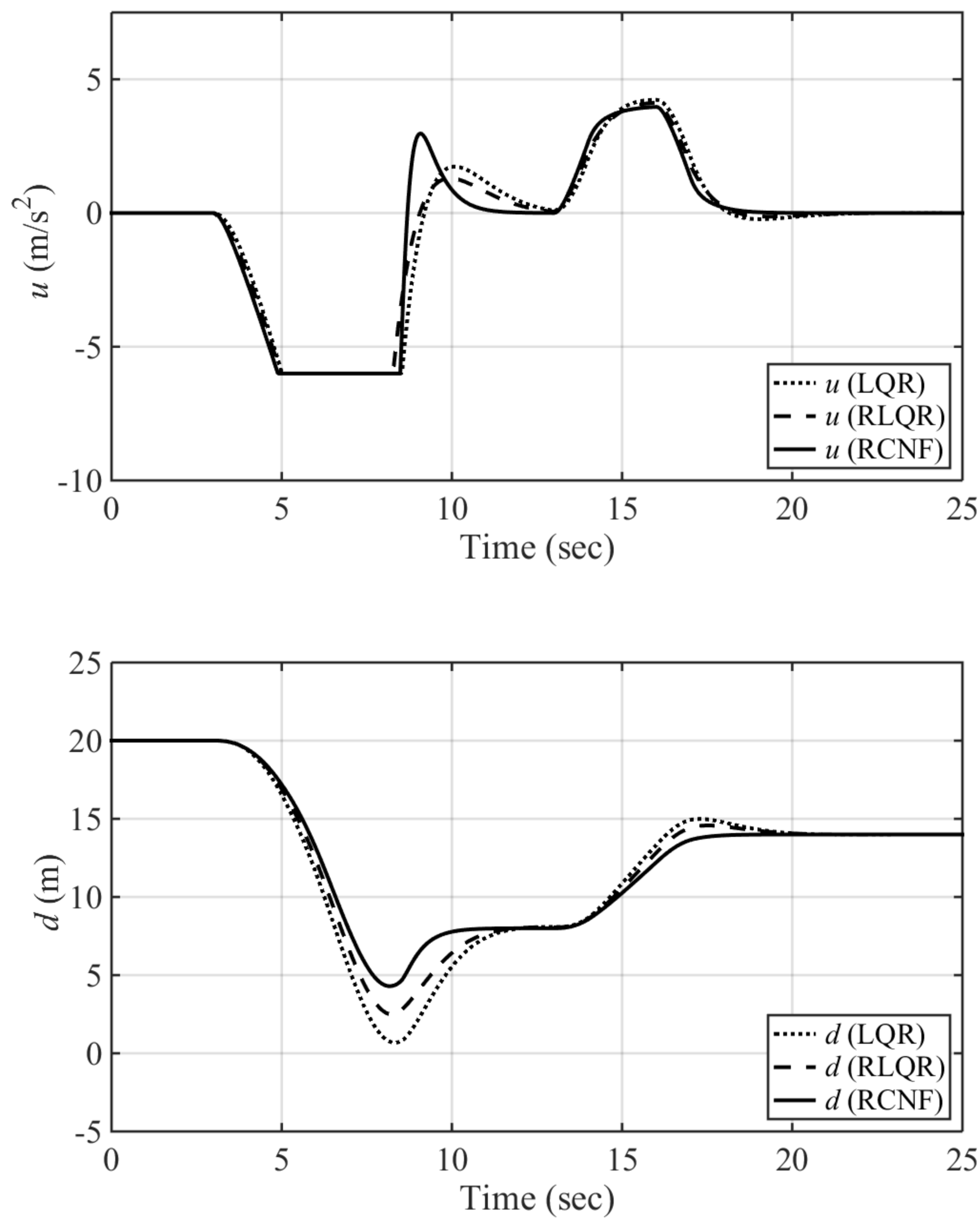

Figure 4.14 Simulation results for u and d in Case V (Comfort with (R)LQR)

The results denote a decent ability for RLQR and LQR to not only maintain the safety but provide a comfortable ride, which can the shown in Figure 4.14 where the control input u varies with smoother ascending and descending edges than RCNF.

But compared with that in Case I, the decelerating distance increases for LQR and RLQR, which may cause danger in real world practice. Therefore, the stopping distance d_0 should be set larger than normal cases with comfort taken into consideration.

For a summary, RCNF is generally a better controller in ACC system design with concerns on safety aspects, which is robust to braking ability limitation, vehicle aging and mechanical problems which cause vehicle delays. RLQR should be considered when concerns switched to comfort, but the stopping distance d_0 should be redesigned for safety reasons.

4.3.2 Vehicle Level Controller Simulation

In this section, an ADRC controller and a PID controller are designed and simulated simultaneously with results being analyzed.

According to Figure 4.1, vehicle level controller is designed to reject noise in the plant. Therefore, the robustness to noise should be considered as a performance indicator.

Note that the reference received by vehicle level controller is the desired speed of following vehicle, which is integrated from desired acceleration outputted from supervisory controller, as shown in Figure 4.1.

For real practice on commercial vehicles, the cruising speed (i.e. initial speed $v_{f0} = 30m/s$ for the situation in this thesis) should be set as the input saturation to vehicle plant, which indicates the mechanism of ACC which was presented in Figure 4.3.

But for the purpose of demonstration, and a consideration of later experiments, the input reference r to vehicle level controller (i.e. the desired speed of following vehicle) is set to be $r = 2m/s$, which is far smaller than normal passenger vehicles but as much as $2/3$ of the maximum speed of the experimental robot.

The observer gain ω_0 and closed-loop bandwidth ω_c can be chosen according to sample time. And, b should be large enough to reduce input chattering.

These parameters are selected as:

$$\omega_0 = 10000,\ \ \omega_c = 5000,\ \ b = 20000$$

With the simulation sample time selected as $T_s = 0.0001s$. For the PID system, parameters are given by:

$$P = 100,\ \ I = 0,\ \ D = 0$$

Note that I and D do not have a great influence on control results, thus they are set to be 0.

To reflect the noise level in vehicle level, a Gaussian distributed random number generator is chosen with the variance $R_v = 0.1$ and sample time $R_s = 0.01$, which is plotted below:

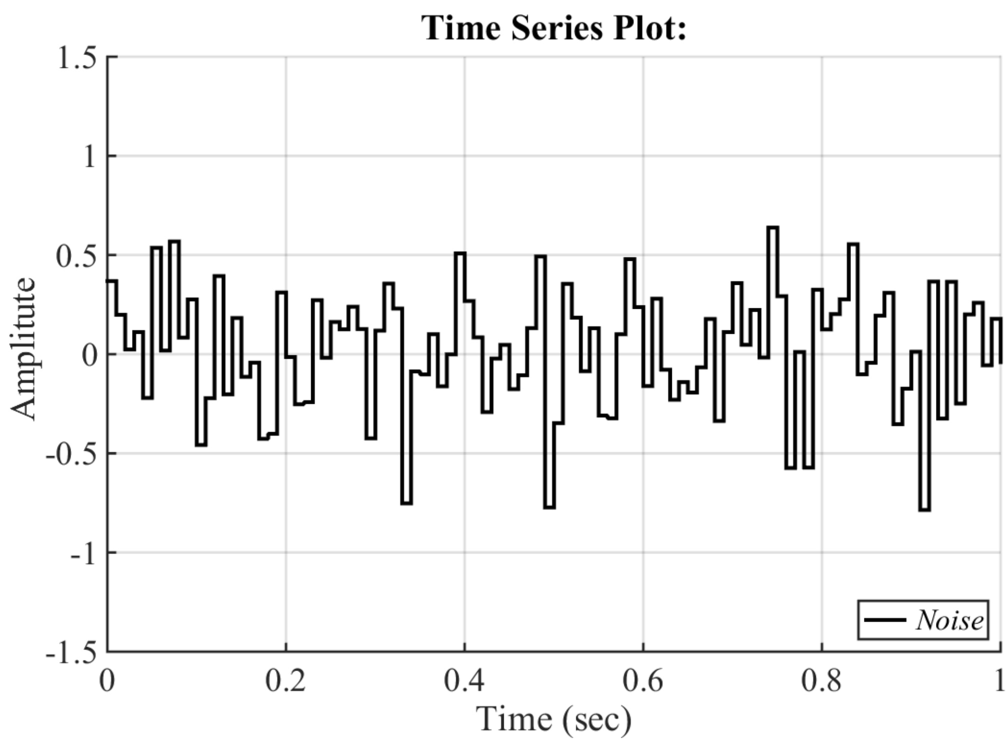

Figure 4.15 Random generated noise

The noise shown in the figure above will also be delayed according to T_L, which is set to 0.1 in this case, when applied to vehicle plant.

Simulation results are as follows:

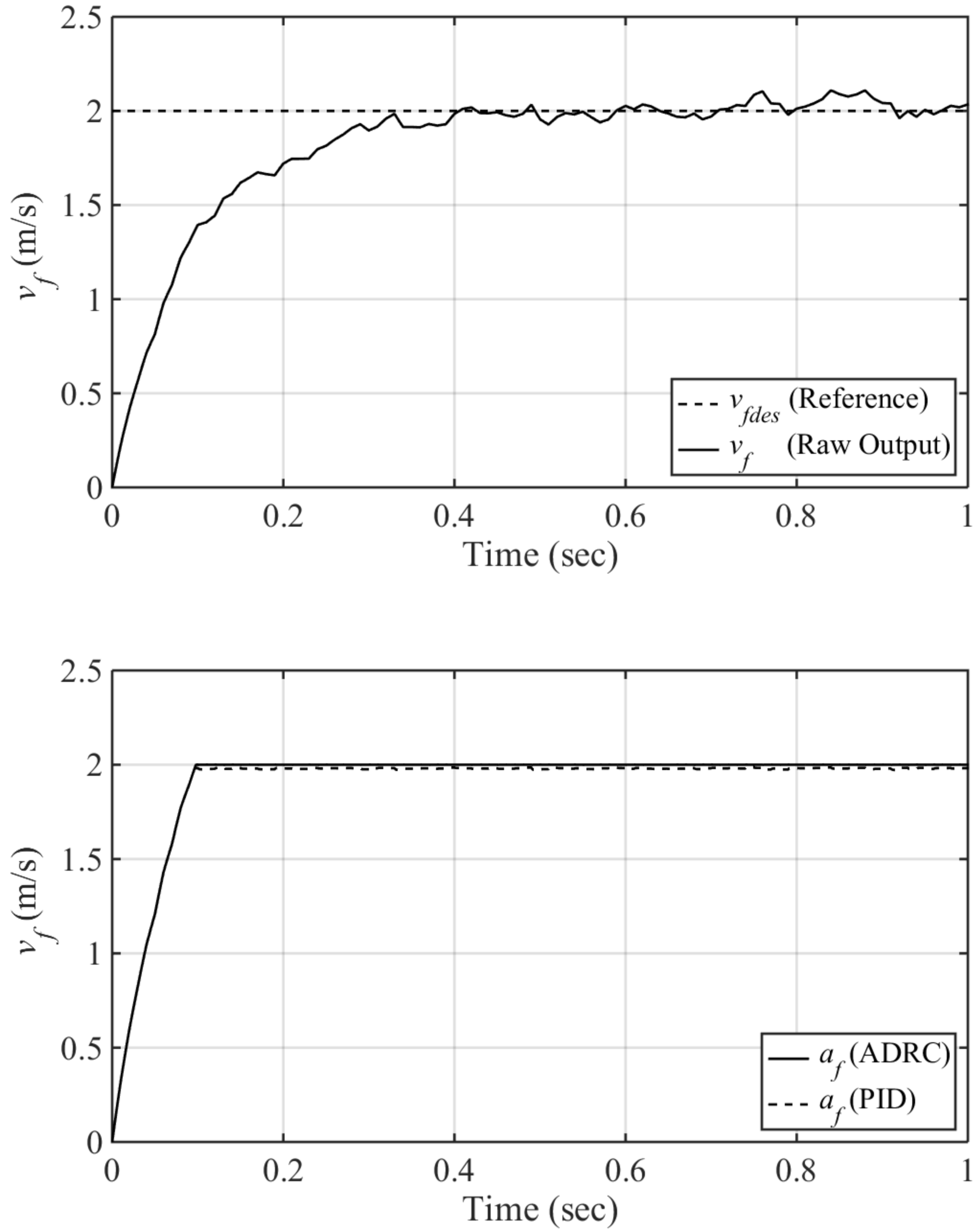

Figure 4.16 Reference, raw output and noise rejected speed feedback

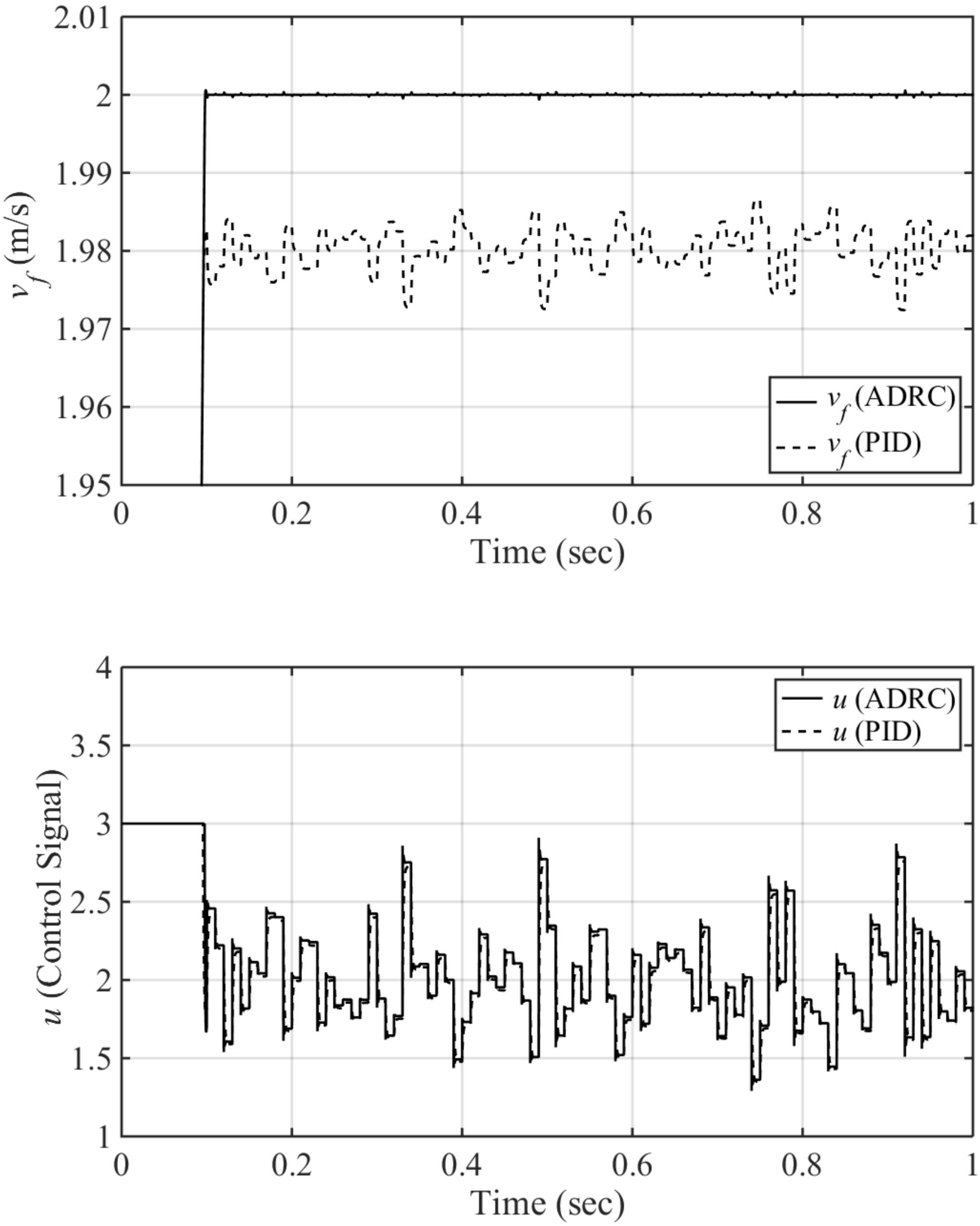

Figure 4.17 Noise rejected speed feedback and control signal to vehicle plant

The dashed line in the upper graph of Figure 4.16 denotes the reference signal r, and the solid line denotes the uncontrolled raw output (i.e. motor speed feedback). The noise rejected speed feedbacks by ADRC and PID are presented in Figure 4.16, and partially magnified in Figure 4.17. The difference between control results are apparent, while ADRC denotes a higher precision and less overshoot. Control signals (i.e. speed command sent to plant by PWM method) can also be found in Figure 4.17, where ADRC possess a quicker response but with a little overshoot.

In Chapter 5, the ADRC controller will be applied in experiments, firstly tested onboard solely to test its performance, then together with supervisory level controllers to form a complete ACC control system.

CHAPTER 5

EXPLERIMENTAL VALIDATION

5.1 Experimental System Configuration

In the previous chapters, a hierarchical control architecture is described with a workflow of such architecture demonstrated in Figure 4.1. In this chapter, a more detailed configuration of the hierarchical architecture will be illustrated, which contains not only controllers but other components such as motors, batteries and sensors, which work together to serve as the experimental platform, which is constructed as shown:

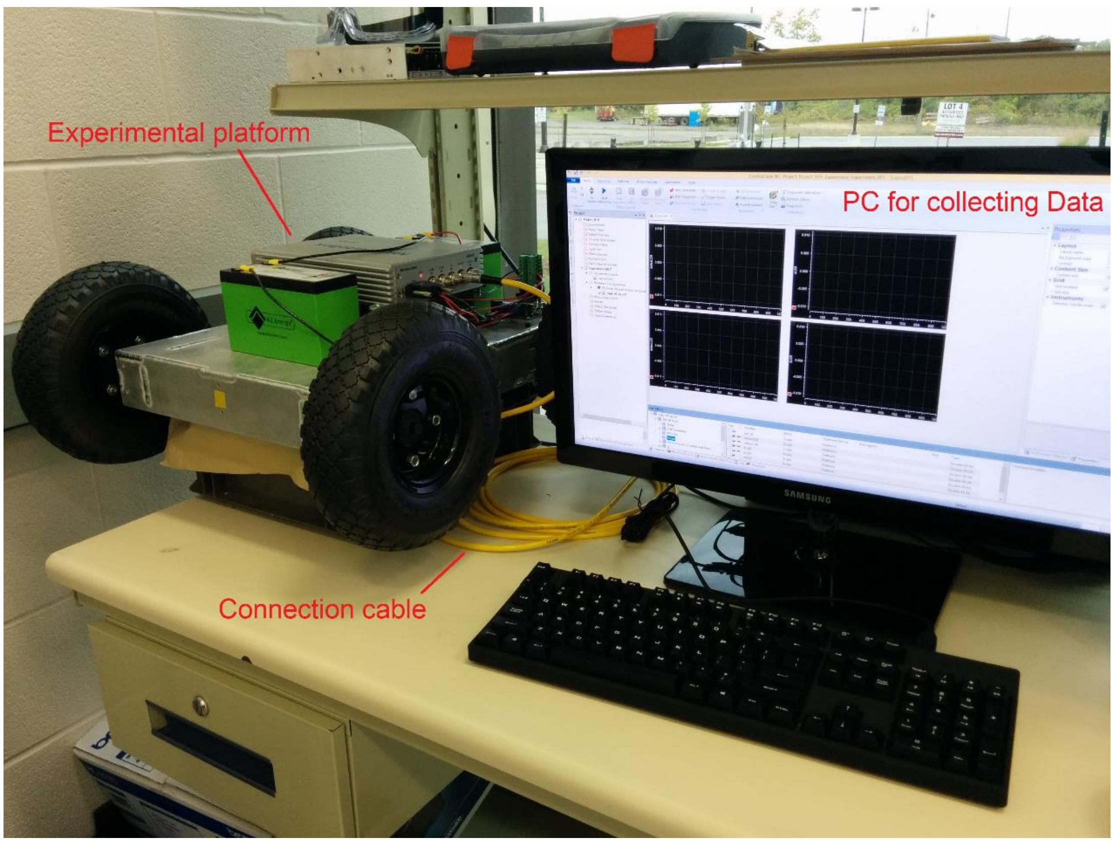

Figure 5.1 Experimental sets

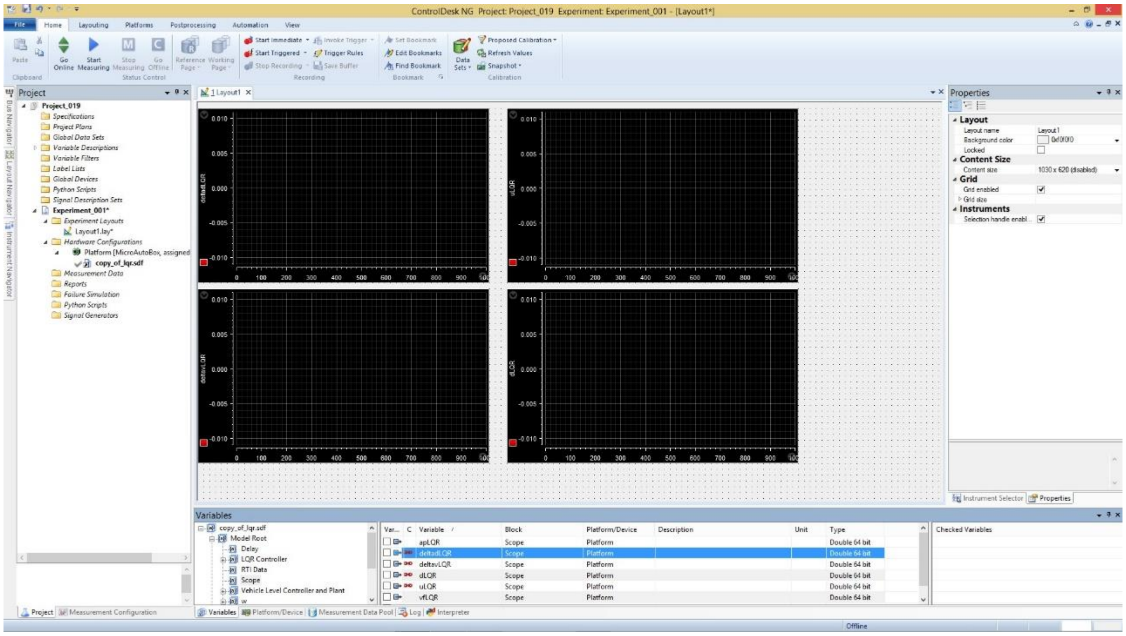

Figure 5.2 dSPACE ControlDesk for data collection

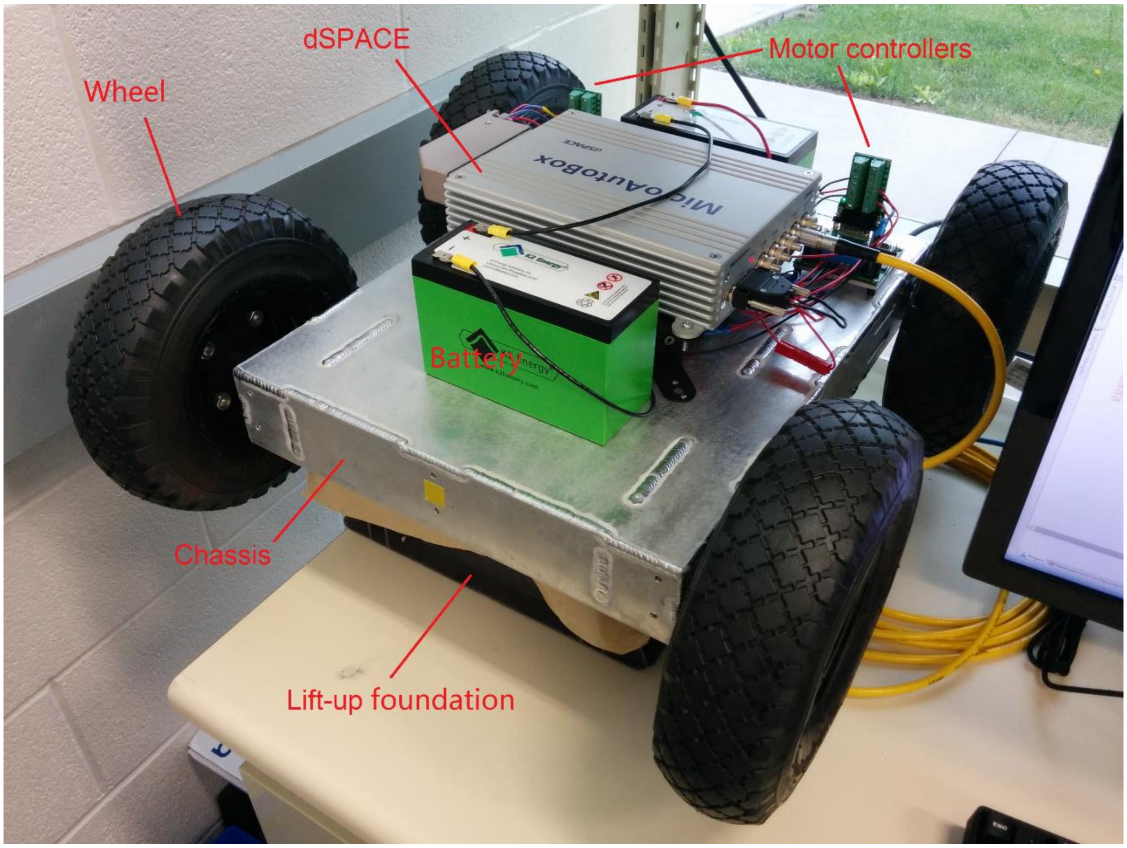

Figure 5.3 Experimental platform

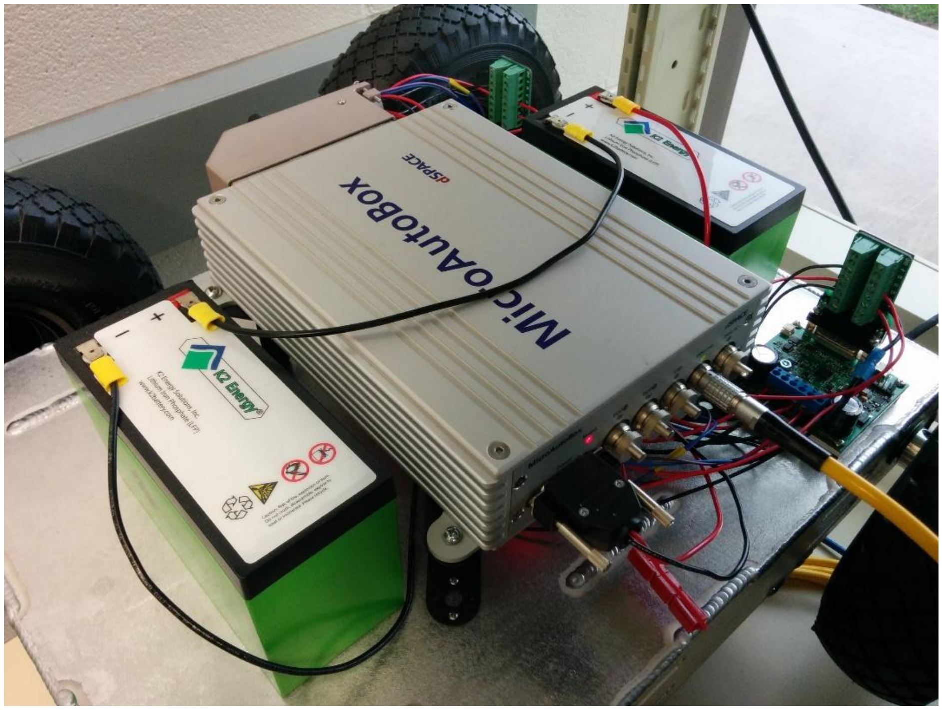

Figure 5.4 Experimental components on upper deck

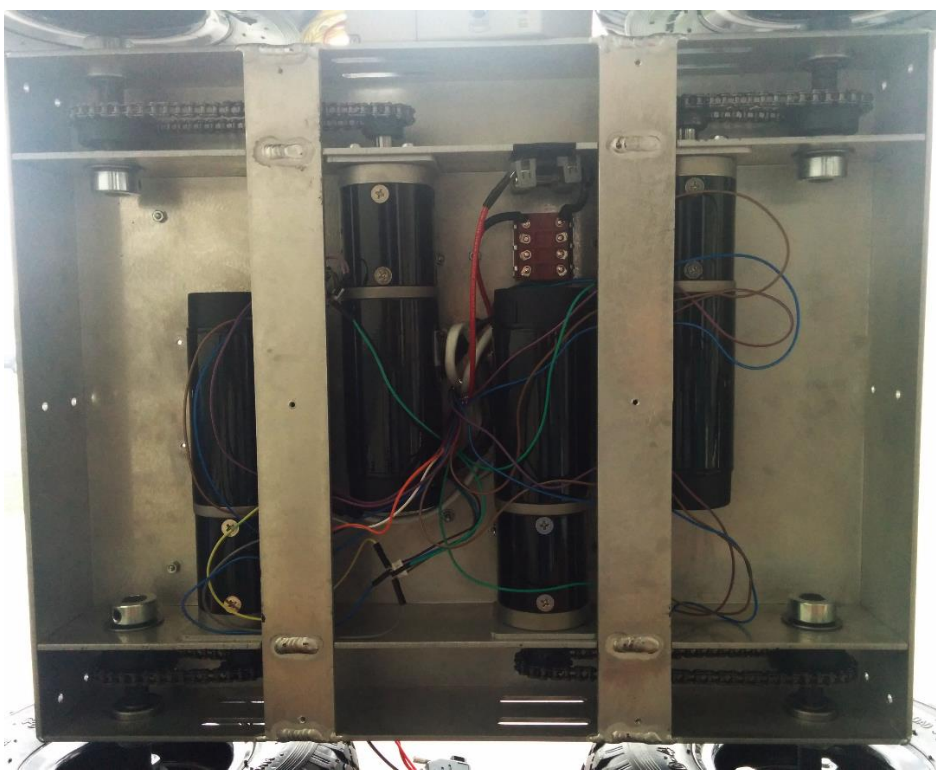

Figure 5.5 Experimental components within chassis

The experimental platform is linked by connection cable with PC, where the program dSPACE ControlDesk is used for real time data collection. And physical positions and appearance of different components are shown from Figure 5.3 to Figure 5.5.

Details for some components are given in the table below, others such as wires and switches are neglected:

Position	Components Selected
Supervisory Controller	dSPACE MicroAutoBox II 1401/1511
Vehicle Level Controller	RoboteQ SDC2130 (2 pieces)
Motor	IG52-04 Gear Motor with Encoder (4 pieces)
Battery	K2 12.8V LiFePO4 Battery (2 pieces)
Sensor	HRLV-MaxSonar-EZ4 Ultrasonic Range Finder

Table 5.1 Components Selection Table

The structure of the experimental platform is given by:

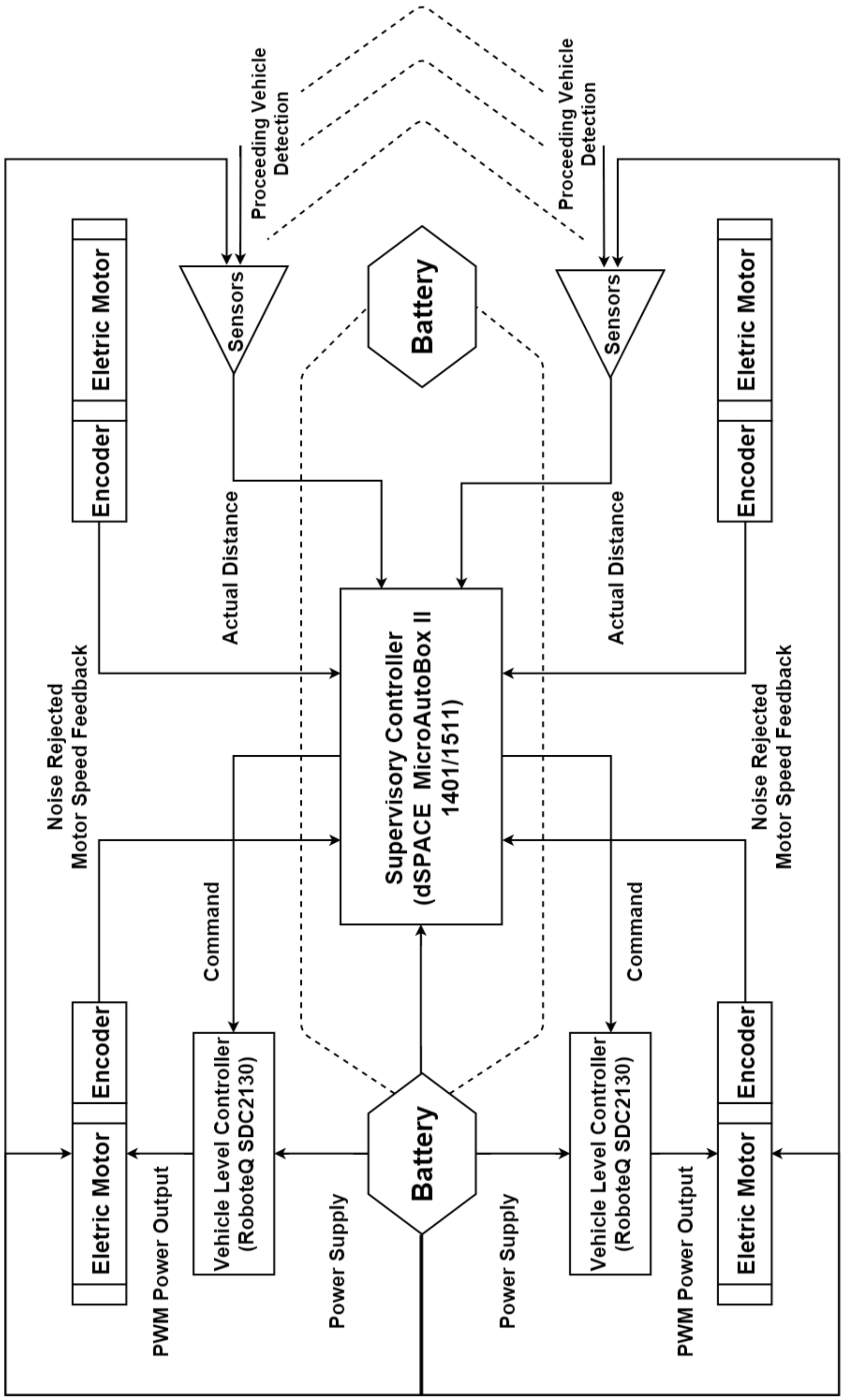

Figure 5.6 Electric robotic vehicle architecture

The diagram above also reflects the physical position for different parts of the electric robotic vehicle.

The two batteries are connected to offer power supply to the other components. The proceeding vehicle is detected by sensors, which deliver the range signal back to supervisory controller, where these signals are calculated with the motor speed feedbacks to generate the control law. The desired acceleration is calculated and integrated as desired speed, then sent to vehicle level controller, which calculates the ultimate motor command according to the desired speed and motor speed feedbacks to reject noise.

Note that because of the selection of ADRC as the vehicle level control strategy, the motor controller SDC2130, which is suitable for PID, does not possess the ability to calculate the algorithms for ADRC. Therefore, the task of vehicle level controller is achieved in dSPACE, while the motor controllers SDC2130 are used to receive speed command and generate PWM power output to motors. Therefore no motor speed feedbacks go into SDC2130, which can be indicated from Figure 5.6.

A simplified diagram of power stage operation of motor controller SDC2130 is given below. For there is no feedback exists, the power output is linked proportionally to speed commands.

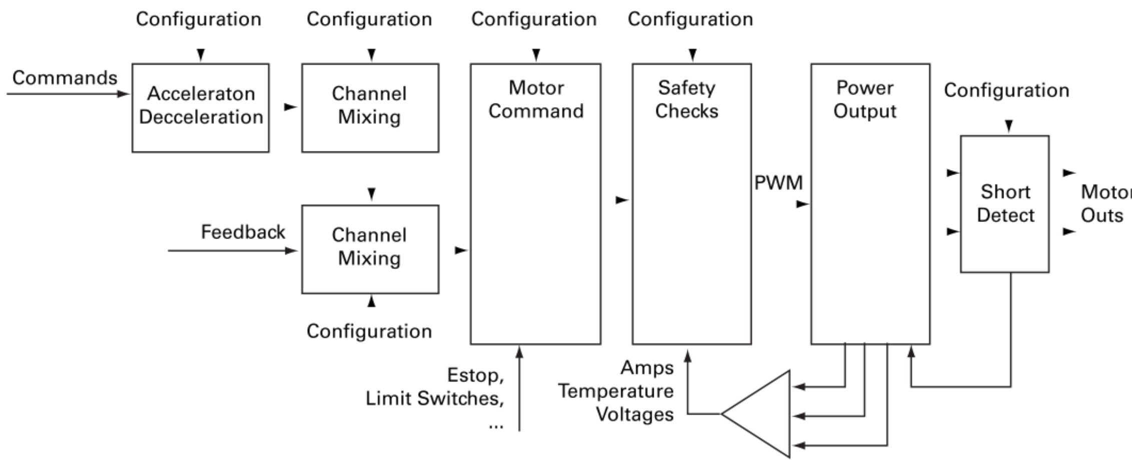

Figure 5.7 Simplified diagram of power stage operation for motor controller SDC2130

5.2 Performance Validation for Vehicle Level Controller

As mentioned in previous chapters, the responsibility for vehicle level controller is to reject noise generated in vehicle plant. In this section, ADRC control strategy will be tested in practice to judge its robustness compared to raw input signals.

The output of ADRC and the raw signals are sent respectively as motor speed command to motor controller SDC2130, which gives out a PWM power output to actuate motors. The encoders of motors will send the RPM information back as frequency, which is received by dSPACE to read the actual speed of motors then recalculate it into vehicle speed.

The objective is to maintain the vehicle speed at $v = 2\ m/s$. Note that this electric robotic vehicle is heavy duty oriented, of which the maximum speed is only around

$3m/s$ $(about\ 10km/h)$, and the motors are design to carry full load with a maximum RPM of $285r/min$. The gear ratio between motor and wheel is $14:21$, which further reduces the maximum speed to some degree. Therefore, the experimental will be carried out with reduced magnitudes, as presented in next section.

With ADRC control method and raw signal input, experiments are carried out respectively and motor speed feedbacks are recalculated as vehicle speeds shown as follows:

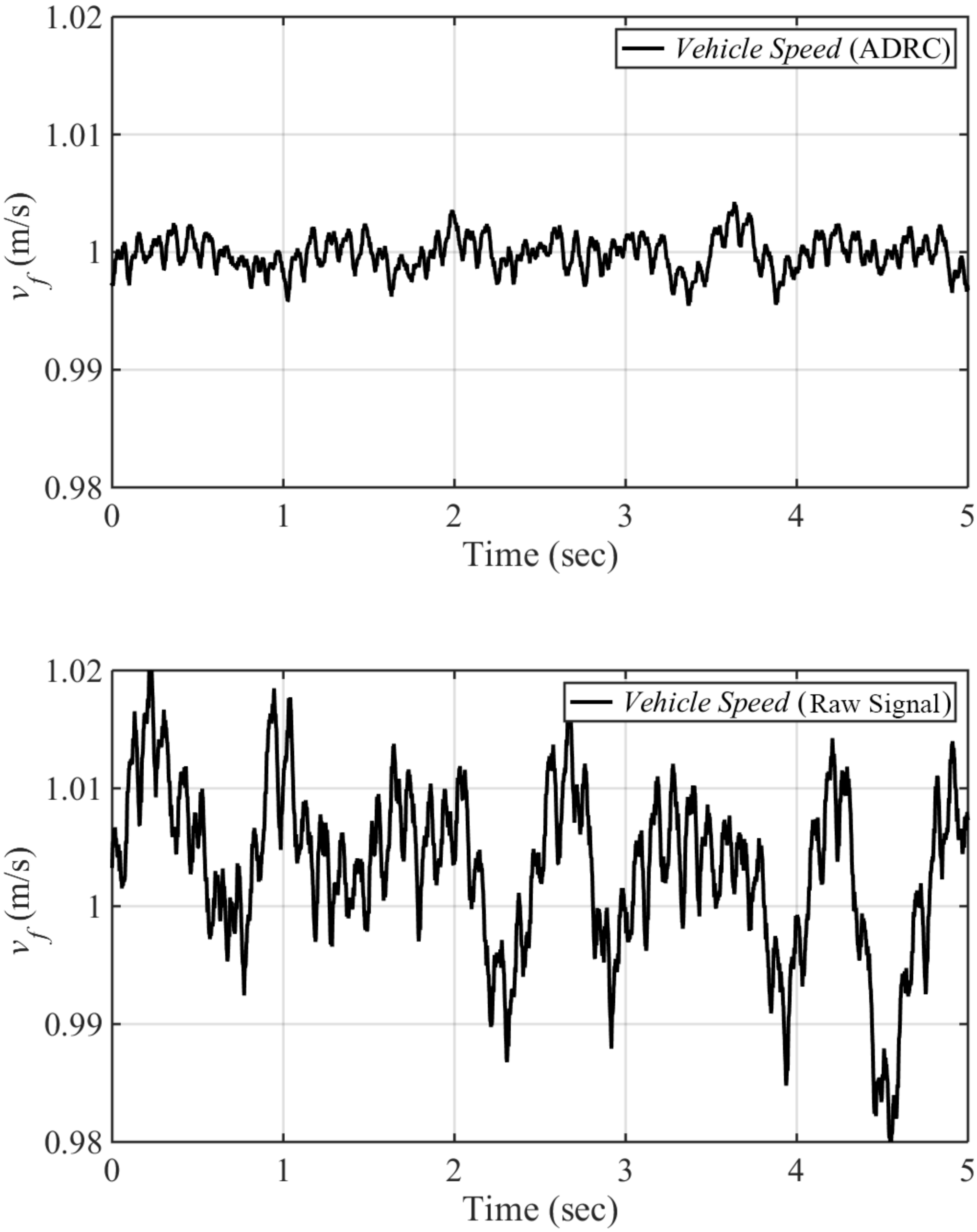

Figure 5.8 Vehicle speed with ADRC control and raw signal input

Note that these two experiments are performed not simultaneously. Results are posted in different graph for clearer illustration. By comparing the magnitude of these two feedback signals with noise, a conclusion can be driven explicitly that ADRC greatly reduce the noise level and offers a smooth run.

5.3 Comprehensive Experiments

On contrary to the simulation, where the two level controllers are better separated for a more explicit demonstration of performance, controllers will be linked together in experiments to offer the best results.

LQR, RLQR, and RCNF are applied separately as supervisory controllers. ADRC will be kept in use for the whole process. The experiments are divided into four parts similar with that in previous simulations.

Because ACC is generally activated in vehicle with high speed, especially on highways, modification needs to be made to some parameters to demonstrate the control algorithm on a low speed robot.

The input saturation u_{max} is resized to 0.48 and 0.8 from 6 and 10, which denotes two different configurations respectively. The stopping distance d_0 and the initial distance between two vehicles d_i are resized to the same size 0.4 to let $\Delta d = 0$ at $t = 0$.The initial speed of two vehicles are set to 2.4. The acceleration of proceeding vehicle (i.e. the disturbance) is also reset to its 0.08 times, figured as follows:

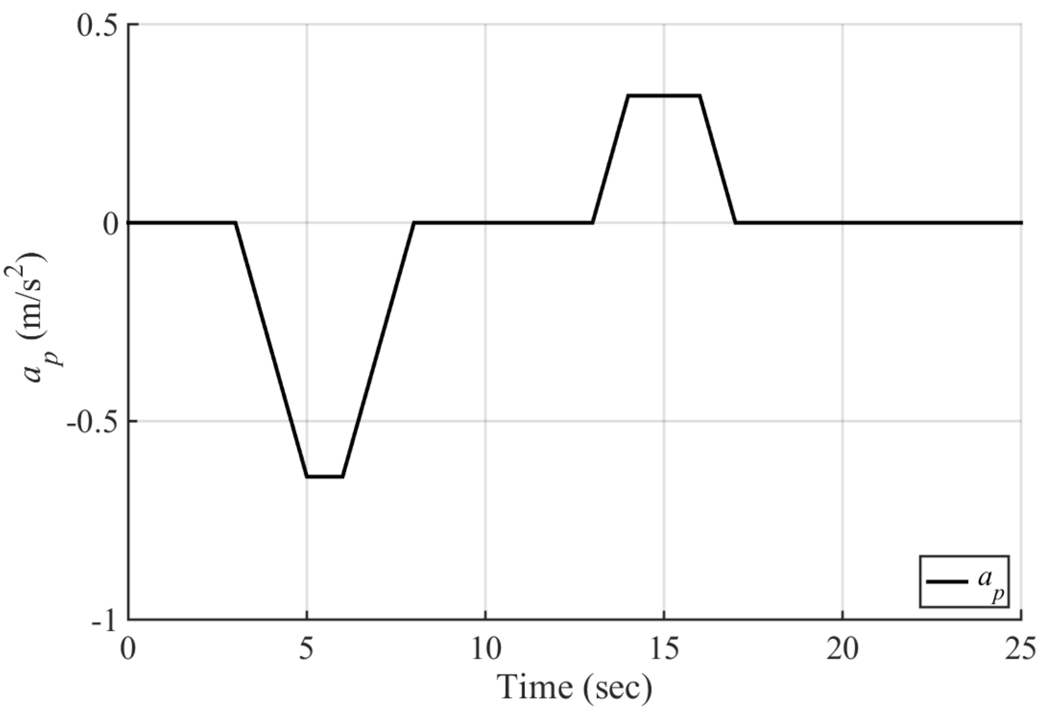

Figure 5.9 Resized acceleration of proceeding vehicle

And the parameters chosen for ADRC controllers are:

$$w_o = 200,\ \ w_c = 301.2,\ \ b = 100000$$

Other parameters retain their original sizes.

A summary of parameter selection in experiments can be given as follows, where resized parameter are in bold:

	$\tau_h = 0.5$	$d_0 = 0.4$	$V_{f0} = 2.4$	$d_i = 1.6$
	$x_0 = [0\,;0\,;0]$		$K_L = 1$	$T_s = 0.001$
RCNF	$\alpha = 10$		$\beta = 20$	$r = 0$
	$Pole_1 = [-5 + 0.1i \;\; -5 - 0.1i \;\; -2]$			
	$Pole_1 = [-5 + 0.1i \;\; -5 - 0.1i]$			$W = 0.01I_3$
ADRC	$\omega_0 = 200$		$\omega_c = 301.2$	$b = 100000$

Table 5.2 Parameter selection in experiments

Experiments are conducted in four cases shown as below, which are similar to Case I, II, IV and V of simulations:

Case	u_{max}	Q	R	Remark
I	0.48	$\begin{bmatrix} 10 & 0 \\ 0 & 1 \end{bmatrix}$	1	General Case
II	0.8	$\begin{bmatrix} 10 & 0 \\ 0 & 1 \end{bmatrix}$	1	Effective Braking
III	0.48	$\begin{bmatrix} 10 & 0 \\ 0 & 0.01 \end{bmatrix}$	0.01	Safety with (R)LQR
IV	0.48	$\begin{bmatrix} 20 & 0 \\ 0 & 5 \end{bmatrix}$	10	Comfort with (R)LQR

Table 5.3 Parameter selection for different experimental cases

Where the time delay constant of vehicle plant T_L, which was applied for denoting the delay properties for a better demonstration in simulations, is no more considered in experiments due to the physical existence of delay in experimental devices.

Experiments are shown from Figure 5.10 to 5.17, and each two figures denote a case.

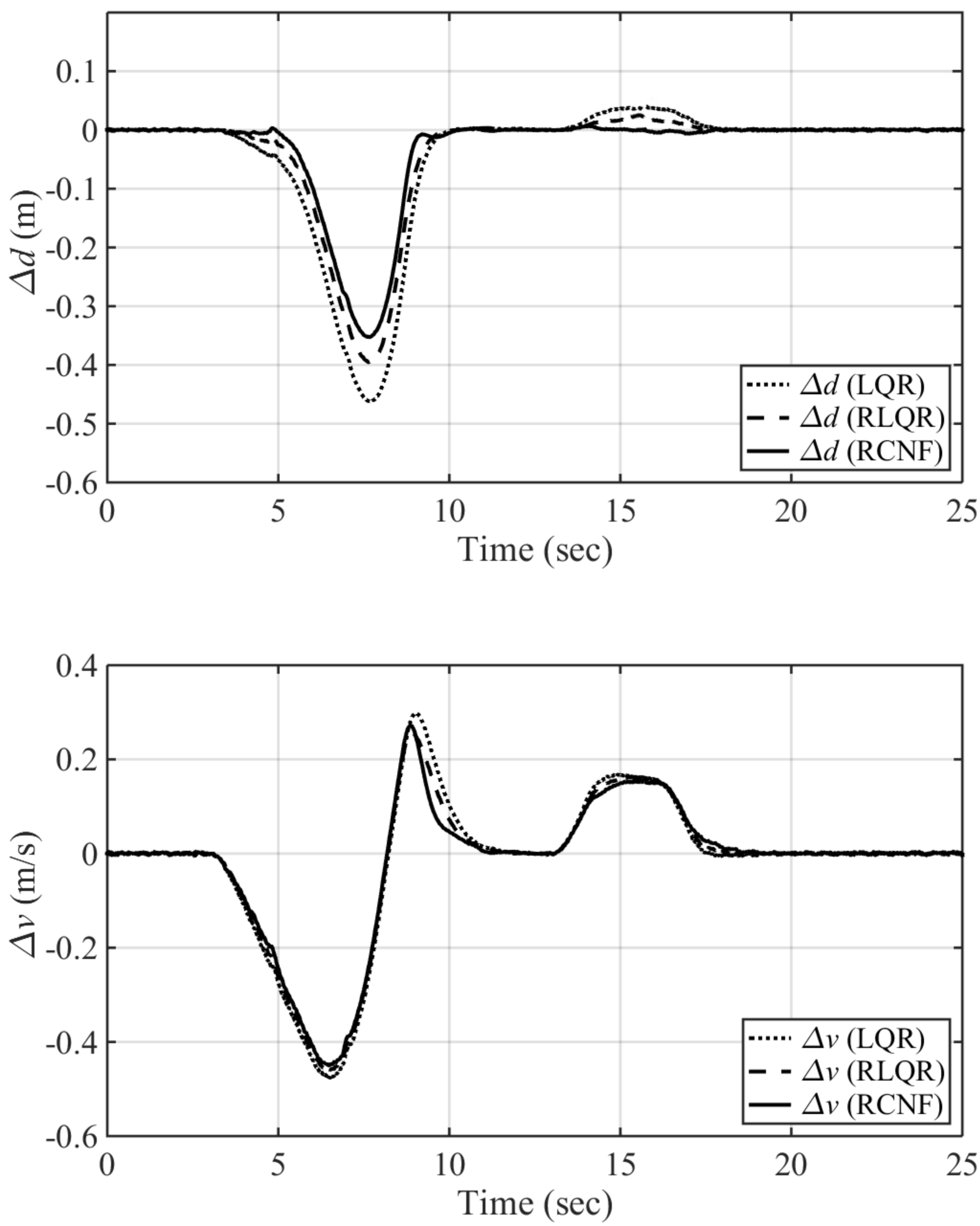

Figure 5.10 Experimental data for Δd and Δv in Case I (General Case)

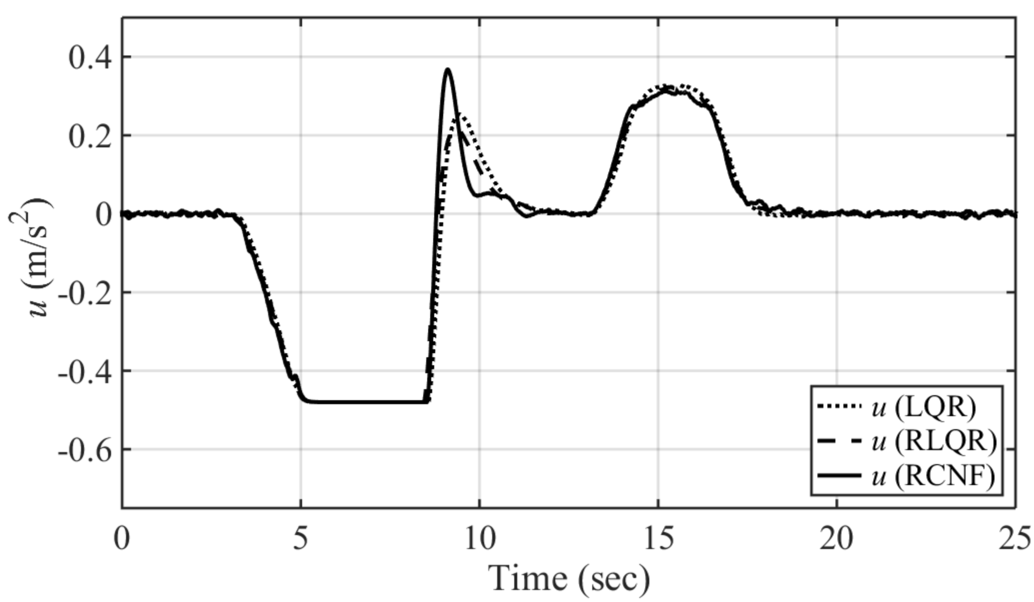

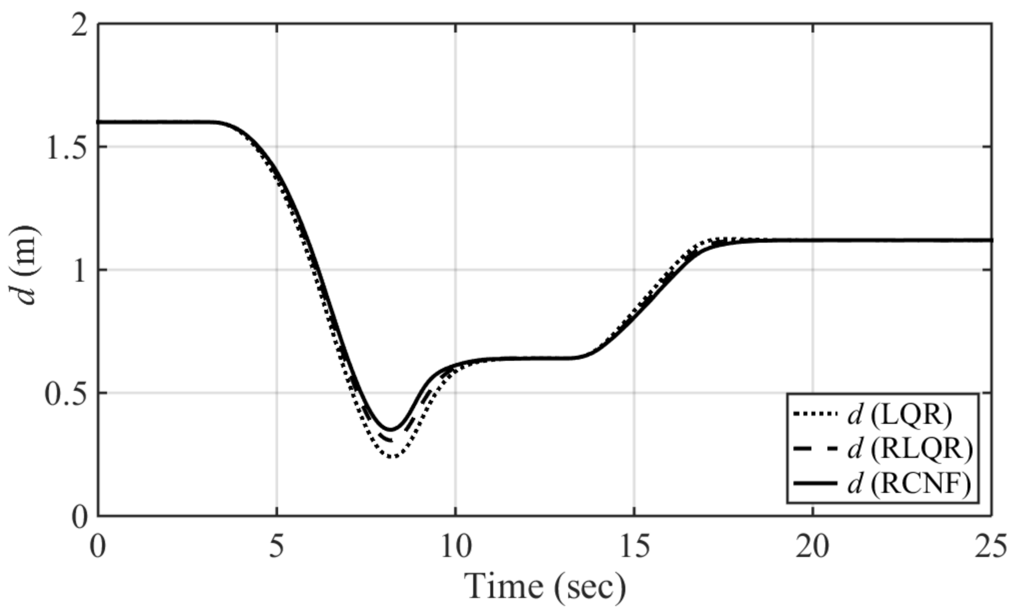

Figure 5.11 Experimental data for u and d in Case I (General Case)

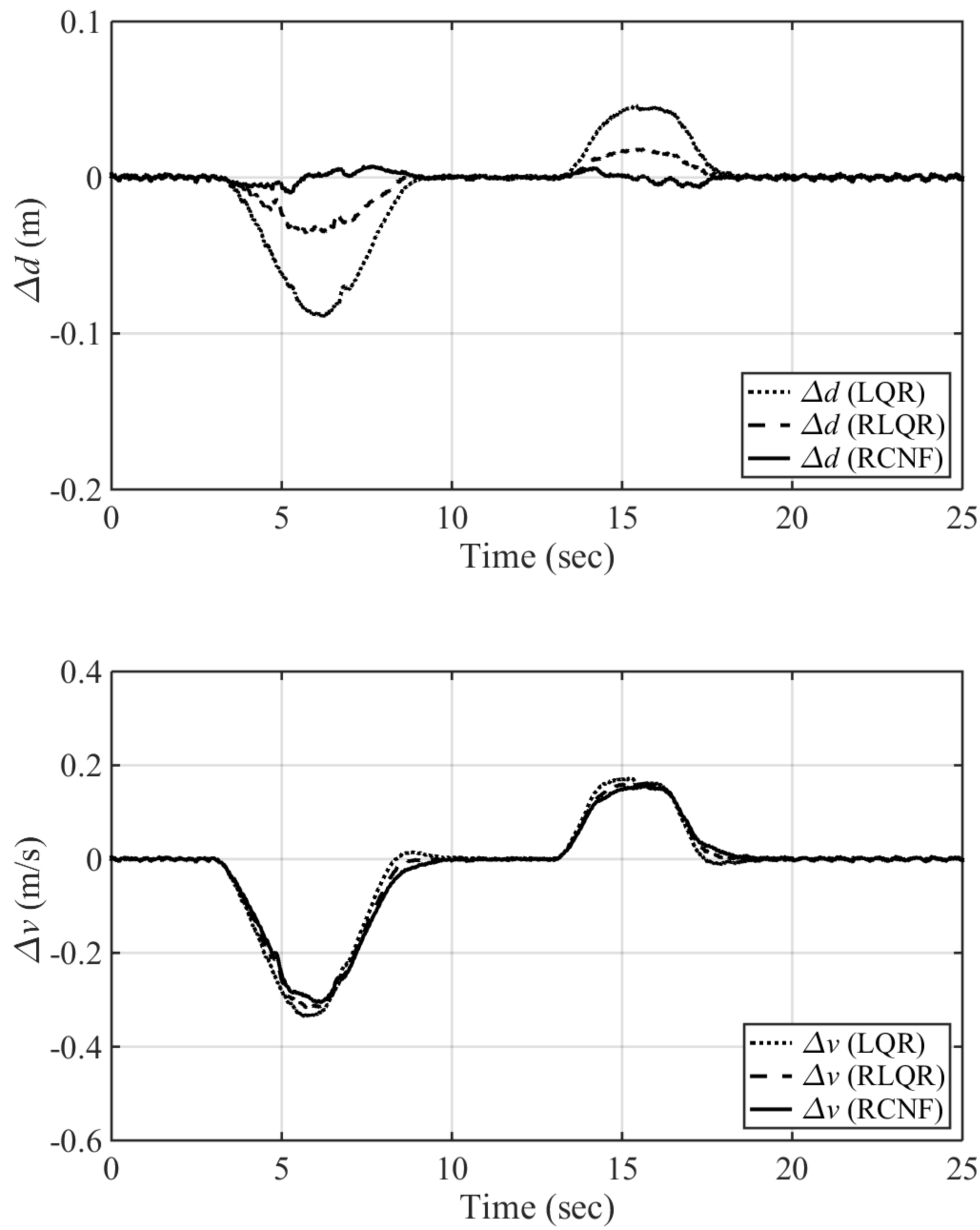

Figure 5.12 Experimental data for Δd and Δv in Case II (Effective Braking)

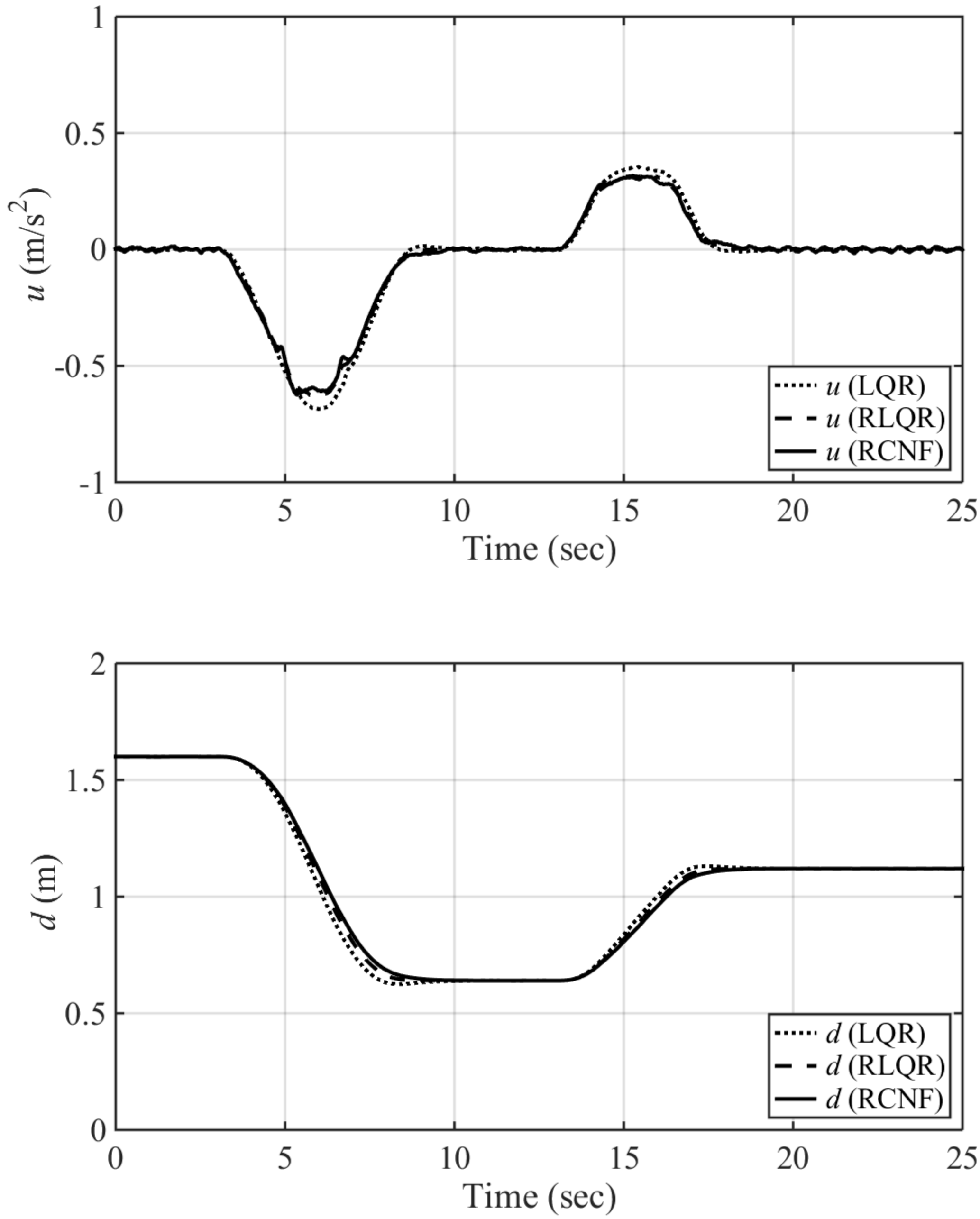

Figure 5.13 Experimental data for u and d in Case II (Effective Braking)

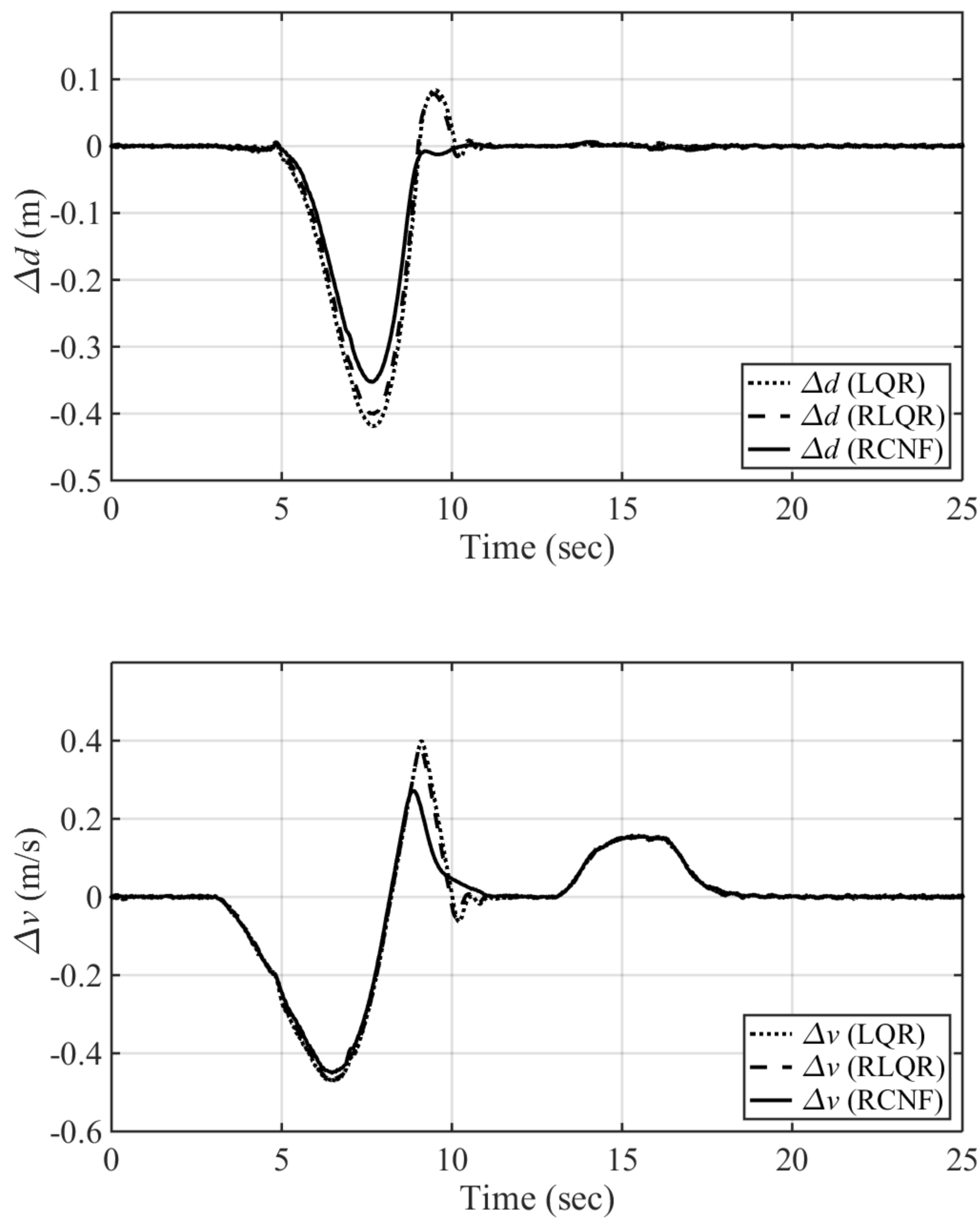

Figure 5.14 Experimental data for Δd and Δv in Case III (Safety with (R)LQR)

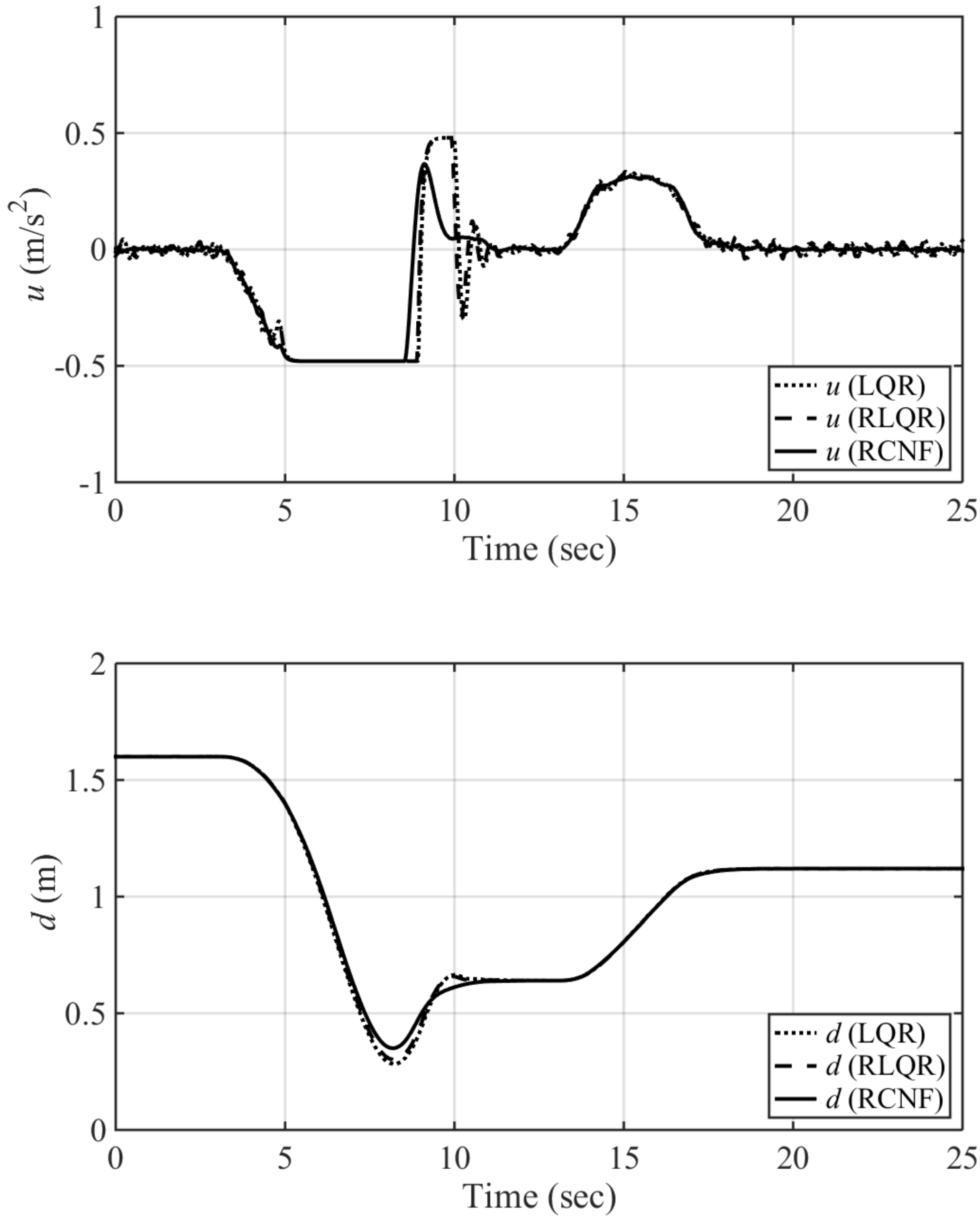

Figure 5.15 Experimental data for u and d in Case III (Safety with (R)LQR)

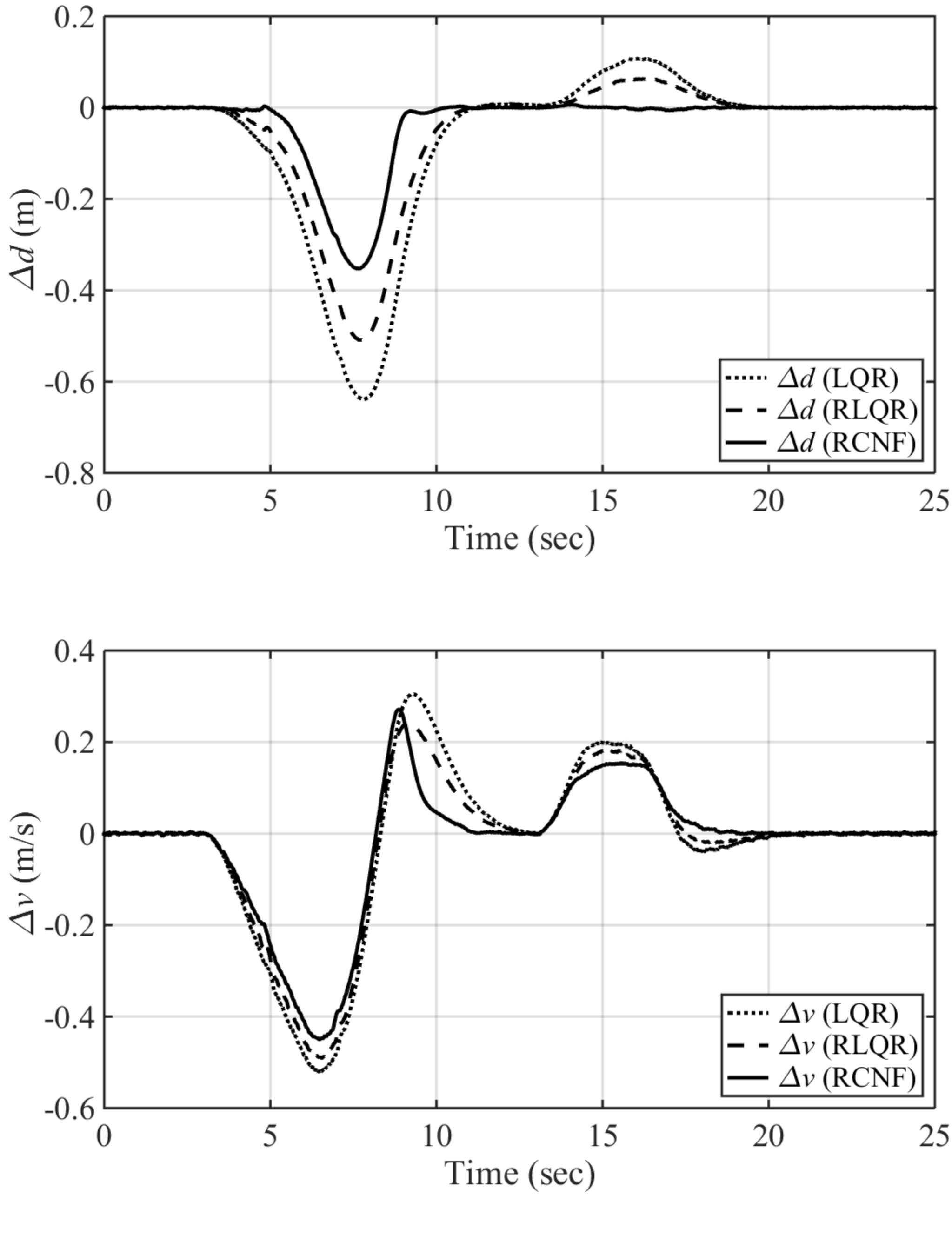

Figure 5.16 Experimental data for Δd and Δv in Case IV (Comfort with (R)LQR)

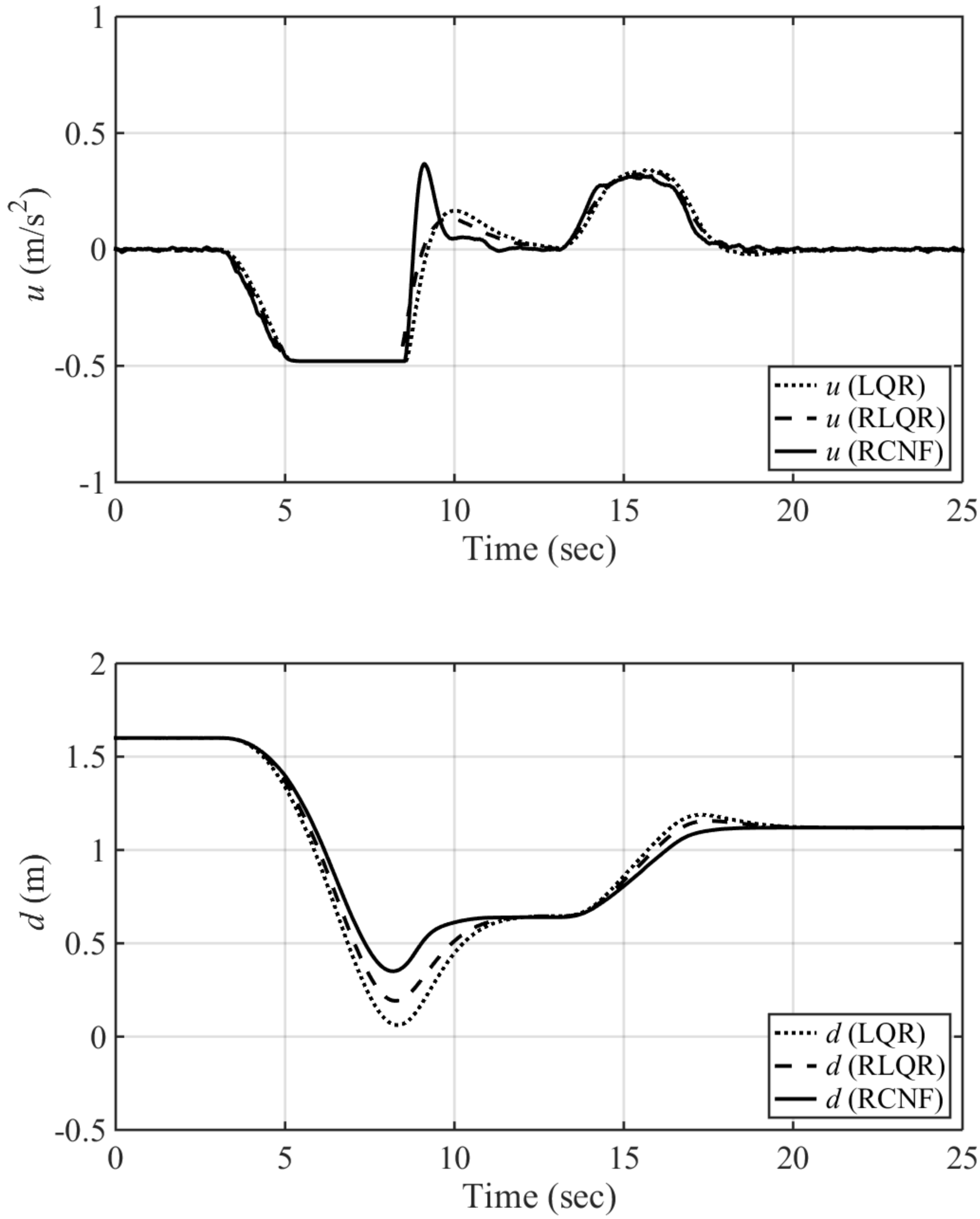

Figure 5.17 Experimental data for u and d in Case IV (Comfort with (R)LQR)

As demonstrated through simulations, RCNF possesses the quickest response time of input u among the three controllers, which converges Δd to 0 with less time and overshoot. RLQR is still the second best choice in these cases, which offers a tradeoff between safety and comfort with the flexibility to select various sets of parameters.

The input u demonstrates a similar pattern with that in simulation, and the actual distance d demonstrates again the superiority in tracking performance of RCNF controller.

In Case II, with enough deceleration, all three controllers can maintain a safe distance with little overshoot, within which the RCNF denotes a better controlling performance, but it also brings larger chattering into inputs, especially while the vehicle is maintaining a constant speed.

Experimental results in Case III are slightly different with simulations. The input of LQR and RLQR appears chattering, which is probably caused by system delays.

In Case IV, input u of LQR and RLQR both presents a less variation rates, offering a smoother running compared to RCNF, but also a weaken ability to stabilize Δd. Therefore, the stopping distance should be resized greater in this case for safety concerns, especially for LQR method.

5.4 Summary

In Chapter 5, the experimental platform is configured where ACC control strategies are validated with effectiveness.

Properties about the platform and its architecture are given in the form of diagrams and tables. The vehicle level controller ADRC is tested for its performance, which denotes highly contribution to reject noise. Experiments are conducted in different cases, which demonstrates again the characteristics, advantages and disadvantages of different control mechanisms, where RCNF denotes a better tracking ability but less comfort, while LQR and RLQR demonstrate their flexibility to focus on different design objectives.

CHAPTER 6
CONCLUSIONS AND FUTURE WORK RECOMMODATION

Adaptive Cruise Control (ACC), which can be considered as an extension version of Conventional Cruise Control, has been proposed for decades on a purpose to improve driving condition and road safety. It's the doorway to autonomous vehicles, which are just around the corner to change the world we live.

The control theory of ACC systems is already well developed, covering a wide range, including human behavior based fuzzy logic or neural network, and mathematical based algorithms. Hierarchical architecture is commonly adopted, with a supervisory controller and one or several vehicle level ones.

In this thesis, three control strategies, LQR, RLQR and RCNF are respectively adopted as the supervisory controller, and ADRC is selected as vehicle level one. Detailed design procedure is proposed with discussion on different controllers.

An electric robotic vehicle was built up in MARC to validate the feasibility of selected control strategies. The characteristics of these controller are summarized and compared through simulations and experiments.

For future work recommendation, more complex models for vehicle plant can be constructed and control system can be further tested on a full size vehicle. And the experimental platform is feasible to validate most longitudinal control strategies, while lateral control may be practical by setting different speeds to different sides of wheels. The robot can also be built into semi or fully autonomous platforms, which possesses the ability to carry various sensors and components like robotic arms to perform complicated tasks.

REFERENCES

[1] Anon, Car accident statistics, 2008.Available at http://www.car-accidents.com.

[2] A. Peters and J. Peters, Automotive Vehicle Safety, Taylor & Francis, London, 2002.

[3] Bennett, S. (1993). A History of Control Engineering 1930-1955. London: Peter Peregrinus Ltd. On behalf of the Institution of Electrical Engineers. ISBN 0-86341-280-7.

[4] C. Liang, Traffic-friendly adaptive cruise control design, Ph.D. Diss., University of Michigan, 2000.

[5] C. Liang and H. Peng, Optimal adaptive cruise control with guaranteed string stability, Veh. Syst. Dyn. 31 (1999), pp.313–330.

[6] H. Diamond and W. Lawrence, The development of an automatically controlled highway system, University of Michigan. Transportation Research Institutes's Report UMR1266, 1966.

[7] S. Levine and M. Athans, On the optimal error regulation of a string of moving vehicles, IEEE Trans. Autom. Control 11 (1996), pp. 355–361.

[8] S. Shladover, Review of the state of development of advanced vehicle control systems (AVCS), Veh. Syst. Dyn. 24 (1995), pp. 551–595.

[9] R. Fenton, R. Cosgriff, K. Olson, and L. Blackwell, One approach to highway automation, Proc. IEEE 56 (1968), pp. 556–566.

[10] R. Fenton and J. Mayhan, Automated highway studies at the Ohio state University –An overview, IEEE Trans. Veh. Technol. 40 (1991), pp. 100–113.

[11] J. Bender and R. Fenton, On the flow capacity of automated highways, Trans. Sci. 4 (1970), pp. 52–63.

[12] J. Bender, R. Fenton, and K. Olson, An experimental study of vehicle automatic longitudinal control, IEEE Trans. Veh. Technol. 20 (1971), pp. 114–123.

[13] P. Ioannou, Automated Highway Systems, Plenum Press, New York, 1997.

[14] I. Catling, Advanced Technology for Road Transport: IVHS and ATT, Artech House, Boston, 1993.

[15] R. French, E. Case, Y. Noguchi, C. Queree, and O. Sviden, A comparison of IVHS progress in the United States, Europe, and Japan, 31 December, DOT/FHWA 150278, 1993.

[16] F. Broqua, G. Lerner, V. Mauro, and E. Morello, Cooperative driving: Basic concepts and a first assessment of ‘Intelligent Cruise Control’ strategies, Advanced Telematics in Road Transport, Proceedings of the DRIVE Conference, Brussels, 1991.

[17] X. Zhang, Intelligent driving – PROMETHEUS approaches to longitudinal traffic flow control, Proceedings of Vehicle Navigation and Information Systems Conference, Dearborn, MI, 1991.

[18] X. Zhang and T. Benz, Simulation and evaluation of intelligent cruise control, IVHS J. 1 (1993), pp.181–190.

[19] DIATS Deliverable 1, State-of-the-art review of ATT systems, manufactures and users, RO-96-SC.301, CEC, DGVII, Brussels, Belgium, 1996.

[20] M. Brackstone and M. McDonald, A comparison of EU and US progress in the development of longitudinal advanced vehicle control and safety systems (AVCSS), Transp. Rev. 20 (2000), pp. 173–190.

[21] R. Bishop, Intelligent Vehicle Technology and Trends, Artech House, Boston, 2005.

[22] R. Betsold, R. Braun, G. Briges, R. Ervin, W. Harris, B. Hodge, and D. Willis, Mobility 2000 presents intelligent vehicles and highway systems, DOT/FHWA Summary 101018, 1990.

[23] L. Saxton, Mobility 2000 and the roots of IVHS, IVHS Rev. 1993, pp.11–26.

[24] P. Fancher, R. Ervin, and J. Sayer, Intelligent cruise control field operational test (interim report), University of Michigan Transportation Research Institute Report, Report No. UMTRI-97-1, 1997.

[25] P. Fancher, R. Ervin, and J. Sayer, Intelligent cruise control field operational test (final report) Vol. I, Tech. Rep., University of Michigan Transportation Research Institute Report, Report No. UMTRI-98-17, 1998.

[26] S. Bogard, P. Fancher, and R. Ervin, Intelligent cruise control field operational test (final report) Vol. III, Performance of a String or Cluster of ACC-Equipped Cars, University of Michigan Transportation Research Institute's Report, Rep. No. UMTRI-98-28, 1998.

[27] W. Najm, M. Stearns, H. Howarth, J. Koopman, and J. Hitz, Evaluation of an automotive rear-end collision avoidance system, DOT-VNTSC-NHTSA-06-01, April 2006.

[28] T. Nakahara and N. Yumoto, ITS development and deployment in Japan, IEEE Conference on Intelligent Transportation System, Boston, MA USA, 1998.

[29] H.Winner, S.Witte, W. Uhler, and B. Lichtenberg, Adaptive cruise control system: Aspects and development trends, SAE International, SAE Paper 961010, 1996.

[30] M. Goodrich and E. Boer, Designing human-centered automation: Tradeoffs in collision avoidance system design, IEEE Trans. Intell. Transp. Syst. 1 (2000), pp. 40–54.

[31] M. Hoedemaeker, Drivers' needs and behaviour, Handbook of the International Conference on Traffic and Transport Psychology, Valencia, 1996.

[32] C. Rudin-Brown and H. Parker, Behavioural adaptation to adaptive cruise control (ACC): implications for preventive strategies, Transp. Res. F 7 (2004), pp. 59–76.

[33] W. Choi and S. Darbha, Assessing the safety benefits due to coordination amongst vehicles during an emergency braking maneuver, Proceedings of the American Control Conference, Arlington, VA, 2001.

[34] A.Touran, M. Brackstone, and M. McDonald, Acollision model for safety evaluation of autonomous intelligent cruise control, Accid. Anal. Prev. 31 (1999), pp. 567–578.

[35] J. Koziol, J. Inman et al., Evaluation of the intelligent cruise control system Volume I – Study results, NHTSA Report No. DOT-VNTSC-NHTSA-98-3, 1999.

[36] DIATS Deliverable 15, Assessment of the safety issues relevant to the deployment of ATT test scenarios, RO-96-SC. 301 CEC, DGVII, Brussels, Belgium, 1998.

[37] T. Chira-Chavala and S.Yoo, Potential safety benefits of intelligent cruise control systems, Accid. Anal. Prev. 26 (1994), pp. 135–146.

[38] T. Benz, Checking ICC in a realistic traffic environment, Proceedings of the 1stWorld Congress on Applications of Transport Telematics and Intelligent Vehicle: Highway Systems, Paris, 1994.

[39] J. VanderWerf, S. Shladove, and M. Mille, Effects of adaptive cruise control systems on highway traffic flow capacity, Transportation Research Record 1800, Paper No. 02-3665, 2002, pp. 78–84.

[40] A. Kesting, M. Treiber, M. Schohof, and D. Helbing, Extending adaptive cruise control to adaptive driving strategies, J. Transp. Res. Board 2000 (2007), pp. 16–24.

[41] M. McDonald, J.Wu, and M. Brackstone, The integrated impacts of autonomous cruise control on motorway traffic flow, Proceedings of the 5th Annual World Congress on ITS, Seoul, Korea, 1998.

[42] A. Bose and P. Ioannou, Environmental evaluation of intelligent cruise control (ICC) vehicles, 2000 IEEE Intelligent Transportation Systems Conference Proceedings Dearborn (MI), USA, 2000.

[43] A. Bose and P. Ioannou, Analysis of traffic flow with mixed manual and intelligent cruise control vehicles: Theory and experiments, California PATH Research Report, UCB-ITS-PRR-2001-13, 2001.

[44] A. Bose and P. Ioannou, Evaluation of the environmental effects of intelligent cruise control vehicles, Transp. Res. Rec. 1774 (2003), pp. 90–97.

[45] P. Fancher, R. Ervin, and J. Sayer, Intelligent cruise control field operational test (final report) Vol. I, Tech. Rep., University of Michigan Transportation Research Institute Report, Report No. UMTRI-98-17, 1998.

[46] P. Zhang and M. McDonald, Manual vs. adaptive cruise control – Can driver's expectation be matched? Transp. Res. C 13 (2005), pp. 421–431.

[47] N. Stanton and P. Marsden, From fly-by-wire to drive-by-wire: Safety implications of automation in vehicles, Saf. Sci. 24 (1996), pp. 35–49.

[48] A. Bkarel, D.Waard, andW. Janssen, Behavioural impacts of advanced driver assistance systems –An overview, EJTIR 1 (2001), pp. 245–253.

[49] M. Brackstone and M. McDonald, Behavioral response: Still a major concern for AVCSS? ITS J. 5 (2000), pp. 363–382.

[50] DIATS Deliverable 13–14, User preference and behavioural changes from ATT systems, RO-96-SC.301 CEC, DGVII, Brussels, Belgium, 1998.

[51] K. Syverud, Liability and insurance implications of IVHS technology, SAE International, SAE Paper 901507, 1990.

[52] K. Chen and R. French, Organizational response to intelligent vehicle highway systems, SAE International, SAE Paper 911673, 1991.

[53] J. Costantino, Overcoming institutional barriers to IVHS, Transp. Q. 48 (1994), pp. 3–13.

[54] DIATSDeliverable 16, Assessment of the legal issues relevant to the deployment ofATTsystems, RO-96-SC.301 CEC, DGVII, Brussels, Belgium, 1998.

[55] R. Van der Heijden and K. Van Wees, Introducing advanced driver assistance systems: Some legal issues, EJTIR 1 (2001), pp. 309–326.

[56] K. VanWees and K. Brookhuis, Product liability for ADAS: Legal and human factors perspectives, EJTIR 5 (2005), pp. 357–372.

[57] R. Rajamani, Vehicles Dynamics and Control, Springer, New York, 2006.

[58] K. Jurgen, Adaptive Cruise Control, SAE International, PA, 2006.

[59] R. Abou-Jaoude, SAE international ACC radar sensor technology, test requirements, and test solutions, IEEE Trans. Intell. Transp. Syst. 4 (2003), pp. 115–122.

[60] R. Widmann and K. Daniels, Comparison of lidar-based and radar-based adaptive cruise control systems, SAE International, SAE paper 2000-01-0345, 2000.

[61] E. Feldman, Development and integration of a vision-based sensor for adaptive cruise control, M.sc Thesis, University of California, Berkeley, 2002.

[62] E. Russell and A. Crain, Millimeter-wave radar sensor for automotive intelligent cruise control (ICC), IEEE Trans. Microw. Theory Tech. 45 (1997), pp. 2444–2453.

[63] J. Carsten and N. Merat, Human machine interaction and safety of traffic in Europe, HASTE Final Report 3.1, November 2005.

[64] L. Xiao and F. Gao, “A comprehensive review of the development of adaptive cruise control systems,” *Veh. Syst. Dyn.*, vol. 48, no. February 2015, pp. 1167–1192, 2010.

[65] Anon, Adaptive cruise control system overview, The 5th Meeting of the US Software System Safety Working Group, Anaheim, California, 2005.

[66] K. Egawa and K. Satou, Development of adaptive cruise control with low speed following capability, SAE International, SAE Paper 2005-01-1483, 2005.

[67] M. Ichinose, A. Yokoyama, and T. Nishigaito, Hardware-in-the-loop simulator with auto building vehicle model for adaptive cruise control system, SAE International, SAE Paper 2004-01-1243, 2004.

[68] A. Pipes, An operational analysis of traffic dynamics, J. Appl. Phys. 24 (1953), pp. 274–281. [40] D. Morag, Operating policies for personal rapid transit, U.S. DOT Urban Mass Transit Administration, Report No. RDD-8-74-2, 1974.

[69] D. Mackinnon, High capacity personal rapid transit system developments, IEEE Trans. Veh. Technol. 24 (1975), pp. 8–14.

[70] L. Garrard, J. Gaudill, and L. Kornhauser, State-of-the-art of longitudinal control of automated guideway transit vehicles, High Speed Ground Transp. J. 12 (1978), pp. 35–67.

[71] J. Wang and R. Rajamani, Should adaptive cruise control systems be designed to maintain a constant time gap between vehicles? IEEE Trans. Veh. Technol. 53 (2004), pp. 1480–1490.

[72] J. Zhou and H. Peng, Range policy of adaptive cruise control vehicle for improved flow stability and string stability, Proceedings of the 2004 IEEE international Conference on Networking, Sensing and Control, Taipei, Taiwan, 2004.

[73] D. Han and K. Yi, A Driver-adaptive range policy for adaptive cruise control, Proc. IMechE 220 (2006) pp. 321–324.

[74] S. Darbha, K. Hedrick, C. Chien, and P. Ioannou, A comparison of spacing and headway control strategy for automatically controlled vehicles, Veh. Syst. Dyn. 23 (1994), pp. 597–625.

[75] F. Lattemann, K. Neiss, S. Terwen, and T. Connolly, “The predictive cruise control—A system to reduce fuel consumption of heavy duty trucks,” SAE International, Warrendale, PA, 2004-01-2616.

[76] J. Zhang and P. Ioannou, “Longitudinal control of heavy trucks in mixed traffic: Environmental and fuel economy considerations,” IEEE Trans. Intel. Transport. Syst., vol. 7, no. 1, pp. 92–104, Jan. 2006.

[77] J. Jonsson, “Fuel optimized predictive following in lower speed conditions,” M.S. thesis, Dept. Elect. Eng., Linköping Univ., Linköping, Sweden, 2003.

[78] P. Ioannou and Z. Xu, “Throttle and brake control systems for automatic vehicle following,” IVHS J., vol. 1, no. 4, pp. 345–377, 1994.

[79] K. Yi and Y. Kwon, “Vehicle-to-vehicle distance and speed control using an electronic-vacuum booster,” JASE Rev. vol. 4, pp. 403–412, 2001.

[80] M. Persson, F. Botling, E. Hesslow, and R. Johansson, “Stop and go controller for adaptive cruise control,” in Proc. IEEE Int. Conf. Control Appl., 1999, pp. 1692–1697.

[81] A. Higashimata, K. Adachi, T. Hashizume, and S. Tange, "Design of a headway distance control system for ACC," J. JSAE Rev., vol. 22, pp. 15–22, 2001.

[82] D. Corona, M. Lazar, B. Schutter, and M. Heemels, "A hybrid MPC approach to the design of a smart adaptive cruise controller," in Proc. IEEE Int. Conf. Control Appl., Germany, 2006, pp. 231–235.

[83] D. Corona and B. Schutter, "Adaptive cruise control for a SMART car: A comparison benchmark for MPC-PWA control methods," IEEE Trans. Control Syst. Technol., vol. 16, no. 2, pp. 365–372, Mar. 2008.

[84] Holzmann, H., Halfmann, C., Germann, S., Wurtenberger, M., Isermann, R., 1997. Longitudinal and lateral control and supervision of autonomous intelligent vehicles. Control Engineering Practice, 5(11):1599-1605. [doi: 10.1016/ S0967-0661(97)10015-6]

[85] D. Pomerleau, "Neural network vision for robot driving," in The Hand- book of Brain Theory and Neural Networks, M. Arbib, Ed. Cambridge, MA: MIT Press, 1995.

[86] A. Eskandarian and S. Thiriez, "Collision avoidance using a cerebellar model arithmetic computer neural network," Computer-Aided Civil Infrastructure Eng., vol. 13, pp. 303–314, Sept. 1998.

[87] Naranjo, J. E., Gonzalez, C., Reviejo, J., Garcia, R., & Pedro, T. (2003). Adaptive fuzzy control for inter-vehicle gap keeping. IEEE Transactions on Intelligent Transportation Systems, 4, 132–142.

[88] Naranjo, J., Gonzalez, C., Garcia, R., & Pedro, T. (2007). Using fuzzy in automated vehicle control. Intelligent Transportation Systems, 22, 36–45.

[89] Abdullah, R., Hussain, A., Warwick, K., & Zayed, A. (2008). Autonomous intelligent cruise control using a novel multiple-controller framework incorporating fuzzy-logic-based switching and tuning. Journal of Neurocomputing, 71, 2727–2741.

[90] L. Ng, C. Clark, and J. Huissoon, "Reinforcement learning of dynamic collaborative driving—Part I: Longitudinal adaptive control," Int. J. Vehicle Inf. Commun. Syst., vol. 1, no. 3, pp. 208–228, 2008.

[91] Shakouri P, Ordys A, Laila DS. Adaptive cruise control system: comparing gain-scheduling PI and LQ controllers, 18th IFAC world congress, August 28– September 2, Milano, Italy; 2011.

[92] V. Bageshwar, W. Garrard, and R. Rajamani, "Model predictive control of transitional maneuvers for adaptive cruise control vehicles," IEEE Trans. Veh. Technol., vol. 53, no. 5, pp. 365–374, Sep. 2004.

[93] S. Li, K. Li, R. Rajamani, and J. Wang, “Model predictive multi-objective vehicular adaptive cruise control,” *IEEE Trans. Control Syst. Technol.*, vol. 19, no. 3, pp. 556–566, 2011.

[94] D. Caveney and J.K. Hedrick, Single versus tandem radar sensor target tracking in the adaptive cruise control environment, Proceeding of the American Control Conference, Anchorage, Alaska, May, 2002.

[95] I. Moon, K. Yi, D. Caveney, and J.K. Hedrick, A multi-target tracking algorithm for application to adaptive cruise control, J.Mech. Sci. Technol. (KSME Int. J.) 19(9) (2005), pp. 1742–1752.

[96] D. Caveney, B. Feldman, and J.K. Hedrick, Comprehensive framework for multi-sensor multi-target tracking in the adaptive cruise control environment, Proceedings of the 6th International Symposium on Advanced Vehicle Control (AVEC), Hiroshima, Japan, 2002, pp. 697–702.

[97] R. Möbus and U. Kolbe, Multi-target multi-object tracking, sensor fusion of radar and infrared, 2004 IEEE Intelligent Vehicles Symposium University of Parma, Italy, 2004, pp. 732–737.

[98] C. Yukun, S. Xicai, and L. Zhigang, Research on Kalman-filter based multisensor data fusion, J. Syst. Eng. Electron. 18(3), (2007), pp. 497–502.

[99] M. Maehlisch, W. Ritter, and K. Dietmayer, De-cluttering with integrated probabilistic data association for multisensor multitarget ACC vehicle tracking, Proceedings of the 2007 IEEE Intelligent Vehicles Symposium Istanbul, Turkey, June 13–15, 2007.

[100] S. Miyahara, J. Sielagoski, and F. Ibrahim, Radar-based target tracking method: Application to real road, 2005 SAEWorld Congress Detroit, Michigan, April 11–14, 2005.

[101] Y. Bar-Shalom and W.D. Blair (eds.), Multi-target Multi-sensor Tracking: Application and Advances, Vol. 3, Artech House Edition, Norwood, MA, 2000.

[102] D. De Bruin, J. Kroon, R. Van Klaveren, and M. Nelisse, “Design and test of a cooperative adaptive cruise control system,” in Proc. IEEE Intell. Vehicles Symp. 2004, pp. 392–396.

[103] G. Naus, R. Vugts, J. Ploeg, M. Van de Molengraft, and M. Steinbuch, “Towards on-the-road implementation of cooperative adaptive cruise control,” in Proc. 16th World Congr. Exhib. Intell. Transp. Syst. Serv., Stockholm, Sweden, 2009.

[104] M. van Eenennaam, W. Wolterink, G. Karagiannis, and G. Heijenk, “Exploring the solution space of beaconing in VANETs,” in Proc. IEEE VNC, 2010, pp. 1–8.

[105] D. Swaroop, K. Hedrick, C. Chien, and P. Ioannou, “Comparison of spacing and headway control laws for automatically controlled vehicles,” Vehicle Syst. Dyn., vol. 23, pp. 597–625, Nov. 1994.

[106] J. Gerdes and K. Hedrick, “Vehicle speed and spacing control via co-ordinated throttle and brake actuation,” Control Engineering Practice, vol. 5, pp. 1607–1614, Nov. 1997.

[107] W. Schiehlen and A. Fritz, “Nonlinear cruise control concepts for vehicles in convoy,” Vehicle Syst. Dyn. Supplement, vol. 33, pp. 256–269, 1999.

[108] --------, “Comparison of engine models and distance sensors for vehicle longitudinal control: Analysis and test results in PATH,” in Proc. Annu. Meet. ITS America, Washington, DC, 1995, pp. 61–68.

[109] R. Mayr, “Nonlinear vehicle distance control in longitudinal direction,” Int. J. Syst. Sci., vol. 27, pp. 705–712, Aug. 1996.

[110] H. Raza, Z. Xu, B. Yang, and P. Ioannou, “Modeling and control design for a computer-controlled brake system,” IEEE Trans. Control Syst. Technol., vol. 5, pp. 279–296, May 1997.

[111] K. Yi and J. Chung, “Nonlinear brake control for vehicle CW/CA systems,” IEEE/ASME Trans. Mechatron., vol. 6, pp. 17–25, Mar. 2001.

[112] M. Druzhinina, A. Stefanopoulou, and L. Moklegaard, “Compression braking control for heavy-duty vehicles,” presented at the 2000 American Control Conf., Chicago, IL, 2000.

[113] M. Druzhinina, L. Moklegaard, and A. Stefanopoulou, “Speed gradient approach to longitudinal control of heavy-duty vehicles equipped with variable compression brake,” IEEE Trans. Control Syst. Technol., vol. 10, pp. 209–220, Mar. 2002.

[114] M. Druzhinina, A. Stefanopoulou, and L. Moklegaard, “Adaptive continuously variable compression braking control for heavy-duty vehicles,” ASME Dyn. Syst., Meas. Contr., vol. 124, pp. 406–414, Sept. 2002.

[115] M. Druzhinina and A. Stefanopoulou, “Speed control experiments for commercial heavy vehicles with coordinated friction and engine compression brakes,” presented at the Proc. American Control Conf., Anchorage, AK, 2002.

[116] Maxwell, J.C. (1868). "On Governors". Proceedings of the Royal Society of London 16: 270–283. doi:10.1098/rspl.1867.0055. JSTOR 112510.

[117] Brain D. O. Anderson and John B. Moore (1989), Prentice-Hall, Inc. ISBN 0-13-638651-2.

[118] H. Shakir and W. J. Kim, “Nanoscale path planning and motion control with maglev positioners,” IEEE/ASME Trans. on Mechatronics, vol. 11, no. 5, pp. 625-633, 2006.

[119] M. Basina, J. Rodriguez-Gonzaleza, and L. Frid- manb, “Optimal and robust control for linear state-delay systems,” Journal of the Franklin Institute, vol. 344, no. 6, pp. 830-845, 2007.

[120] J. Zhou, “Stabilisation of individual generators with SVC designed via phase plane partitioning,” IET Control Theory and Applications, vol. 4, no. 4, pp. 601-612, 2010.

[121] V. Dragan, H. Mukaidanih, and P. Shi, “The linear quadratic regulator problem for a class of controlled systems modeled by singularly perturbed it to differential equations,” SIAM Journal on Control and Optimization, vol. 50, no. 1, pp. 448-470, 2012.

[122] X. Liu, Y. Wu, Y. Zhang, and S. Xiao, “A control method to make LQR robust: A planes cluster approaching mode,” *Int. J. Control. Autom. Syst.*, vol. 12, no. 2, pp. 302–308, 2014.

[123] B. M. Chen, T. H. Lee, K. P. K. Peng, and V. Venkataramanan, “Composite nonlinear feedback control for linear systems with input saturation: theory and an application,” *IEEE Trans. Automat. Contr.*, vol. 48, no. 3, pp. 427–439, 2003.

[124] --------, Robust and Control. London, U.K.: Springer-Verlag, 2000.

[125] G. Cheng and J. Hu, "A Robust Nonlinear Feedback Control Approach for the Two-inertia Servo Drive systems," pp. 7822–7827, 2014.

[126] J. Han, "From PID to active disturbance rejection control," *IEEE Trans. Ind. Electron.*, vol. 56, no. 3, pp. 900–906, 2009.

[127] Z. Gao, "Active disturbance rejection control: a paradigm shift in feedback control system design," *2006 Am. Control Conf.*, p. 7 pp., 2006.

[128] Z. Gao, "Scaling and Parameterization Based Controller Tuning," Proc. of the 2003 American Control Conference, June 2003, pp. 4989-4996.